The Study of Pancreatic Circulating Tumor Cells *via* Isolation with an Integrated Microfluidic Immunomagnetic (IMI) Device

by

Rhonda Martha Jack

A dissertation submitted in partial fulfillment
of the requirements for the degree of
Doctor of Philosophy
(Chemical Engineering)
in the University of Michigan
2017

Doctoral Committee:

Associate Professor Sunitha Nagrath, Chair
Professor Erdogan Gulari
Assistant Professor James Moon
Dr. Diane M. Simeone
Assistant Professor Greg Thurber

Dedication

I dedicate this thesis to my older sister Legena Henry whose constant encouragement, guidance and sound advice made the journey all the more bearable. Beyond engineering and science, her adeptness in what seems like every aspect of her life continues to be a deep source of inspiration for me; to my parents Harrington and Miriam, who have sacrificed, nurtured and loved me unconditionally, especially at my lowest points. Their unwavering support touches my heart every time I reflect on it; to all of my siblings and their families who have brought me unceasing joy throughout the journey; to my advisor Prof. Sunitha Nagrath who has believed in me and mentored me with deep wisdom, kindness and patience. She gave me room to grow and to explore science in ways that really spurred my curiosity and innovativeness.

Acknowledgements

Without the help, guidance and collaborative input of a number of individuals, this work would not be possible. Firstly, I acknowledge my advisor Prof. Sunitha Nagrath whose intuition, insight and unmitigating conviction in the true value of the work we do in the Nagrath group have been a constant source of energy for me. After each one-on-one meeting with her, I left with a deep sense of purpose and increased zeal to execute my research. My lab mates have also been a tremendous source of encouragement to me. Their ingenuity, intellectual curiosity and their remarkable work ethics have shaped and impacted me in many ways. I want to specifically acknowledge Dr. Meggie Grafton, a past group member who directly trained me when I initially joined the team.

I am immensely thankful to my thesis committee Prof. Gulari, Prof. Thurber, Prof. Moon and Dr. Simeone as their guidance, advice and timely feedback throughout the process have caused me to take greater ownership of the work I've done. I am deeply grateful to Dr. Simeone for providing all of the patient samples described in the work and Dr. Heather Cameron who did a spectacular job at coordinating the process. Also, I would like to acknowledge Dr. Muneesh Tewari and Dr. Maria Giraldez for their expertise and collaborative involvement with the molecular profiling work. I am truly grateful for the remarkable collaborative work the Nagrath group does with Dr. Max Wicha, and the Wicha lab, in particular for Dr. Ebrahim Azizi and Shamileh Fouladdel assistance with the gene profiling work. To the UROP program and the undergraduate students I mentored, I can't say thank you enough. Without the diligence and quality efforts of students like Danika Rodrigues and Khadijah Hussain, among others, this work would be incomplete. I am indebted to Rackham for the Conference Travel Grants I received as well as the Talwar Award/Rackham research grant which contributed directly to my development as a researcher and PhD student. Additionally, I am deeply grateful to the experts and staff at the Lurie Nanofabrication Facility (LNF), the Microscopy and Image Analysis Lab (MIL) and the Mechanical Engineering machine shop at the University of Michigan.

To the members of SMES-G, SCOR and PCWID who all made my time at Michigan a happier and more fulfilling experience, I say thank you from the bottom of my heart. To DNW and my C-WBN family, I could not have done it without your love and support.

Table of Contents

List of Tables

List of Figures

Abstract

In 2016 alone, it is projected that over forty thousand Americans will succumb to pancreatic cancer. One avenue that holds promise in developing accurate predictive tools and effective therapeutic agents to mitigate cancer mortality lies in the analysis of circulating tumor cells (CTCs). CTCs describe a subset of tumor cells that have acquired the ability to disseminate from primary and metastatic sites and intravasate into the circulatory system to subsequently spur new metastases. As such their detection in peripheral blood has been recognized as a potential tool in the diagnosis of cancer and in the prevention of metastasis. CTCs can be accessed from facile, non-invasive patient blood draws compared to complex surgical procedures traditionally employed to obtain tumor tissue biopsies. However these cells are quite rare, occurring on the order of 1:1 billion among other blood cells. Therefore the need to enrich these cells to achieve better detection is exigent.

This thesis delineates the development and the implementation of an integrated, polymer-based microfluidic CTC sorting device that enables significant enrichment of CTCs in a continuous, high-throughput manner (24mL/hr). The device operates via strategic combination of size-based inertial cell sorting, on-chip CTC immunomagnetic-microbead labeling, and magnetic cell sorting. Targeted isolation of as few as 10s of cancer cells from millions of WBCs with average CTC purities of 82.5%±23.5 (n=14) is enabled through this process. Moreover, CTCs were detected in 100% of patient samples, at >13 CTCs/mL across all patients, (median = 69 CTCs/mL, mean = 146± 231 CTCs/mL), demonstrating the ability of the approach to distinguish between diseased and healthy samples.

Subsequently, the work outlines CTC molecular characterization, by way of both messenger- and micro- RNA profiling, of CTCs isolated using the optimized integrated device. Messenger RNA (mRNA) profiling revealed that expression of seven mRNAs, Zeb1, KLF4, cMYC, BRCA1, HER2, CD3D, and HPRT1 were significantly higher in metastatic versus borderline profiles. Also, CTC microRNA profiling showed that miRs-221-3p, -23a-3p, -143-3p and -21-5p, were among those most abundantly expressed. These miRNAs have all been previously reported to be PDAC associated. Also, we report that miRs 17-5p, 19b-3p, 320b and let7a-5p were among those most highly expressed by the profiled PDAC CTC samples. Through network analysis of the miR expression data, we also found that pathways involving MAP2K1/2 and Smad2/3 are implicated in PDAC CTC biology.

Additionally, two separate studies, which analyze distinct aspects of the heterogeneity that exits among CTCs, have been reported. In one study, CTCs were sorted and compared according to a continuum of expression of EpCAM, a surface protein of paramount interest. Interestingly, CTCs of varying EpCAM levels were isolated from patient samples using this sorting method suggesting an observable level of heterogeneity at the protein level among these patients CTCs. In another study, CTCs have been studied based on a dual isolation approach where a combination of surface protein of interest, EpCAM and CD44, have been used to immunomagnetically enrich and probe these rare cells. Among borderline patients, CTC mRNA profiles hint at differences at the molecular level between patients classed as resectable from those not identified as resectable. Finally, preliminary studies on the synthesis and use of differentially synthesized micron particles, with the potential to isolate unique cancer cell subpopulations have been reported.

The development of an integrated platform to isolate CTCs with high purities allows for CTC-specific downstream genomic characterization. Molecular characterization of pancreatic cancer-derived CTCs revealed several mRNAs and microRNAs that were associated with the patient disease. Furthermore, studies were carried out to characterize CTCs based on their heterogeneity, a phenomenon that appears to be indispensable to cancer metastasis. Ultimately, sensitive CTC interrogation as described opens the doorway to identifying biological pathways and molecular targets that can be exploited in the fight against cancer.

Chapter 1
Introduction

1.1 Motivation

The coming of age of more sensitive and reproducible techniques for detection, capture and isolation of circulating tumor cells (CTCs) has led to the emergence of these rare, blood-borne cells as potential biomarkers in the prognosis and treatment of many solid tumors including breast, prostate, lung, pancreatic and colon cancers. Furthermore, through the availability of improved isolation platforms, more research avenues have opened up to explore the role of CTCs beyond rudimentary CTC enumeration, towards disease prognosis and therapeutic testing. Notwithstanding the major developments in CTC isolation platforms, CTC isolation purities have been moderate, which has ultimately led to suboptimal CTC molecular assays. The need for improved CTC isolation purities via methods that provide viable cells has been recognized. This thesis describes the development of an integrated microfluidic immunomagnetic platform that was used in the isolation and study of CTCs in pancreatic disease. Through the ultra-pure isolation of viable CTCs, the potential to perform CTC-specific molecular characterization was demonstrated, the results of which will be further presented.

1.2 Microfluidic Applications in the Study of Cancer

1.2.1 Circulating Tumor Cells in the Study of Cancer

The ability of a subset of tumor cells to disseminate from a primary tumor through the vasculature to an anatomically distant site, while still maintaining similar traits to the tumor of origin, was first reported in the nineteenth century by Ashworth.[1] Evidence suggests that tumor cell dissemination may be a result of passive shedding of tumor cells or as a result of acquired characteristics of cells through a process of epithelial to mesenchymal transition (EMT).[2, 3] These cells, which are known as circulating tumor cells, (CTCs), are believed to be responsible for the persistence and spread of cancer in many solid tumor cancers even after the resection of detectable tumors.[4] In fact, it is believed that metastasis, which is ultimately responsible for 90% of cancer-induced fatalities, initiates when primary tumor growth occurs coupled with processes of angiogenesis, alongside the transition of a small subset of tumor cells from an epithelial phenotype to a more mesenchymal-like cell. The mesenchymal-like cells, which become more motile then extravasate from the primary tumor site into the blood stream and invade a distant site, leading to the process of metastasis (see Figure1.1). [5, 6]

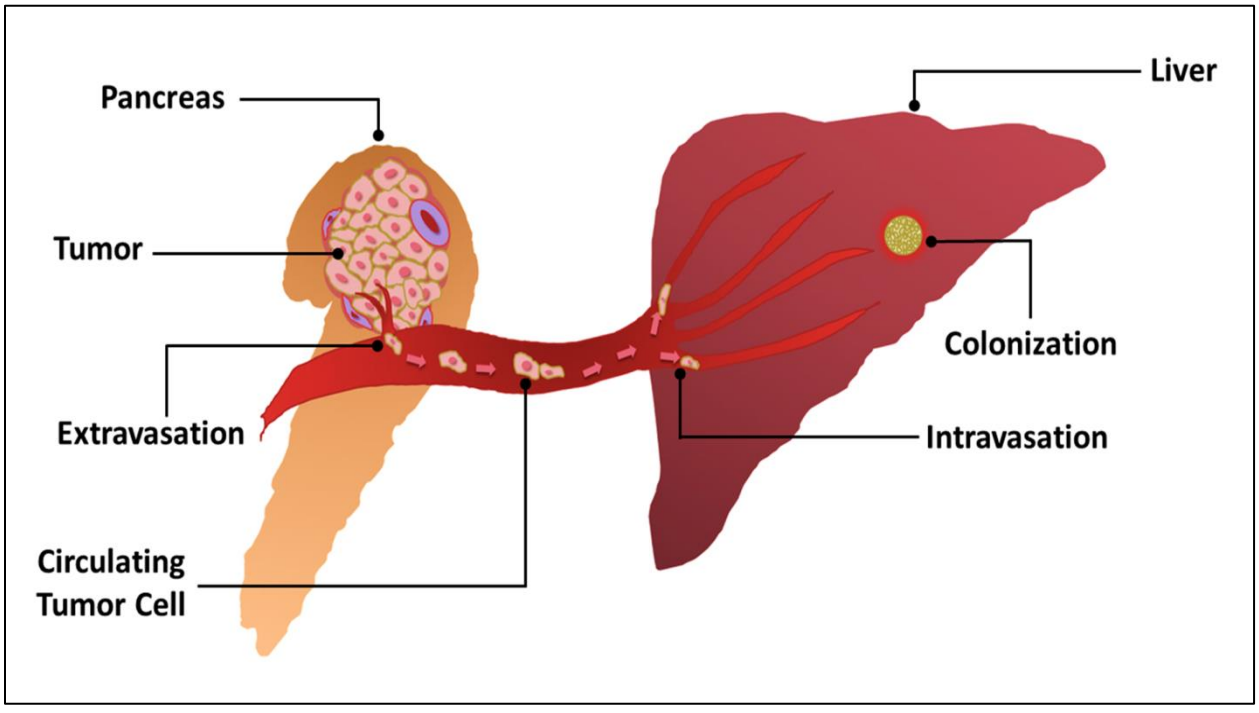

Figure 1.1: Role of CTCs in the metastatic cascade. A small fraction of tumor cells have the ability to extravasate from the primary tumor into the blood stream and then intravasate into a distal organ where there colonize the new organ in the process of metastasis.

The number of circulating tumor cells in peripheral blood is typically quite low (~1 CTC for every 10^7 blood cells), which leads to significant technical challenges in their detection and isolation from other blood components. Yet the anticipated breadth of clinically relevant information that can be harvested from these rare cells has spurred great efforts to develop sensitive platforms that help to identify, enrich and then study CTCs. As such, these efforts have resulted in routine access to CTCs from a simple blood draw and therefore represent what has been described as a liquid biopsy, since these cells originate from the tumor.[7]

Numerous platforms have been developed to isolate these rare cells, the majority of which can be categorized under immunoaffinity based methods or as approaches that exploit the distinct physical properties of CTCs compared to other blood cells (see Figure 1.2) Isolation of these cells presents a non-invasive alternative to ultimately diagnose and treat cancer. Furthermore, with the potential for real time access to CTCs via routine blood sampling during cancer treatment, a patient's response to therapy can be sensitively monitored. Overall, it can be seen that CTCs represent a potent tool in the treatment and management of cancer.

Several studies involving solid tumor malignancies such as metastatic breast, colorectal, prostate and lung cancers, have demonstrated preliminary correlations between CTC burden and clinical outcomes.[8-11] For instance, in a study using CellSearch system, (Janssen Diagnostics, Raritan, NJ) to isolate CTCs, Cristofanilli and colleagues set out to determine whether the level of CTCs in patients with metastatic breast cancer, (MBC) would yield any predictive value. Their study demonstrated that progression free survival and overall survival could be predicted independently by the level of CTCs a patient had before treatment.[8] In a follow up study involving the same cohort of MBC patients, it was found that the levels of CTCs measured in the blood were indicative of disease progression during treatment and overall survival.[9] Similarly, Moreno et al found that in a study involving patients with metastatic prostate cancer, higher levels of CTCs in a patient's blood correlated with poorer overall survival.[10] Cohen et al reported in a study of metastatic colorectal cancer (mCRC) patients, that unfavorable baseline CTC levels (>3 CTCs/7.5mL of blood) correlated with shorter progression free survival (PFS) and overall survival (OS). [11]

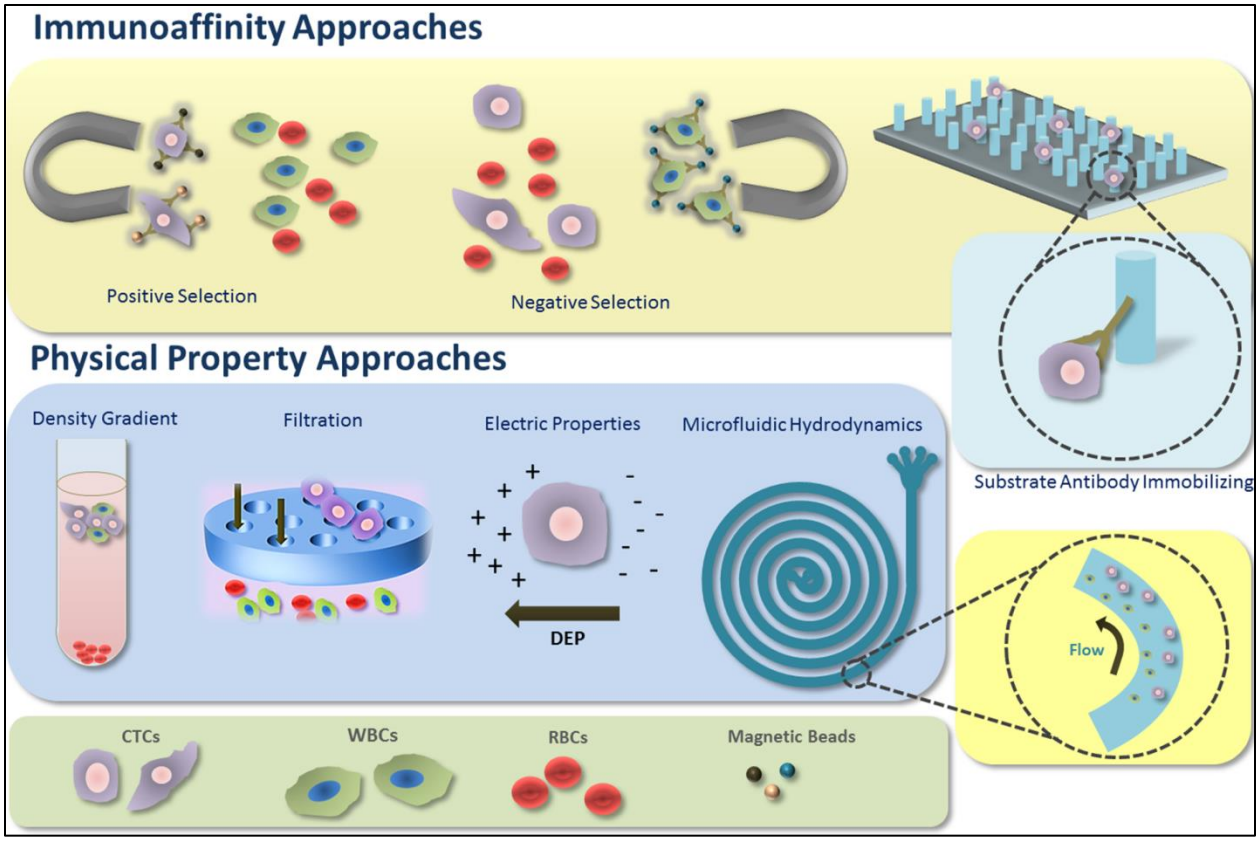

Figure 1.2: CTC isolation approaches. Methods that exploit both the physical or biochemical properties of CTCs that make them different form other blood cells are employed in their isolation.

More recently, another CTC study that involved patients with non-small-cell-lung cancer, (NSCLC) demonstrated that stage IV (more advanced) cancer patients had higher numbers of CTCs than patients with either stage IIIB or IIIA (less advanced) cancer. Furthermore, the study showed that among other indicators, CTC levels was the strongest predictor of OS and that PFS and OS were shorter for patients having ≥5 CTCs/7.5mL of blood.[12] Nesteruk et al studied CTCs in nonmetastatic patients with rectal cancer who were treated with preoperative radiotherapy. They reported that CTC detection in peripheral blood 7 days after surgery independently predicted local disease recurrence among the patients.[13] Earlier findings as such, have inspired efforts towards the development of more sensitive platforms, with higher sample processing capacities to meet the challenge of CTC enrichment, in anticipation of the clinical utility of CTC studies.

For many solid tumor cancers, evidence points to the heterogeneity among CTCs even within the same patient. For instance, differences have been observed among CTCs that are shed

from the primary tumor, tumor cells that encompass the primary tumor and tumor cells sourced from secondary metastases within the same patient. [14-16] One aspect of CTC heterogeneity is in the range of cell diameters observed, with reported sizes for breast and castrate resistant prostate cancers being 7.05-8.94μm and 15-30μm respectively.[17, 18] Using fiber-optic array scanning technology in a study of 659 breast cancer CTCs from a single patient, Marrinucci and colleagues reported that a significant extent of pleomorphism was observed among the CTCs, inclusive of the nuclear to cytoplasm ratio, and phenotypic changes associated with different stages of apoptosis.[16]

Microfluidic-based single cell CTC transcriptional analysis of breast cancer CTCs also demonstrated remarkable transcript heterogeneity when profiled for 87 cancer-associated and reference genes, compared to cell lines which showed tight transcription clustering.[19] In fact, a significant extent of heterogeneity was observed among CTCs shed from the same tumor in breast, prostate and gastrointestinal cancers.[15, 19] It is believed too, that CTCs shed from secondary metastases are responsible in part for the heterogeneity observed among the CTCs. [20, 21] Physiological changes associated with EMT may also be another source of CTC heterogeneity. While the concept of EMT still holds elements of a controversial nature, evidence points to capacity of epithelial tumor cells to progressively take on a more mesenchymal phenotype and thereby acquire greater motility, resistance to apoptosis as well as invasiveness in many epithelial cancers.[22-24]

In several cancer types, cancer stem cells (CSCs) have been studied in the context of representing a subset of CTCs of particular interest. In fact data in preclinical models suggests that CSCs may be an important component of CTCs[25]. The identification of a subpopulation of pancreatic cancer cells having CD44+CD24+ESA+ surface markers that were highly tumorigenic and demonstrated self-renewal abilities was reported by Li et al.[26] These cells which were identified as CSCs were found to comprise 0.2-0.8% of human pancreatic cancer cells and showed the capacity to give rise to differentiated progeny. CSCs were observed to play a regulatory role in signaling pathways involving sonic hedgehog and Bmi-1.[27] What makes these cells of particular interest in the study of metastasis is their resistance to standard therapies which may contribute to the malignant nature of pancreatic and other types of cancer.

In a mouse model study of circulating pancreatic cells (CPCs) that was reported by Rhim et al, cells were found to invade and enter the blood stream, even before any signs of malignancy

were detected. Interestingly, these cells demonstrated stem cell properties.[25] The study found that the CPCs seeded the liver and that invasiveness was abundant at inflammatory foci, with induced pancreatitis increasing the CPC counts.[25] While such studies point to the importance of stem cells in disease progression, more thorough studies in human samples are required to affirm the role of CSCs in CTC biology. Indeed there is data to support the clinical role that CTCs can facilitate in various forms of cancer and the relatively non-invasive means of ascertaining these rare cells make them an attractive tool in studying disease progression. With many forms of cancer, there is significant difficulty in routinely accessing tumor tissue. Moreover, understanding of the complexities involved in disease onset and progression are limited. Studying CTCs has the potential to improve our insights on disease advance and in the long run, develop tools that can effectively fight cancer in a practical manner.

1.2.2 Exploiting Microfluidic applications to isolate CTCs

The design and development of devices with micron-size dimensions proffer precise control of tiny volumes of fluids under flow, whether during processes of transporting, mixing or separation.[28] These devices, collectively known as microfluidic devices, offer many benefits when handling small entities like blood cells, which are on the same length-scale as features in these devices.[29] In fact, microfluidics represents an expansive avenue of CTC enrichment, where quite a number of technologies have been developed to isolate CTCs from blood samples under flow in devices, with features and channels on the micron scale.

In 2007 Nagrath et al reported on the feasibility of a microfluidic based method for viable CTC capture form whole blood.[30] In addition they demonstrated that this approach was more sensitive than previously used platforms, yielding higher number of CTCs. Blood samples were assessed for CTCs from patients with metastatic lung, prostate, pancreatic, breast and colon cancer using a microfluidic approach, the "CTC-Chip."[30] The platform which consists of an array of 78,000 microposts coated with EpCAM, demonstrated the ability to detect CTCs in more than 99% of patients. Patient blood sample is flowed through the device at 1mL/h and as cells expressing the EpCAM antibody encounter the EpCAM coated microposts, they become attached to the microposts. To preserve and identify CTCs, on-chip fixation and immunofluorescent staining take place subsequently. The transparent device allows for visualization of fluorescently labeled CTCs for enumeration where CTCs events are those cells that have cytokeratin and DAPI nuclear stains while they are negative for CD45.[30]

Since then, additional microfluidic platforms that incorporate immunoaffinity CTC capture have emerged. Table 1.1 summarizes some of these methods. One such platform is the "herringbone chip". It represents an advance to the CTC-chip by employing a ridged upper wall which produces micro-vortices that increase the collision frequency and therefore the chance of capture of CTCs with the EpCAM coated micro-posts.[31] Related is the establishment of the which consists of nano pillars coated with EpCAM on a silicon substrate with sinuous micron channels that give rise to enhanced mixing when flow is established. This in turn allows greater capture efficiency of microvilli and filopodia of EpCAM expressing CTCs.[32, 33] The nano-velcro chip technology has since been incorporated in an optimized version.[34] While such platforms have improved the sensitivity of CTC detection and capture, the low flow rates necessitated by these platforms are not conducive to processing appreciable volumes of patient samples for higher yields of CTC capture. Moreover, immobilizing CTCs on fixed surfaces raise problems with cell release from the surface for subsequent genomic analysis and cell based assays.

Quite a few more platforms have incorporated surface enhancement of the microfluidic chips through chemical or physical means to improve CTC capture. For example Hughes et al developed a microfluidic CTC capture device functionalized with epithelial markers and E-selectin, that was enhanced with halloysite nanotube coating. They used the device to isolate CTCs form 12 patient samples with a reported isolation range of 20-704 viable CTCs per 3.75mL of blood and purities of 18-80%.[35] Gleghorn et al developed a geometrically –enhanced differential immunocapture (GEDI) microdevice that they used to isolate prostate cancer CTCs. The device consisted of staggered obstacle arrays that could maximize how streamlines of fluid containing CTCs would interact with prostate specific membrane antigen (PSMA) coated posts, based on their size compared to other non-target blood cells. Purities of 62% were reported using this platform. [36]Adams et al reported on a high aspect ratio microchannel device containing 51 channels coated with EpCAM antibody that could detect low numbers of CTCs as the channels divide the whole blood samples into 190μL volumes for probing the samples. The channels are arranged sinusoidally and the chip was augmented with a conductivity sensor that could detect and enumerate CTCs released from the chip using trypsin. Since the CTCs could be detected without the need for staining, this makes the process more time efficient and less expensive. Recovery rates of 97% were reported with almost 100% detection rates of cancer cells with the single cell conductivity sensor.[37]

Earhart et al reported on the ongoing development of the magnetic sifter, a magnetic separation device that isolates CTCs from whole blood through immunomagnetic capture, where CTCs prelabeled with magnetic nanoparticles are temporarily captured by magnetic pores on a microfluidic chip. Blood samples are processed by mixing the nanomagnetic particles with the samples in a bulk fashion before magnetic CTC isolation using flow rates of 10mL/hr. The device is made of a dense array of magnetic pores, with 200pores/mm2 and once the magnetic field is removed, cells can be released from the pores. Six metastatic NSCLC patients were evaluated using the device and CTCs were detected in all samples ranging from 31-96 CTCs/mL.[38]

Our group recently reported on the OncoBean Chip, a microfluidic platform which exploits the velocity gradients that develop from radial flow compared to linear flow in order to enhance CTC capture from whole blood. Additionally, microposts were designed with a bean shape to enhance capture efficiency, even at a flowrate of 10mL/hr. CTCs were detected from lung, breast, and pancreatic cancer patient samples.[39]Additionally we developed a microfluidic CTC capture chip for sensitive cell capture with as little as 3-5 CTCs/mL through the use of graphene oxide (GO) nanosheets affixed to patterned gold posts. The nanosheets are functionalized with EpCAM to capture CTCs from patient samples, at a flow rate of 1mL/hr. Cancer cell recoveries of 73%±32.4 (n=10) at spike rates of 3-5cells/mL, with 100% recovery in 5 of 10 samples were demonstrated. The high sensitivity of the platform enabled CTCs to be detected even among early stage BC patients.[40]

One drawback of methods that depend solely on affinity based capture to sort CTCs, such as the use of EpCAM based approaches, is the discrepancies in the level of EpCAM or other surface antibodies that CTCs express even within the same patient sample. A few studies done among breast cancer patients have demonstrated that EpCAM expression can range from 35% to 100% among different patients.[41-44] While Went et al reported that adenocarcinomas of the pancreas showed 78% of tumors having strongly positive EpCAM expression, CTCs are believed to undergo epithelial to mesenchymal transition which may result in decreased expression of EpCAM among these circulating cancer cells.[41]

Microfluidic device technologies primarily based on the physical properties of CTCs and on size-sorting CTCs have also been reported in their successful isolation and enrichment. Table 1.2 summarizes some of these methods. One such method was reported by Lim et al in the

design of a silicon microsieve with pores to enrich CTCs from blood based on both the size and deformability of CTCs compared to other blood cells. The device was augmented with a peristaltic pump to regulate flow rate of samples with a process rate of 1mL/min. A cancer cell recovery rate of >80% was reported using this platform.[45]

Another such method, though dependent on immunoaffinity, combines selective size amplification (SSA) and multiple obstacle architecture (MOA), and has been designated SSA-MOA. This approach amplifies the size of CTCs by polymer microbead coverage through immunoaffinity, followed by applying a filter chip system to isolate the CTCs with a reported 92% tumor cell recovery rate. The platform was tested for specificity of EpCAM bead coverage with breast cancer cell lines that were either EpCAM positive (MCF-7) or negative (MDA-MB-231), the results of which showed that the polymer beads specifically bind to, and size-enhance the EpCAM positive cancer cells. The filter gaps on the filter chip ranged from 8-30μm to facilitate the heterogeneity of CTC radii. [46] Kim et al report using flow rates of 20μL/min. While the platform shows high recoveries and purities, efficiency of bead labeling in whole blood may not be as high as pre-spiked cells and therefore, the device performance with patient samples may not yield as high recoveries. Furthermore, CTCs are rare in blood and so appreciable CTC yields may necessitate high sample volumes and so higher processing rates. The relatively low flow rates and throughput of the system may limit its clinical applicability.[46]

The use of microtraps designed with a series of crescent shaped, perforated gaps that specifically trap CTCs and allow other smaller cells to squeeze through the perforations, has also been reported. This technology takes advantage of both the size and deformability differences of CTCs compared to other blood cells. CTCs can be recovered by applying a backflow of buffer to recover the cells that are not immobilized by chemical bonds, with a reported CTC recovery rate of 80%.[47] This platform allows for recovery of viable cells and allow for isolation of a wider range of CTCs irrespective of surface protein expression, compared to affinity and immune-based methods. Tan et al were able to demonstrate the applicability of the method to a range of adenocarcinomas.[48] Some of the drawbacks of this approach would be the relatively low flow rates that such an approach would require, the nonspecific capture of contaminating cells that the microtraps capture, as well loss of CTCs that occur if microtraps are already occupied along the path of a CTC through the device. Zheng et al developed a 3D microfilter device for CTC capture by incorporating 2 parylene filters through which 1mL of patient sample is processed.

The additional lower filter is supposed to support the cells and promote viability of the enriched CTCs. Recovery rates of ~86%, comparable to a 2D model previously reported, was again reported. [49]

Additionally, size dependent inertial sorting has been reported for CTC enrichment where hydrodynamic forces focus blood cells at distinct streamlines in fluid under flow, based on the diameter of the cells.[50-53] Since the different cell types in blood typically behave as spheres with unique radii characteristic of the cell type, inertial forces which are directly dependent on radii are able to separate cells at distinct streamlines along a microfluidic channel. Device outlets can be designed to collect the stream enriched for a target cell type. For instance CTCs can be separated from other blood cells using such an approach. Once again, stand-alone technologies like inertial sorting that are based on size inevitably isolate non-target blood cells that are of similar size or lose CTCs that are outside of the predicted CTC size range of the technology.

Some platforms have enhanced size-dependent inertial sorting of CTCs through device modifications that allow for more specific CTC isolation from samples under the given flow conditions. For instance, Sollier et al combined inertial size-based particle focusing with generation of on-chip micro-scale vortices to separate CTCs from patient samples in a viable and high throughout manner. They tested 4 breast cancer patients and detected 25-51 CTCs/7.5mL of blood and 8 lung cancer patients, where CTCs ranged from 23-317/7.5mL blood.[54]

Other platforms have leveraged the use of additional inertial focusing that arises from more detailed channel geometry and design. Bhagat et al developed a method they described as pinched flow couple shear-modulated inertial microfluidics for isolating CTCs from patient blood where the channels were patterned with a contraction-expansion array. This pattern allowed particles to be aligned based on their size such that CTCs would focus in the middle of the channel. They report that the device allows for 80% recovery of cancer cells. The process requires that blood be diluted to x20 and flow rates of 400μL/min were achieved using this platform.[55] Hou et al designed an inertial spiral microchannel that also exploits the predicted size of CTCs where patient blood sample flowing through the microfluidic channel gives rise to inertial forces that focus the CTCs away from other blood cells based on the radii of the CTCs and other blood components. Through introduction of curvature to the channels Dean forces arise that further focus smaller particles away from the CTCs to improve the purity of the CTCs. The method, termed Dean flow fractionation, demonstrated 85% recovery of viable CTCs in

suspension from whole blood. This label-free approach precludes the need for additional cell release from the device. Furthermore, the absence of a reliance on immunoaffinity should leads to recovery of CTCs regardless of the level of their surface marker expressions.[55, 56]

Similarly, Sun et al reported on a double spiral microchannel that allows for label free separation of CTCs from other blood components using hydrodynamic forces that arise when diluted blood under flow is driven through the microchannel. The double spiral design proved to enhance focusing of smaller blood components compared to a single spiral channels which led to improved depletion of other contaminating blood cells. To test the system, whole blood was diluted x50. A recovery rate of 88.5% of cancer cells was reported. [57]

Also Warkiani et al developed a slanted inertial microfluidic spiral chip with a trapezoidal cross-section to isolate CTCs from blood using flow rate of 1.7mL/min with isolation efficiency ranging from 80-90%. The slanted design of the channel allowed for enhanced focusing of smaller cells so that CTCs could be collected in a distinct device outlet, away from the other contaminating blood cells. [58]

Regarding isolation methods that leverage the physical properties of CTCs, it is known that CTCs express heterogeneity in size and therefore to rely on a technology that predicts a size range for CTCs will inevitably lead to losses from cells that fall outside the predicted range of CTC radius. Furthermore, it has been shown that malignant tumor cells are irregular in shape and that metastatic potential of cells is associated with changes such as increased nuclear to cytoplasmic ratio.[59, 60] The overlap of physical dimensions and properties of CTCs with leukocytes coupled with the fact that leukocytes far outnumber CTCs remain a challenge for separating CTCs from leukocytes.

Ideally, the capacity of a platform to reach both high rates of purity and yield of viable CTCs, together with high throughput, increase its desirability. With the current state of the art technology that allows for single cell manipulation for genetic profiling studies, having high number of isolated CTCs may not be as crucial as the purity rate of the CTCs. For studies that require CTC enumeration, the ability to get high CTC yields is important so as to accurately reflect the level of CTCs in patient blood.

More recently, several microfluidic platforms have incorporated a combination of both size based and immunoaffinity based approaches to develop integrated systems that improve CTC recovery, as well as purity at which CTCs are isolated from other blood cells. For instance

Ozkumur et al reported on the i-chip which is a microfluidic device that combines hydrodynamic sorting, inertial focusing and then magnetic sorting of pre-labeled CTCs from blood. The platform is amenable to both EpCAM positive selection and then negative WBC depletion using CD45 and CD15 WBC surface markers. It consists of an array of microposts with 32μm gaps for deterministic lateral displacement, used for waste cell depletion. The second component allows for additional CTC purification through inertial sorting in an asymmetrically curved channel while the third component uses immunomagnetic cell sorting. The i-chip, which operates at 8mL/hr of whole blood, demonstrates a purity rate of >0.1% purity.[61] Another integrated microfluidic approach, IsoFlux was reported by Harb et al in which CTCs are isolated through immunomagnetism. The method also allows for instant molecular assaying of the CTCs that are retrieved.[62]

Chang et al recently developed a parallel flow micro-aperture chip system that enriches CTCs by mixing samples with antibody functionalized magnetic beads, then processing the sample through an 8μm filter aperture chamber to which a magnet is attached, at the bottom of the filter system. Magnetically labeled cells are drawn through the filters to the magnets. A detection system has also been added to the device to quantify CTCs on chip. The parallel flow system allows for multiple circulation of the patient sample through the system to improve separation of CTCs from other contaminating cells. Cancer cell recovery rates of 89% were reported and CTC detection in 49/50 patients with either NSCLC or pancreatic cancer was also reported. [63]

Some level of blood cell contamination persists with the CTC isolation platforms reported. Microfluidic platforms have demonstrated significant improvements in the purity and recovery rates for tumor cells and offer the advantage of being relatively cost effective to produce. A number of platforms have reported on high throughput devices that can process patient sample in a timely manner, giving results that are reproducible. Furthermore, the devices allow for subsequent analysis and characterization of CTCs whether on chip in the case of capture platforms or in suspension with platforms that allow for substrate free CTC isolation. Indeed, as platforms continue to emerge that demonstrate greater levels of purities and yield, the increased availability of CTCs may lead to more telling studies about the process of metastasis.

Table 1.1: Immunoaffinity based CTC Isolation Methods.

Method	Enrichment (%)	Capture Efficiency	Volume	Throughput	Detection	Number of Patients	CTC Detection Summary	Reference
Immunoaffinity								
EpCAM beads with MagSweeper	51±18	62±7	9mL	9mL/hr	IF	17	100% in metastatic breast cancer patients	(Talasaz, Powell et al. 2009)
EpCAM beads with MagSweeper	--	--	9mL	9mL/hr	RT-PCR	50	70% in primary and metastatic breast cancer patients	(Powell, Talasaz et al. 2012)
EpCAM beads with Magnetic sifter	17.7±9.3	91.4%	0.9-3.3mL	10mL/hr	IF	6	100% in lung cancer patients	(Earhart, Hughes et al. 2014)
AdnaTest® BreastCancer	--	--	10mL	--	RT-PCR	42	52% in metastatic breast cancer patients	(Tewes, Aktas et al. 2009)
AdnaTest® BreastCancer	--	--	10mL	--	RT-PCR	86 70	19% in Pre surgery ovarian cancer 27% in Post Chemotherapy ovarian cancer	(Aktas, Kasimir-Bauer et al. 2011)
AdnaTest® BreastCancer	--	--	10mL	--	RT-PCR	502	19% in primary breast cancer patients	(Kasimir-Bauer, Hoffmann et al. 2012)
EpCAM microposts with CTC chip	>47	>60	0.9-5.1mL	1-2mL/hr	IF	123	99% in metastatic and early prostate cancer patients	(Nagrath, Sequist et al. 2007)
PSMA microposts with GEDI chip	68±6	85±5	1mL	1mL /hr	IF	20	90% in prostate cancer patients	(Gleghorn, Pratt et al. 2010)
EpCAM microposts in herringbone chip	14±0.1	91.8±5.2	4mL	1.5-2.5mL/hr	IF	15	93% in metastatic prostate cancer patients	(Stott, Hsu et al. 2010)
EpCAM beads / CD45, CD15 Beads with iChip	0.02-4.3	98.6±4.3	6-12	8mL/hr	IF	42	88% in metastatic cancers patients	(Ozkumur, Shah et al. 2013)
EpCAM nanopillars with Nano-Velcro chip	--	>95	1mL	1mL/hr	IF	26	77% in prostate cancer patients	(Wang, Liu et al. 2011)
Selectin with EpCAM/PSMA microtubes	66±3.9	50	7.5	4.8mL/hr	IF	14	100% in metastatic cancers patients	(Hughes, Mattison et al. 2012)
EpCAM medical guidewire	--	--	3-6L/hr	1.5-3L	IF	24	92% in breast and lung cancer patients	(Saucedo-Zeni, Mewes et al. 2012)

EpCAM bean-shaped microposts with OncoBean Chip	1060-1240WBCs/mL; 390-740 WBCs/mL	>80%	10mL/hr	1, 10mL/hr	IF	6	100% in breast (2), lung (2), pancreatic cancer patients	(Murlidhar, Zeinali et al. 2014)
EpCAM/EGFR/VMT or EpCAM/CEA magnetic beads with	10E3.6-10E4	89%	2mL/min	8mL	IF	38 12	100% in NSCLC patients 91% in pancreatic cancer patients	(Chang, Huang et al. 2015)

Table 1.2: Isolation methods based physical properties of CTCs.

Method	Enrichment	Capture Efficiency	Volume	Throughput	Detection	Number of Patients	CTC Detection Summary	Reference
Physical Properties								
Density gradient separation with Ficoll-Paque®	--	--	10mL	--	RT-PCR	58	41% in colorectal cancer	(Weitz, Kienle et al. 1998)
Density gradient /size separation with OncoQuick®	*632	87	10-30mL	--	RT-PRC	37	30% in gastrointestinal carcinoma patients	(Rosenberg, Gertler et al. 2002)
Density gradient /size separation with OncoQuick®	--	70.6	20mL	--	IF	123	24% in primary and metastatic breast cancer patients	(Muller, Riethdorf et al. 2012)
Density gradient /size separation with OncoQuick®			15mL		IF	61	23% in metastatic carcinoma patients	(Balic, Dandachi et al. 2005)
Leukapheresis with CellSearch®			4.5L		IF	29	72% of carcinoma patients	(Fischer, Niederacher et al. 2013)
Microfilter ISET® method			6mL		Cytomorph-ology	44	52% in primary liver cancer patients	(Vona, Estepa et al. 2004)
Microfilter ISET® method			7.5mL		Cytomorph-ology	60	95% of metastatic cancer patients	(Farace, Massard et al. 2011)

Microfilter ISET® method	10E7	92±14	7.5mL	225mL/hr	IF	57	89% of metastatic cancer patients	(Lin, Zheng et al. 2010)
Size/deformability with crescent microtraps	--	--	1-3mL	--	IF	5	100% in metastatic lung cancer patients	(Tan, Lakshmi et al. 2010)
Inertial size-based pinched flow device	*5.5-7.1	80%	--	1.2mL/hr	--	--	--	(Bhagat, Hou et al. 2011)
Inertial size-based microvortex device	57-94%	20.7%	7.5mL	22.5mL/hr	IF	12	100% in breast and lung cancer patients	(Sollier, Go et al. 2014)
Inertial size-based Spiral cell sorter	10%	>85%	6mL	3mL/hr	IF	20	100% in metastatic lung cancer patients	(Hou, Warkiani et al. 2013)
Inertial size-based double spiral cell sorter	*19	88.5%	--	20mL/hr	IF	--	--	(Sun, Li et al. 2012)

1.3 CTCs in the study of Pancreatic Cancer

1.3.1 Background

Over 85% of all pancreatic cancers originate in the pancreatic duct, a condition termed pancreatic ductal adenocarcinoma (PDAC).[64] To date pancreatic cancer, apart from most other cancers, has been associated, categorically, with the term "lethal" [64, 65]. This association stems from the fact that pancreatic cancer has a median survival rate of less than 6 months after diagnosis, and a bleak 5-year survival rate of 3-5 percent.[64] PDAC demonstrates a particularly aggressive biology with resistance to both conventional and targeted therapeutics so that by the time a patient receives diagnosis, the disease has already advanced to an incurable state.[64] Frequent and early dissemination of the disease coupled with ambiguous symptoms and the absence of early biomarkers for detection inevitably result in late detection.[66, 67]

Furthermore, obtaining tissue from pancreatic cancer patients has significant challenges that prevent early histological diagnosis because the pancreas has limited anatomic accessibility. The inherent difficulty in obtaining and studying tumors and their pharmacodynamic responses during clinical trials limit the ability to develop predictive information about PDAC. Indeed, the paucity of extensive, temporal studies of pancreatic tumor biology perpetuates a lack of predictive information about PDAC. In turn, lack of early and reliable screening tests are said to be responsible for the fact that 80% of patients have already reached the terminal stage at the time of diagnosis.[67] With the use of CTCs derived from PDAC patients, the hope is that they can be used as reliable biomarkers for early detection, and other clinically relevant indicators such as prognostication and therapy monitoring, among others.

Furthermore, studies have been reported that support the significance of heterogeneity among PDAC primary tumors and metastatic growths, as well as the existence of inter-tumor heterogeneity. [68-70] In an effort to identify the molecular subtypes of PDAC, Collisson et al combined transcription profiles of primary tumor samples from multiple studies as wells as profiles from human and mouse cell lines and used the data to identify three PDAC subtypes.[68] They were able to demonstrate that the three subtypes, namely classical, quasi-mesenchymal and exocrine-like had associated with them, gene signatures, clinical outcomes and therapeutic response.

Recently, proteome studies of metastasized liver, lung and peritoneum cells from a single pancreatic cancer patient were reported which were geared at understanding the extent to which genetic heterogeneity in PC affects proteomics and signaling pathways. Interestingly, cells from the three metastatic sites showed distinct patterns of proteome expression as well as tyrosine kinase activity, which in turn affected the unique sensitivity of the different sites to targeted small molecule kinase inhibitors. [70]

Taken together, these studies highlight the necessity of understanding PDAC tumor subtypes as the information gathered can potentially inform decisions that affect patient treatment and outcomes. The ability to isolate and study CTCs that contain information about these tumor subtypes, holds promise for improved understanding about how cancer metastasizes and therefore in identifying effective drug targets to manage cancer. Ultimately, CTC studies may facilitate in the development of personalized therapeutics to treat the different nuances of PDAC cases.

The advantages of access to CTCs as a "liquid biopsy" have been explored in several types of malignancies including pancreatic cancer. Pancreatic cancer is unique among other type of cancers as it is the single major cancer in which the 5 year survival rate remains in the single digits.[71] While more recent advances in imaging to diagnose pancreatic cancers, there are instances that specifically warrant biopsy procedures such as with preoperative tissue diagnosis. Moreover, biopsies are required in the recognition of rare tumors, in deciding to administer adjuvant and neo-adjuvant therapy, in disease confirmation for the purpose of counseling and in instances of diagnostic doubt, for example.[71] However, the modest results associated with biopsy techniques such as the low sensitivities, characteristic of brush cytology, and the safety concerns raised with fine needle aspiration biopsies (FNAB), have led to a diminished reliance on tissue biopsies. Indeed, with increasing studies geared towards developing reliable fingerprints of CTCs and disease prognosis and staging, CTCs hold potential for safer, less painful and less risky biopsies.

1.3.2 Isolation Approaches in Pancreatic Cancer

To date, several studies have been published describing the use of a variety of isolation strategies to detect CTCs in patients with pancreatic cancer. Here we describe studies in which 15 or more pancreatic cancer patients were enrolled in the study to determine CTC counts and or

biomarker information based on CTC analysis. Preliminary investigations into CTC counts were reported as well as limited findings on biomarkers from the CTCs, without any attempts to correlate findings to disease prognosis or survival outcomes. Table 1.3 gives a summary of these studies.

One of the earlier CTC studies was done by Allard et al in 2004 to determine the effectiveness of CellSearch in isolating CTCs from 12 major carcinomas including pancreatic cancer. The CellSearch system which allows for positive selection of EpCAM cells in circulation, employs the criterion of >5 CTCs in 7.5mL of patient blood as confirmation of CTC detection in a given sample.[7, 72, 73] Of the 16 pancreatic cancer patients examined, 37.5% showed detectable CTCs in 7.5mL of blood. The study found that pancreatic cancer had one of the lowest CTC detection rates among all the cancers tested using the platform.[7]

In a landmark study that demonstrated significant improvements upon existent methods to detect and capture CTCs with increased sensitivity and specificity, Nagrath et al reported on the use of the CTC chip to detect CTCs in 99% of 115 patient samples tested. Of the 115 patients, 15 of them were metastatic pancreatic cancer patients. They found that CTCs ranging from 9-831/mL could be detected in patient samples compared to 0 CTCs in healthy controls. The device showed a cancer cell yield of 99% and a purity rate of >47%. Additionally, temporal studies of therapy response in 3 pancreatic cancer patients treated with chemotherapy revealed that CTC numbers decreased with tumor volume.[30] The prognostic value of CTCs has been studied in a number of cancers where CTC counts have been monitored throughout the course of patient treatment to determine any associations involving treatment response.

Table 1.3 CTC Enumeration Studies in Pancreatic Cancer

Method	Detection	# of Patients	Markers	Summary	References
Density gradient separation	Nested RT-PCR	28	CK-20 mRNA	79% of patients CK-20 mRNA positive ; no significance between CK-20 mRNA levels and CEA or CA19-9 level	(Chausovsky, Luchansky et al. 1999)
EpCAM beads with CellSearch	IF	16	CK-19, CK-18, CK-8	6/16 patients with detectable CTCs	(Allard, Matera et al. 2004)
EpCAM microposts with CTC chip	IF	15	CKs	15/15 patients with detectable CTCs ranging from 9-831/mL	(Nagrath, Sequist et al. 2007)
RBC lysis before CD-45 WBC depletion	Immunocyto-chemistry	41	CK8/18, CA19-9	33/41 patients with detectable CTCs before chemotherapy and 12/41 patients 1 week after chemotherapy	(Ren, Han et al. 2011)
EpCAM beads	Nested PCR	25	CK-20, CEA, h-TERT, C-MET mRNAs	21/25 CK-20 mRNA positive ; 20/25 CEA mRNA positive ; 25/25 patients h-TERT mRNA positive , 20/25 C-MET mRNA positive	(Zhou, Hu et al. 2011)
None	Immunocyto-chemistry	18	CKs	9/18 patients with CTCs detected	(Marrinucci, Bethel et al. 2012)
Size-Based filtration with ScreenCell	Cytomorphology CA19-9 serum levels	40	CA19-9	15/27 patients with detectable CTCs. Diagnostic accuracy of CTCs was 70% compared to 85% with FNA. CTC detection sensitivity and specificity were 55.5% and 100% respectively. No statistical association with CTC detection and tumor size, metastatic status, vascular invasion, CA19-9 levels, lymph node involvement	(Iwanicki-Caron, Basile et al. 2013)

Capillary action, size-based filtration with MetaCell	Histochemistry Immunocyto-histochemistry	24	CK-18	CTCs detected in 16/24 patients; 88.9% of grade III tumor patients with detectable CTCs. Same percentage of CTCs detected in metastatic and nonmetastatic patients	(Bobek, Gurlich et al. 2014)

Table 1.4 CTCs and Prognosis in Pancreatic Cancer

Method	Detection	#of Patients	Markers	Summary	References
Density gradient separation	Immunocyto-chemistry	105	CK-19, CK-7, CK-20, AE1/AE3, glycoproteins	CTCs detected in 3/32 resectable patients, in 24/73 unresectable patients; Trend towards association between CTC detection and disease progression.	(Z'Graggen, Centeno et al. 2001)
Density gradient separation	Nested PCR	20	CEA mRNA	6/20 patients CEA mRNA-positive; 5/6 of them with disease recurrence while 2/12 CEA mRNA-negative patients with recurrence (p=0.007)	(Mataki, Takao et al. 2004)
Density gradient separation	Nested PCR	154	CK-20 mRNA	52/154 patients with detectable CTCs; CTC detection correlated with shorter overall survival (p=0.05)	(Soeth, Grigoleit et al. 2005)
RBC lysis, Density gradient separation	Compared Nested PCR to RT-qPCR	37	CK-19 mRNA	RT-qPCR detected 24/37 patients CK-19 mRNA positive before surgery. Levels decreased after surgery; trend towards association between CK-19mRNA detection and survival	(Hoffmann, Kerner et al. 2007)
EpCAM beads with CellSearch	IF	26	CK-19, C18, CK-8	CTCs detected in 11/26 patients ; CTC detection correlated with shorter overall survival (p<0.001)	(Kurihara, Itoi et al. 2008)
EpCAM beads	IF,	53	EpCAM CK-19,	ISET detected more CTCs; trend towards decreased survival for patients with CTCs	(Khoja,

with CellSearch; ISET	immunocyto-chemistry		CK-18, CK-8, CK-7, Vimentin, E-Cadherin	detected y CellSearch	Backen et al. 2012)
RBC lysis then density gradient separation	RT-qPCR	48	EpCAM mRNA	12/48 patients EpCAM mRNA positive before surgery compared to 31/48 after surgery; trend towards association between EpCAM mRNA levels and survival before surgery	(Sergeant, Roskams et al. 2011)
EpCAM/MUC-1 magnetic beads	RT-qPCR	34	EpCAM, CK-19, MUC-1, CEACAM-5, BIRC-5 mRNAs	16/34 patients with at least 1 detectable CTC mRNA ; correlation with CTC mRNAs and shorter progression free survival	(de Albuquerque, Kubisch et al. 2012)
Various	Various	623	Various markers	Meta-analysis of 268 CTC-positive and 355 CTC-negative patients with Stata 12.0; Significant association with poor PFS and CTC positive patients (p=.001). Worse OS in CTC positive versus negative patients (p<.001)	(Han, Chen et al. 2014)
CD-45 depletion, antibody microposts capture	IF	22, 3, 6	FISH (CEP-8), CK	22 pancreatic cancers, 3 borderline pseudopapillary tumors, 6 benign tumors tested; Enriched cells classified as CK+/CD45-/DAPI+/CE8=2, CK+/CD45-/DAPI+/CE8>2, CK-/CD45-/DAPI+/CE8>2, CK-/CD45-/DAPI+/CE8=2 and CK+/CD45+/DAPI+/CE8>2 or =2. Based on CTC criteria CTC counts decreased 3 days after surgery and increased 10days after surgery. CTC positive patients showed metastasis and worse OS at 1.5 years follow-up	(Zhang, Wang et al. 2015)
EpCAM beads with CellSearch	IF	79	EpCAM	CTCs detected in 5% patients before treatment and 9% patients after treatment; CTCs of LAPC patients assessed before and 2 months after chemotherapy; CTC detection associated with poor tumor differentiation (p=0.04) and shorter OS (p=0.01)	(Bidard, Huguet et al. 2013)
cell capture with collagen adhesion matrix	DNA microarray analysis	50	Gene Expression	Prospective clinical trial with advanced PDAC patients; Chemotherapy regimens predicted as effective using previous PGx model provided clinical benefit compared to those predicted as ineffective with respect to PFS (10.4 mo vs 3.6 mo , p<0.0001) and OS (17.2 mo vs 8.3 mo, p=0.0249)	(Yu, Ricigliano et al. 2014)

Ren et al performed a similar study among 41 advanced pancreatic cancer samples from patients who were previously untreated. Through CTC enrichment via immunomagnetic negative depletion of leukocytes from patient samples, the team examined the effect of the chemotherapy agent 5-fluorouracil on CTC counts as well as on expression levels CA 19-9, a sensitive pancreatic cancer marker. The study found that after the first cycle of chemotherapy, the percentage of patients with >2 detectable CTCs dropped from 80.5% (range of 0-59) before treatment, to 29.3% (range of 0-40) after 7 days of treatment. Among advanced cancer patients, they also found that apoptotic CTCs could be observed after chemotherapy, and may be indicative of chemotherapy efficacy in patients. Additionally, the appearance of granular, bubble-like CTC morphologies with CA19-9 and CK8/18 staining were observed, which the study reported could be reflective of apoptosis.[74] The use of negative depletion sought to decrease the chances of losing CTCs through targeted antibody labeling of CTCs.

Decreasing the probability of CTC loss by lysing unwanted RBCs and then distinguishing among nucleated cells to identify CTCs is another CTC enrichment strategy. Using what they described as fluid phase biopsy, Marrinucci and colleagues reported on developing a CTC isolation approach that is label free, requiring no surface-protein based enrichment and so allows a wider range of CTCs to be identified regardless of their surface protein expression. The protocol involves lysis of blood samples and subsequent collection and immunofluorescent staining for the remaining nucleated cells followed by CTC detection using fiber-optic array scanning technology. (FAST) They analyzed blood samples from 18 pancreatic cancer patients and were able to identify CTCs in 50% of patients. [75, 76]

Developing platforms that make viable CTCs available, which can later be cultured or gene profiled for example, has been a topic of interest for some time. In one study, 24 pancreatic cancer patients were enlisted to evaluate the performance of the CTC isolation platform MetaCell and to subsequently attempt CTC cultivation on the filter. Of the 24 samples tested, CTCs were detected in 16 patients. The study showed that 88.9% of patients with grade III tumors had detectable CTC levels.[77]

One of the anticipated clinical uses of CTCs is as a non-invasive diagnostic tool for cancerous lesions. In 2013 Iwanicki-Caron et al reported on a study done with 40 PDAC patients to determine the usefulness of CTC detection from blood compared to conventional use of endoscopic ultrasound-guided fine needle aspiration (EUS-FNA) as a first diagnostic procedure.

The ScreenCell platform was used to detect CTCs in 10mL of peripheral blood. Interestingly, the study found that CTC detection had a 70% diagnostic accuracy compared to 85% for EUS-FNA. The conclusion was made that CTC detection could be used as a first-line diagnostic procedure, with the aim of avoiding the invasive EUS-FNA procedure in about 50% of patients that present with a solid mass in their pancreas in need of a tissue diagnosis.[78] Despite the fact that CTCs are yet to be proven as a biomarker for decision making among oncologists, such studies point to their potential clinical usefulness as well as the urgency to understand the extent to which they can be used.

A spectrum of studies has been carried out on PDAC derived CTCs, from attempts to determine the technical feasibility of isolating them to preclinical studies to determine their clinical potential. However, robust studies that allow clinicians and other scientists to draw any impactful conclusions are yet to be reported. Before CTCs can be used as a routine tool in treating patients with pancreatic disease, more extensive, multicenter, prospective randomized trials need to be conducted on human samples to establish metrics that can be used based on CTCs. Standardized protocols and objective data analysis need to be deployed that encompass the multiple forms and presentations of PDAC.

1.3.3 Molecular Technologies to Assess CTCs

Once CTCs have been isolated, sensitive and reproducible assessment of cells is integral to the clinical impact they can have. Moreover, the platforms used to enrich CTCs determine both the downstream assessment methods that can be used as well as the specificity with which CTCs can be evaluated. The caveats associated with various platforms can impact upon the subset of CTCs that are isolated and thereupon, information that CTC assessments give. In light of the inherent differences among the various platforms when it comes to CTC enrichment, rigorous characterization of each platform to determine recovery and purity rates, as well as false positive expectations will be useful in pooling data among CTC studies in PDAC. Assessments of CTCs at both the cellular and molecular level have taken several directions some of which are further discussed.

<u>Protein Expression:</u>

So far, one of the more standard approaches of CTC evaluation is immunostaining to identify proteins that characterize putative CTCs. As described by the FDA approved CellSearch® system, protein expression patterns of CTCs include a positive stain for cytokeratins, (CKs) combined with a positive stain for nuclear content using DAPI, and negative staining for CD45 expression, which is a putative leukocyte surface protein. These three criteria are the bare minimum criteria for CTC identification through immunofluorescence (IF). Therefore, the availability of three fluorescent channels with distinct spectral ranges is required to image and confirm CTCs with immunofluorescence techniques.[8-11, 79] Additionally, protein immunostains that are specific to solid tumor malignancies have been used to further corroborate the presence CTCs in peripheral patient blood. For instance several studies have incorporated protein immunostains for PSA and PSMA which are specific to prostate cancer.[80-82] Moreover, CTCs have been assessed for protein expression of clinically relevant proteins, such as HER2 which has important implications about therapy selection. [83-85]

Protein expression assessment has also been leveraged in a number of studies to support the existence of distinct subset of populations of tumor cells within a given patient sample. For instance, Theodoropoulos and colleagues reported on the use of triple marker IF to assess stem cell marker expression of CD44, CD24 and ALDH1 in metastatic breast cancer, (MBC) CTCs. Results from the study supported the existence of stem cell-like CTC subpopulations in the peripheral blood of MBC patients.[86] Similar studies have been carried out for other EMT and stem cell marker expression in CTCs in attempts to deepen what is known about the existence and role of certain tumor cell populations in cancer metastasis.[87-89]

Proteins shed, secreted or released from CTCs have also been used to detect viable CTCs in patients using the ELISPOT assay and to study CTC protein expression patterns that may be relevant to metastatic disease.[90, 91] Additionally, Alix-Panabieres reported on evaluating the release of CK-19 and mucin-1 to detect viable CTCs in breast cancer patients as well as the secretion of fibroblast growth factor, FGF2, a stem cell growth in prostate cancer CTCs.[21]

Assessment of CTC protein expression has been useful to date in characterizing patient CTCs beyond simple enumeration however, the presence of contaminating cells with current CTC isolation platforms can produce RT-PCR results that are not specific to CTCs. Distinguishing the signals specific to CTCs only, represents a technical challenge. Furthermore,

with IF techniques that necessitate distinct fluorescent channels for IF imaging, there is a limit to the number of proteins that can be detected per sample.

RNA, DNA, FISH

The availability of CTCs with relatively high purity rates from microfluidic platforms and other technologies have opened up many possibilities for interrogating CTC genetic material at the DNA and mRNA levels. Specifically, genetic mutations and aberrations that are associated with patient outcomes and their response to therapy have been uncovered. Such findings can ultimately enable clinicians to make better decisions about patient treatment regimens. For instance CTCs captured using an EpCAM based microfluidic platform from patients with NSCLC were studied for EGFR mutations which have been implicated in drug resistance to EGFR targeted therapies.[92] DNA was recovered from CTCs using allele specific polymer chain reaction (PCR) amplification, and EGFR mutational analysis was performed on the CTCs alongside matched plasma DNA as well as primary tumor DNA. The study found that the T790M mutation, which is responsible for drug resistance was detected in CTCs of patients who had received drug therapy. Moreover, serial CTC analysis revealed additional EGFR mutations in some cases where tumor progression was observed.[92]

Established gene expression technologies and protocols have also been applied to CTCs to determine whether any information of diagnostic or prognostic value could be yielded. In one study, RT PCR was used to detect prostate specific antigen, (PSA) mRNA among 122 men with androgen-independent prostatic carcinoma (AIPC) in order to investigate whether mRNA detection could be used as a cancer specific biomarker. Interestingly, the study showed a significant correlation between mRNA detection and decreased survival. PSA detection based on RT PCR was also found to be independent of, and of higher quality than serum PSA.[93] In a related study, real time RT PCR of localized or castration-refractory prostate cancer CTCs revealed close associations with detection of KLK mRNAs and survival.[94]

Moreover, Aktas and colleagues used multiplex RT-PCR to study patterns of expression of EMT markers (Twist1, Akt2, PIK3α) and the stem cell marker, ALDH in CTCs from breast cancer patients.[95] Similar studies have been done to evaluate the expression of genes hat have been deemed important in clinical decision making, such as HER2, estrogen receptor, (ER) and progesterone receptor (PR).[96-98] Notably, RNA sequencing has been integral in revealing pathways implicated in cancer metastasis. In attempts to establish the genomic signatures of

pancreatic cancer CTCs, Yu et al used a pancreatic cancer mouse model to capture mouse CTCs and performed single molecule RNA sequencing, which identified Wnt2 as an enriched gene in pancreatic cancer CTCs.[99] These findings were corroborated in 5 out of 11 patients with pancreatic cancer. The study found that WNT2 expression in cells suppresses anoikis and increases metastatic capacity in vivo. Sphere formation was also enhanced with WNT2 expression.[99]

Ting et al reported on a mouse model study that compared genome-wide expression profiles of CTCs with their corresponding primary tumors. CTC isolation was performed using an epitope free approach in order to isolate CTCs independent of their surface marker expressions. Single cell RNA sequencing was performed on the CTCs, revealing that CTCs showed lower proliferative signatures and high gene expression for ALDH1a2 which is a stem cell associated marker, compared to primary tumor cells and tumor derived cell lines. CTCs also demonstrated biphenotypic expression of both epithelial and mesenchymal markers as well as lgfbp5, a gene associated with the epithelial stromal interface. The study also showed that CTCs from both mouse and human origin demonstrated high expression of stromal derived extracellular matrix proteins, which may contribute to signals that enhance the spread of cancer.[100]

The prevalence of somatic alterations to gene copy number, associated with many solid tumor malignancies, has garnered a lot of interest as they can potentially be used as cancer biomarkers associated with important clinical outcomes. Fluorescence in-situ hybridization (FISH) provides a rigorous platform to identify these types of alterations. For instance, through the use of FISH, HER2 genomic alterations have been observed in CTCs isolated from breast cancer patients that were not in accordance with the HER2 status of primary tumors.[101] Similarly, a multi FISH assay was used to confirm the amplification of the androgen receptor (AR) locus and increased androgen signaling observed among late-stage prostate cancer patients using a multi-color FISH assay.[102]

More recently, the use of FISH to monitor genomic alterations during therapy has been reported. Using FISH, gene amplification of EGFR in CTCs from NSCLC patients was monitored during tyrosine kinase inhibitor-based therapy. Of the 20 patients monitored, 5 of them showed EGFR amplification, occurring within 85%-100% of EpCAM positive cells.[103] Interestingly, FISH was used in a dual colorimetric quantitative fluorescence assay of RNA to

detect epithelial (CK 5, 7, 8, 18 and 19; EpCAM; cadherin-1) and mesenchymal (fibronectin-1; cadherin-2; serpin peptidase inhibitor, clade E) transcripts from MBC patients. Quantification of RNA-ISH, among other assays, supported the EMT evidence in BC CTCs and the association of mesenchymal markers expression with CTC clusters versus single CTCs. [104]

While there is promise in the clinical relevance of genomic aberrations observed in CTCs, FISH analysis of CTCs still needs to be fully validated before the information can be used routinely in a clinical setting. Furthermore there is still a lot that needs to be understood regarding FISH analysis of PDAC derived CTCs, and in the clinical impact that such analyses may demonstrate in the of treatment PDAC.

Single Cell Analysis:

To circumvent the issues associated with leukocyte or other blood cell contamination of isolated CTCs, and to better understand the heterogeneity that exists among distinct CTCs, several studies have implemented single cell CTC analysis. [15, 19, 105-108] Using some of the commercially available cancer panel amplification platforms such as those provided by TruSeq® Amplicon (Illumina, San Diego, CA) as well as Ion Torrent AmpliSeqTM (Life Technologies, Carlsbad, CA), CTC DNA can be amplified and then genotyped or sequenced to identify genetic mutations and other genomic aberrations.

One of the first reported studies of single cell CTC analysis utilized a PCR based approach to analyze EpCAM or CK positive cells from the bone marrow of cancer patients. These cells may be latent and are thought to play a role in early cancer dissemination. Through the use of comparative genomic hybridization (CGH), genomic aberrations were used to identify cancer cells, among which, extracellular metalloproteinase inducer (EMMPRIN) had one of the highest protein expression rates. [15, 109]

CTC single-cell analysis has been leveraged to determine the extent and nature of mutational heterogeneity among CTCs from the same patient sample. A clinical study which involved EGFR gene amplification and sequencing for KRAS (v-Ki-ras2 Kirsten rat sarcoma viral oncogene homolog), BRAF (v-raf murine sarcoma viral oncogene homolog B1), and PIK3CA (phosphatidylinositol-4,5-bisphosphate 3-kinase, catalytic subunit α) mutations in CTCs enriched from colorectal cancer patients showed that EGFR protein expression varied from CTC to CTC from a single patient. Interestingly, one patient had 2 different PIK3CA mutations in 2 separate CTCs. Of the 44 single CTCs interrogated, no genetic mutations were

detected for BRAF from any patient. PIK3CA mutations were observed in 14 of 36 CTCs from 4 patients while 5 out of 15 patients from a single patient showed KRAS mutations.[110]

To facilitate single cell analysis of CTCs, microfluidic based platforms have been customized to collect and analyze very small amounts of genetic material from single cells. Patterns of gene expression among CTCs can be implicit of putative biological processes that lead to metastasis such as EMT. Using a microfluidics based PCR platform, 38 prostate cancer CTCs sourced from 8 patients were used to study gene expression patterns of 84 genes associated with EMT. Several of the genes associated with a mesenchymal transition, and therefore invasiveness were expressed in the CTCs, though at varied extents and combinations. Of note, the study showed detection of a few genes frequently expressed in cells unique to castration resistant patients compared to castration sensitive cases.[108]

Apart from DNA and genomic studies, single cell analysis has also been used to extract information about active gene transcription and gene expression changes through single CTC mRNA sequencing. Smart-Seq, a single cell mRNA sequencing platform, was used to carryout transcriptome analysis wherein 9 transcripts of membrane proteins specific to melanoma derived CTCs, that were mostly absent in primary melanocytes or immune cells, were identified. Interestingly, there was loss of expression of epithelial cadherin (CDH1) in CTCs, which is associated with increased proliferation and invasiveness, and ultimately cancer spread.[106] Additionally, because of the improved read coverage of the Smart-Seq platform, preliminary studies on single nucleotide polymorphisms of the CTCs were carried out, which revealed thousands of genetic sites with alternative alleles in at least 2 CTCs.[106]

As technologies become more sensitive with improved reading accuracy as well as multiplexing capabilities, the requirements for increased data processing and interpretation of bioinformatics are commensurate. The investments and costs associated with data processing can be a limiting factor. Additionally, there are requirements to determine what genetic information is clinically relevant, and to decipher to what extent some of the observed data can inform clinical outcomes. Another caveat associated specifically with the current technologies for single cell analysis are concerns about amplification errors that are inherent to the high degree of amplification required for propagating information from genetic material of a single cell. Furthermore, there is a need to standardize protocols across studies so that data can be exchanged and compared objectively.

1.3.4 Clinical Utility of CTCs in Management of Pancreatic Cancer

CTCs and Cancer Detection:

The early dissemination of pancreatic cancer, apart from its resistance to targeted therapeutics is thought to be responsible for the particularly aggressive nature of PDAC.[64] While there have been advances in early detection of other cancers such as breast and other cancers, there are currently no reported effective methods for early detection of PDAC. [111]

Klapman et al discussed methods for early screening and detection of pancreatic cancer and detailed the screening program enforced at their respective institute.[111] Criteria for screening patients are limited to those with a high risk of developing the disease based upon factors such as hereditary pancreatic cancer syndrome, familial breast cancer syndrome and familial atypical multiple mole melanoma syndrome. Yet, hereditary and familial factors only account for 10% of pancreatic cancer patients. They concluded that more robust, non-hereditary risk factors need to be established to identify those who will benefit from screening. They also stated that more cost effective, less invasive methods should be developed to use in patient screening.[111]

In a recent study using a genetic mouse model of PDAC, Rhim et al reported on detection of circulating pancreas cells, (CPCs) in the bloodstream of mice even before any tumor could be seen in the mice.[23] Using a Cre-lox-based PDAC mouse model, a RosaYFP allele was introduced to specifically and efficiently label cells originating from the pancreas. Using this lineage tracer, YFP cells were observed in circulation of mutant mice before the detection of invasive cancer. Moreover, through Zeb1 immunostaining and qPCR, EMT cells were identified in mice with premalignant lesions. This data is suggestive of the role of EMT in early disease onset in PDAC. Since EMT is associated with the loss of epithelial phenotype among CTCs, including a decrease in EpCAM expression, EpCAM based technologies with lower sensitivities may prove less efficient in detecting CTCs in pancreatic cancer.

Moreover, Rhim and colleagues, further substantiated the possibility of using CTCs as a biomarker for early detection of pancreatic cancer, before it reaches an invasive stage, in an additional report. Patients with cystic tumor of the pancreas who are at increased risk for the subsequent development of pancreatic cancer and who routinely undergo surveillance in the clinic were studied. Of the 21 patients that had no clinical diagnosis of cancer but had cystic lesions of the pancreas, 3 or more CPCs/mL was detected in the blood of 7 of the patients. Eight

of the 11 patients with confirmed PDAC had 3 or more cells/mL while no CPCs were detected in healthy patients. Since the study suggested the presence of these circulating cancer cells in patients before tumor formation, at the early stages of disease, the authors propose the detection of these cells for risk management in early disease settings. A larger clinical trial to validate these results is currently underway.[25]

Zhou and others proposed the use of CTCs as an early detection platform for pancreatic cancer by examining the RT-PCR expression levels of h-TERT, CK20, CEA and C-MET in circulating cancer cells for 25 patients.[112] Immuno-magnetic particles were used for cancer cell enrichment and the study found that there was a significant difference in the positive expression of the 4 genes. The positive expression rates for h-TERT, CK20, CEA and C-MET were 80%, 100%, 84% and 80% respectively. The study also found that positive expression of C-MET, CK20 and CEA correlated well with tumor stage.[112]

CTCs and Prognosis in Pancreatic Cancer

With respect to pancreatic cancer, in establishing the clinical utility of CTCs, the need for more robust prospective randomized studies becomes apparent. Several studies aimed at evaluating the prognostic value PDAC derived CTCs have been reported (see Table 1.4). Such reports have gone further in establishing the clinical relevance of CTCs by monitoring patients through their clinical course and investigating how CTCs could yield prognostic information They represent a step towards understanding how CTC detection in pancreatic disease can ultimately be used in disease monitoring and treatment.

In order to evaluate whether cancer cells detected in bone marrow aspirates are indicative of micro metastases or give rise to cells in circulation, Z'graggen et al developed an immunocytochemical assay to detect tumor cells in blood and bone marrow. The study enlisted 105 pancreatic cancer patients and 66 control patients and CTCs were isolated using a density separation medium, Nycoprep (Accurate Chemical & Scientific Corporation, Westbury, NY). Tumor cell counts were compared with disease stage, and survival analysis was performed using a multivariate Cox regression. Tumor cells were detected in 26% of blood samples and in 24% of bone marrow specimens. Interestingly, it was seen that tumor cell prevalence increased with tumor stage in blood samples unlike with bone marrow samples (P=0.52). Tumor cell prevalence in blood also correlated with resectability (P=0.02), disease progression, (P=0.08) and with peritoneal dissemination (P=0.003). [113]

Since CTC levels have demonstrated correlations with disease prognosis among several other solid tumor cancers, their potential as a similar biomarker in PDAC would prove quite beneficial, given the inaccessible position of the pancreas to do routine tissue sampling. In an early study involving 26 pancreatic cancer patients Kurihara et al set out to see if CTCs levels, as isolated by CellSearch, could be used for predicting survival in pancreatic cancer. Eleven patients with chronic pancreatitis and 10 healthy volunteers were enlisted. The study showed that 42% of patients had detectable CTCs in 7.5mLs of blood while those with benign conditions showed no CTCs. Among the 15 patients with CTCs, this group demonstrated a median survival time of 110.5 days while the 11 patients with no detectable CTCs showed a median survival time (MST) of 375.8 days ($P<0.001$). For the 14 patients that were at an advanced stage, IVb, the MST of those with and without detectable CTCs were 52.5 and 308.3 days respectively ($P<0.01$).[114]

Given the interest in enumerating CTCs, questions arise about the sensitivity and isolation yields among the commercially available platforms. Khoja et al reported on a pilot study done in 2012 to compare two CTC enumeration and detection platforms across pancreatic cancer blood samples, obtained from 54 patients. They compared CTC numbers using CellSearch, the only FDA approved diagnostic platform for CTCs, with isolation by size of epithelial tumor cells (ISET) technology. ISET detected CTCs in 93% of patients while CellSearch detected CTCs in 40% of patients. Khoja et al report that among the patients with detectable pancreatic CTCs, burden of disease and performance status correlated with CTC numbers as measured by CellSearch.[115]

In efforts to assess the prognostic value of CTC levels in patients with pancreatic cancer Han et al carried out a meta-analysis of previously reported studies.[116] Using an extensive literature search for relevant studies done up to July 2013, the meta-analysis incorporated 9 cohort studies which included 623 pancreatic cancer patients, 268 of which were positive for CTC, and 355 negative. The analysis found that patients who had CTCs were significantly associated with poor progression free survival ($HR=1.89$, 95% $CI=1.25-4.00$, $P<0.001$) and worse overall survival compared to those patients in whom CTCs could not be detected, regardless of platform used.[116]

Detection of CTCs with tumor-associated antigens has garnered significant interest since the presence of these proteins on cells support the tumor origin of CTCs. Soeth et al reported on

a prospective study that investigated the diagnostic potential of Cytokeratin 20 (Ck-20) in detecting disseminated tumor cells (DTCs) in bone marrow and blood samples of patients with PDAC.[117] The study, which involved 172 PDAC patients, also looked at the prognostic value for overall survival. Bone marrow samples and venous blood obtained preoperatively were analyzed using nested CK-20 RT-PCR. The study reported that 47.1% of patients had detectable CTCs with detection rates of 33.3% in bone marrow and 33.8% in blood samples based on CK-20 positivity. Using the Kaplan Meier univariate survival analysis, a statistically significant relationship was observed between overall survival and the radicality of the operation ($P<0.0001$), tumor stage, ($P<0.0011$) and DTC detection in bone marrow and/or blood. [117]

Similarly, Hoffman et al reported on a study that evaluated the diagnostic value of cytokeratin 19 (CK-19) mRNA for CTC detection in blood, peritoneal fluid and bone marrow involving. The study which included 37 pancreatic cancer patients, 16 patients with chronic pancreatitis and 15 patients with benign disease, also sought to distinguish between pancreatitis and pancreatic cancer based on the data obtained. Nested PCR and fluorogenic RT-PCR were used to analyze blood samples that were taken preoperatively, intraoperatively, and postoperatively, as well as bone marrow aspirate and lavage taken preoperatively. CTCs were detected in 15 patients. Results showed that 64% of blood samples from pancreatic cancer patients had elevated CK-19 expression while 30% of lavage samples from cancer patients showed elevated CK-19 levels. A trend towards shorter survival was observed in cancer patients with at least 1 CK-19 positive sample. The study also found that tumor cell detection rate correlated well with disease stage and differentiation in peritoneal lavage.[118]

Multiplexing genes and using multiple cancer specific biomarkers in CTC detection allow more robust confirmation of CTCs, as well as more detailed CTC characterization. A few studies reported on such rigorous methods of CTC detection and the related clinical implications. For instance, De Albuquerque et al developed an immunomagnetic/real time reverse transcript polymerase chain reaction (RT-PCR) assay and assessed its clinical value for detecting CTCs in 34 pancreatic cancer patients. The assessment was done before systemic therapy. CTCs were enriched through the use of immunomagnetic capture with Dynabeads magnetic microbeads, (Invitrogen), coupled to BM7 and VU1D9 antibodies, which target mucin 1 and EpCAM respectively. Real-time RT-PCR analysis of KRT 19, MUC1, EPCAM, CEACAM and BIRC genes was also carried out. The study showed that shorter progression free survival (PFS) was

observed for patients with detectable CTCs before treatment compared to patients having no CTCs before treatment. Using a log-rank test (P=0.01) it was seen that patients with positive CTC detection showed a median progression free survival time of 66 days (95% CI=44.8-87.2) while patients having no detectable CTCs had approximately double the median PFS of 138 days (95% CI= 124.1-151.9). Additionally, correlations were seen between tumor grading and CTC detection rates.[119]

In addition to CTC gene analysis, genomic studies have also been used to detect CTCs arguably with more specificity. Zhang et al reported on one such study where fluorescence in situ hybridization of the chromosome 8, (CEP8) centromere was used to enumerate CTCs. Additionally, patterns of CTC immunostaining with CEP8, CK and CD45, were used for CTC detection in the study which involved 22 pancreatic cancers, 3 borderline pancreatic solid pseudopapillary tumors, 6 pancreatic benign tumors and 30 healthy individuals.[120] CTCs were isolated by negative depletion of white blood cells with CD45 antibodies. Dynamic monitoring of pancreatic patients was performed and the study reported that CTC detection had a sensitivity rate and a specificity of 68.18% and 94.87% respectively. Moreover, they found that CTC counts decreased 3 days after surgery but increased 10 days after surgery in most patients, and patients with increased numbers of CTCs showed enhanced rates of metastasis and worse survival rates at the 1.5 year follow-up.[120]

Many of the reported trends and associations of PDAC CTCs with clinical outcomes are for a heterogeneous collection of CTCs. These data support the eventual use of CTCs to inform clinical decision. With the availability of single cell resolution analysis, studies similar to those reported for other cancer types can be applied to pancreatic CTCs, to better characterize the distinct components that are involved in disease spread. This understanding can potentially facilitate the development of more potent and strategic therapy regimens.

CTCs and therapy monitoring

The relative ease with which CTCs can be obtained and the development of increasingly sensitive and time efficient isolation platforms enable the use of CTCs in real time, routine biopsies. In this vein, CTC detection rates and prognostic value were studied in a prospective cohort of locally advanced pancreatic carcinoma (LAPC) patients by Bidard et al using a subgroup of 79 patients from an LAP07 international center randomized study.[121] The study evaluated whether CTC counts assessed before the start of chemotherapy and after 2 months of

chemotherapy treatment correlated with patient characteristics and survival. To be recruited for the study, patients had to be de novo histologically confirmed stage III LAPC as per UICC classification, without consideration for curative resection, and with a performance status of 0-2, among several other clinical indicators. The treatment course involved an initial random assignment of gemcitabine alone or in combination with erlotinib for 4 months. After 4 months patients with controlled disease were randomly assigned either gemcitabine again or radiation therapy alongside capecitabine. Patients initially assigned erlotinib continued after 4-month phase except when receiving radiation therapy. The study found that CTC detection was associated with poor tumor differentiation (P=0.04) and with shorter overall survival.[121]

In a study that investigated whether pharmacogenomics (PGx) profiling of CTCs from unresectable PDAC patients could predict tumor response, progression and resistance, Yu et al enlisted 50 advanced or locally advanced patients in a prospective preclinical trial. Using single agent response data, a number of chemotherapy agents were profiled including FOLFIRINOX (5-FU, irinotecan, and oxaliplatin), FOLFOX (5-FU and oxaliplatin), Gem-nab (gemcitabine + nab-paclitaxel), Gem-Ox (gemcitabine + oxaliplatin), Gem-Cap (gemcitabine + capecitabine), and GTX (gemcitabine, docetaxel, and capecitabine). [122] Of the 35 patients that were deemed evaluable, analysis of the patients CTCs showed good correlation between PGx predictions of effectiveness of chemotherapy regimens. Specifically, the study showed clinical benefit such as progression free survival, was observed in participants treated with chemotherapy regimens that were predicted to be effective, compared to regimes predicted to be ineffective. These results demonstrate the applicability of CTCs in determining the suitability of chemo regimens to unique patient groups.

Taken together, these preliminary results demonstrate the possibility of CTC biopsies to influence important clinical decisions. Specifically, they underscore the feasibility of using CTCs to predict and monitor patient response to therapies, and the effect of treatment regimens on patient outcomes.

CTC Culture for Therapeutic Drug testing

Attempts have been made to culture CTCs, a foreseeable benefit of which is to generate a replenishable source of these aberrant cells, particularly for therapeutic drug testing. Recently, Yu and colleagues reported on the ex-vivo expansion of EGFR positive breast CTCs in the establishment of 5 CTC cell lines. The cultured CTCs were used to test the effect of standard

clinical regimens as well as targeted drugs as standalone agents or in combination, across the 5 different CTC lines. Studies show that for each cell line, specific drugs were effective based on the genetic mutations that were unique to each cell line. For instance with the BRx-07 cell line, which harbored newly acquired activating mutations in both PIK3CA and FGFR2, the CTCs were very sensitive to the PIK3CA inhibitor BYL719 and the FGFR2 inhibitor AZD4547. Cooperative effects were also observed using combined inhibition of both PIK3CA and FGFR2.[123]

Particularly with early stage cancer patients where CTCs detection rates are typically low, the ability to culture CTCs may provide increased opportunities for molecular characterization and therapeutic testing of CTCs. Our group recently reported on the successful use of pancreatic cancer associated fibroblasts (CAFs) in establishing a 3D co-culture platform to culture early stage CTCs form lung cancer patients. From the CTCs that were cultured in 14 of 19 early stage patients, next generation sequencing (NGS) analysis revealed a number of matched, cancer related mutations between primary tumors and CTCs.[124]

Indeed, these studies show the potential to develop similar platforms that can be customized to explore pancreatic CTC ex vivo drug testing. With the ultimate goal of personalized treatment in mind, future development of such studies can involve detailed genomic analysis of patient tumors to compare the signature of the primary tumor and CTCs in actual patients with expanded CTCs.

CTCs and Xenotransplantation models

Mouse models of pancreatic cancer have allowed for in vivo studies of genetic alterations and other molecular studies that are pertinent to metastasis and the resistant nature of pancreatic cancer. Additionally, they have enabled in vivo CTC studies and access to mouse pancreatic CTCs. Recently, Torphy et al developed patient derived xenograft (PDX) mouse models to study whether CTC burden could be used as a facile biomarker of treatment response in PDAC.[125] Using an orally administered therapeutic agent BKM120, which acts to inhibit phosphatidylinositol-3-kinase, EpCAM positive CTCs were isolated and enumerated to determine CTC burden. A vehicle was used as a negative control and PDX mice were given treatment for 28 days. The study showed that CTC counts had a significant reduction in the BKM120 group after treatment, (26.61 to 2.21 CTCs/250uL, p=0.0207), while the decrease in CTCs from vehicle group was not significant (23.26 to 11.89 CTCs/250uL, p=0.8081). Tumor

growth inhibition correlated with CTC burden and with occurrence of sequenced CTC KRAS G12V mutations, which matched the respective tumors.

The studies described demonstrate the potential and functionality of CTCs in managing cancer. Microfluidic technologies have been pivotal in CTC detection and isolation in a viable manner. As a result, sensitive molecular characterization of CTCs as well as CTC culturing have enabled studies that have enhanced our understanding of mechanisms thought to be important to the invasive metastasis cascade. Additionally next generation sequencing has facilitated genomic characterization of mutations that are potentially relevant to gene therapy. As our understanding of metastasis evolves, development of more effective therapies to treat pancreatic disease is anticipated.

1.3.5 Comparison of CTCs versus circulating cell free DNA

The portion of DNA that is thought to be derived specifically from tumors, and not bound to leukocytes or erythrocytes, and therefore circulates freely in the plasma has been designated circulating free DNA (cfDNA).[126-128] Analysis of cfDNA, released from tumor cells into the blood represents another non-invasive approach to studying cancer.[129, 130] In fact, studies have demonstrated that elevated levels of serum and plasma cfDNA were associated with elevated tumor markers and tumor metastasis in various forms of cancer, including pancreatic, breast, ovarian and prostate.[128, 131, 132]

With the availability of increasingly sensitive technologies to identify characteristic genetic and epigenetic aberrations, genetic profiling of cfDNA fragments can potentially lead to clinical use in prognosis, treatment response assessment and disease recurrence, for instance.[21, 128, 133] As such, some studies have compared the clinical value of cfDNA to that of other tumor markers. These comparisons have yielded data to support greater sensitivity of cfDNA as a predictive marker for recurrence and progression free survival than carcinoembryonic antigen in colorectal cancer patients, and a more reliable marker for tumor burden compared to plasma circulating tumor antigen CA 15-3 in metastatic breast cancer (MBC) patients. [132, 134]

The clinical applicability of cfDNA has also been compared to CTCs among the same cohort of patients. [132, 135] Dawson and colleagues reported on a study of 30 MBC patients who were on systemic therapy, in which radiographic images of tumors were collected along with cfDNA, CTCs and CA15-3 levels.[132] Using detection of somatic alterations, the study identified

gene alterations to cfDNA in 29 of 30 patients while CTCs could be detected in only 26 of 30 patients. Additionally, among 19 patients with progressive disease, increased cfDNA levels was associated with disease progression in 17 patients while increased CTC counts was observed in only 7 of the 19 patients. While both the CTC and cfDNA levels correlated with treatment response, cfDNA levels were more amenable to response monitoring and showed a greater correlation to tumor burden than CTC levels.[132] Interestingly, this study and others outline the ability of cfDNA to give insight into therapy resistance up to 10 months before disease progression occurs.[136-138]

Other studies have demonstrated the clinical potential of cfDNA such as its use in predicting treatment response. With the use of single molecule PCR, activating EGFR mutations that confer resistance to EGFR targeted therapies have been detected in NSCLC patients.[139] In another study, sequencing of advanced cancer patient cfDNA at different time points during treatment allowed for identifying increased mutant DNA associated with onset of therapy resistance.[138] Several studies involving cfDNA have looked at the role of genetic and epigenetic aberrations associated specifically, with pancreatic cancer.[140-142]

Indeed cfDNA isolation and analysis allows for sensitive and dynamic studies of cancer metastasis and hold promise in developing monitoring platforms for cancer treatment and therapy response. Compared to CTCs, the isolation, preparation and characterization platforms are not as technically challenging.[127] However, there are some associated challenges with the use of cfDNA. For instance, in determining which cancer specific cfDNA to monitor, individual somatic mutations have to first be identified to confirm the cfDNA.[127, 132] Moreover, the small amounts of cfDNA in circulation are still few and can present technical challenges. As is the case with CTCs, cfDNA isolation requires very sensitive detection platforms. Furthermore, identification of the source of cfDNA may pose a challenge since cfDNA can be derived both from lysed non-viable cells as well as from intact, viable cells.

With CTCs, since cells are isolated as intact entities, additional and pertinent information such as cell morphology and phenotype can be obtained. Since evidence supports the importance of cellular migration in metastasis, studying cell properties as well as multiple genetic aberrations specific to the same cell may be more telling of metastasis. From one cell, both DNA and mRNA aberrations can be studied to elucidate how mutations and pathways interact. Particularly with the subset of CTCs that persist after therapy, CTC studies allow for direct

analysis of these recalcitrant cells to identify mechanisms of therapy resistance. There is a lot that remains to be understood about the biology of pancreatic cancer and each method provides unique opportunities to do so. There are advantages unique to either of these minimally invasive approaches and combining both approaches may prove beneficial to studying pancreatic cancer metastasis.

Pancreatic cancer maintains one of the more aggressive, untenable disease manifestations of most other cancers, and strides in addressing patient outcomes have been marginal. CTCs isolated from pancreatic cancer patients represent a tool that can be used in several ways to improve our understanding of PDAC onset and metastasis, and to unveil potential therapy targets arrayed against disease spread. Before CTCs can be routinely used in patient treatment, isolation protocols and platforms need to be standardized and data from prospective randomized trials, with specific endpoints need to be conducted.

A deeper understanding of the biology of pancreatic cancer will lead to unraveling important details about the cause and the role of heterogeneity within tumors and how this relates to heterogeneity among CTCs. Identifying and studying CTCs that are resistant to therapy will improve our understanding of more effective therapy targets and regimens. Establishing CTC cultures and development of xenotransplantation models will allow for more extensive testing and revamping of treatment therapies. Furthermore insight into disease onset and early dissemination will be exigent to identifying early biomarkers for PDAC so that the disease can be treated before it is deemed untreatable. Because of their putative role in cancer metastasis, pancreatic cancer CTCs and their studies bring new hope and opportunities for improving patient outcomes. As isolation platforms, as well as molecular assays continue to develop, the ultimate expectation is that CTCs will allow for strides in our understanding of pancreatic disease and thereupon, lead to clinical impact.

Chapter 2

Development of an integrated microfluidic immunomagnetic (IMI) device for CTC isolation in Pancreatic Cancer

2.1 Abstract

While substantial evidence exists to support the clinical potential of circulating tumor cells (CTCs) in elucidating metastasis, achieving high CTC isolation purities from blood remains a challenge. To this end, we report an ultra-specific microfluidic CTC isolation approach that enables significant CTC enrichment in a continuous, high-throughput manner (24 mL hr^{-1}), through strategic combination of size based-inertial, on-chip CTC labeling with magnetic microbeads, and magnetic cell sorting. The clinical relevance of the platform was demonstrated by processing 14 pancreatic ductal adenocarcinoma (PDAC) patient samples, which resulted in unequaled CTC isolation purity rates, averaged at 82.5%±23.5 across 14 PDAC patients. Detection of >13 CTCs/mL was observed in 100% of patient samples (median = 69 CTCs/mL, mean = 146± 231 CTCs/mL). To leverage the availability of the highly enriched CTCs, both MicroRNA and mRNA profiling of CTCs were carried out from CTCs isolated within the system. CTC molecular profiling revealed that RNAs previously reported as PDAC-associated, were among those most abundantly expressed. Overall, we describe a microfluidic platform that enhances CTC purity and permits detailed molecular characterization of isolated CTCs.

2.2 Introduction

Not surprisingly CTC biology has sparked burgeoning interest within recent years because of the postulated role of these rare cells in metastasis. CTCs initiate from the primary tumor and migrate in the blood then occupy a secondary site to subsequently metastasize.[143] They inherently carry information about the tumor that could be useful for understanding metastasis and developing novel therapeutics to more effectively treat these potentially harmful cells. Since CTCs can be isolated from a simple blood draw, they can be used, routinely to yield insight into tumor pathology and treatment response without invasive procedures.[144]

However CTC detection and isolation from whole blood is quite challenging. Firstly, CTCs are rare; there may be only 1 CTC in 7.5mL of blood containing billions of blood cells. Secondly, there is limited knowledge of specific CTC markers, due in part to CTC heterogeneity, such that they vary phenotypically and genotypically among patients.[119] Considering CTC rarity and heterogeneity, engineering a device to isolate them from blood presents an important and interesting challenge.

Two chief approaches used for CTC collection are immunoaffinity capture and label free, size-based filtering.[145] Immune-based methods commonly rely on expression of epithelial cell adhesion molecule (EpCAM), a surface protein, to isolate CTCs and typically require low flow rates (1-3mL hr^{-1}) to ensure that CTCs have sufficient time to be immobilized by functionalized surfaces.[30, 146] Issues concerning cell release of the immobilized cells also arise.[147] In contrast label-free isolation does not rely on specific biomarkers but instead on inherent CTC properties such as size, deformability, or dielectric susceptibility. Size-based sorting usually offers higher throughputs since bulk sorting of appreciable sample volumes is typically used.

Moreover, since the discovery of microfluidic inertial size-based sorting, enhanced size-dependent sorting was demonstrated by incorporating curvature into microfluidic channels. Curvature introduces Dean Forces that augment the inertial forces acting on particles under flow at typical sample flowrates ranging from 500-2000 μL min^{-1}.[51-53, 56]

Whereas label-free methods are rapid, specificity is lacking and operation is limited by overall high blood cell counts. The recently reported CTC iChip combines hydrodynamic,

inertial and magnetic sorting to isolate CTCs from whole blood.[61] A throughput of 8mL hr^{-1} was achieved using positive immunomagnetic selection, with an average of 1500 contaminating white blood cells (WBCs) from 1 mL whole blood. Non-specific WBC labeling with magnetic beads affected purity rates.[61]

We report the development of an ultra-specific microfluidic device that combines inertial microfluidics and immuno-magnetism in a uniquely designed workflow that minimizes non-specific cell labeling for efficient isolation of CTCs from whole blood with ultra-high CTC purity rates and high throughput.[148] We hypothesized that beginning the CTC isolation process by rapid inertial pre-sorting would greatly reduce the number of unwanted cells from whole-blood so that micron-scale, on-chip passive mixing and brief on-chip incubation would facilitate specific and extensive CTC magnetic bead labeling. In turn, reduction in the required incubation time leads to reduced non-specific bead labeling of blood cells, which has been reported with other bulk-labeling approaches. Then, ultra-specific sorting of the pre-enriched magnetized CTCs could be achieved via magnetic sorting.

Specifically, the microfluidic design would allow whole blood to be processed rapidly yet meticulously on a single chip, requiring no blood preparation or long incubation times. This would minimize the extent of non-specific binding to promote CTC isolation purity. Unlike most other platforms, our approach negates bulk CTC labeling and instead uses on-chip CTC-bead labeling which improves the labeling chances of target cell magnetization and successful isolation from blood samples.[148]

Our device, the integrated microchip, is a polydimethylsiloxane (PDMS)-based, microfluidic device, which consists of three distinct modules that have been strategically combined to allow for consecutive processes of inertial sorting, passive mixing coupled with incubation, and continuous-flow magnetic cell sorting. The functionality of each component is illustrated in Figure 2.1, showing cell distribution throughout the device. The first stage of inertial sorting takes an input of whole blood and buffer, simultaneously diluting the blood while depleting the sample of red and white blood cells. Next, the CTC enriched stream from the innermost outlet of the inertial sorter is sent through the passive mixer, where it mixes with pre-labeled magnetic beads for targeted labeling of CTCs via antibody-antigen interaction. After mixing, the sample is briefly incubated on-chip in four reservoirs to ensure magnetic bead attachment.

Finally the suspension of magnetized CTCs in the reservoirs is drained through the magnetic sorter, where proximate permanent magnets deflect the magnetically labeled CTCs away from other unlabeled blood cells to an outlet. The final collection is a highly enriched sample of CTCs in suspension. Each component was designed and tested individually prior to integration in a single system, after which the integrated system was optimized to operate as a seamless entity. The goal engendered for each module was to contribute towards producing a high CTC recovery while concurrently reducing the rate of leukocyte contamination, within a reasonable amount of time.

2.3 Methods

2.3.1 Inertial Sorter module design and development

For size-based inertial sorting of cells, an inertial sorter with a spiral configuration was employed which was fabricated using polydimethylsiloxane polymer. It has been demonstrated that enhanced inertial sorting is achieved in microfluidics by incorporating curvature into microfluidic channels, thereby introducing Dean forces that augment the inertial forces that act on particles under flow[50]. The separation principle of the spiral is based on the concept that particles flowing along a rectangular, curved channel will experience a combination of inertial lift forces, F_L and Dean drag forces, F_D, the magnitudes and directions of which, are dependent on particle size and the relative position of the particle across the channel cross section.

The net lift force is composed of two lift forces that are oppositely directed. F_L focuses different streams of particles within the microchannel and is given by,

$$F_L=\rho G^2 C_L a_p^4$$

where ρ is the fluid density, G, the fluid shear rate is given by $G=U_{max}/D_h$, U_{max} is the maximum fluid velocity and Dh is the hydraulic radius of the channel. C_L represents the lift coefficient which is a function both of the channel's Reynolds number, Re and the particle position along the channel cross section.[52, 53] Particles experience a transverse drag force from the Dean vortices, which is calculated by assuming Stokes drag such that

$$F_D=3\pi\mu U_{Dean} a_p$$

where U_{Dean} is the average Dean velocity given by $U_{Dean}=1.8 \times 10^{-4}De^{1.63}$ where De is the Dean Number given by $De=Re(D_h/2R)^{1/2}$. R is the radius of curvature of the channel and μ is the fluid viscosity. For the spiral device studied, the estimated ratio of F_D/F_L for a CTC (a_p ~20μm) is 2.148 while FD/FL for a WBC (ap ~10μm) is 0.468 so that the 2 particles equilibrate at different cross sectional positions. Essentially, the magnitude of the ratio of F_D/F_L which varies with a_p^3 (a_p being particle diameter), determines the equilibrium position adopted by particles of different sizes.[52]

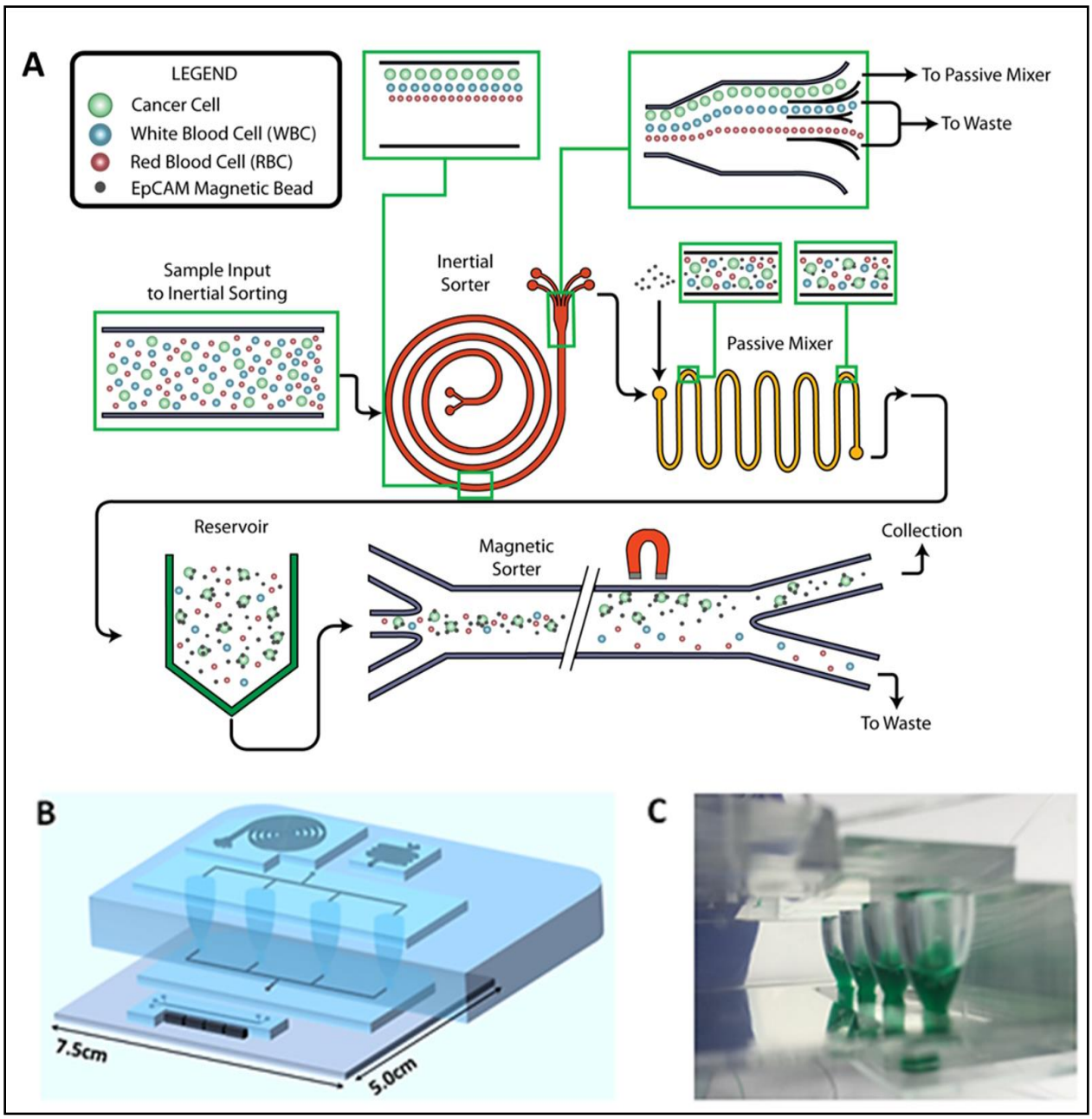

Figure 2.1: Design of ultra-Specific CTC isolation platform (A) Schematic showing inertial sorting, passive mixing with incubation and magnetic sorting (B) 3D illustration of PDMS device (C) Reservoirs allow for brief incubation and flowrate reduction to enable sensitive magnetic sorting.

Thereupon, the spiral device can be engineered so that particles of different diameters occupy single, focused streams along the channel length. Ideally, in the present study, when a patient's blood sample is flowed through the inertial spiral separator, all of the small blood cells

will be focused to the outer wall thus resulting in a suspension consisting mainly of cancer cells and some WBCs in the innermost channel outlet.

In determining the final design configuration of the inertial sorter, routine experiments were carried out using fluorescent polystyrene beads of various sizes (7-20μm) which recapitulate the size, and therefore the anticipated behavior of the various blood cells. By evaluating the flow dynamics of different-sized polystyrene beads along the spiral inertial sorter, design parameters such as height, width and length of the device were modified so that the chosen configuration enabled focusing of the different-sized particles to distinct outlets, thereby separating larger particles (15 and 20μm) from smaller particles (7 and 10μm).

The optimized spiral design for the integrated chip consists of a 500μm wide channel that expands to 1000μm at the outlet and branches into one collection outlet (innermost outlet, width of 200μm) and three waste outlets. The largest radius of the spiral is 15mm and the height of the microfluidic channels is 100μm. The spiral device operates at 1700μL min^{-1} as a stand-alone platform, for effective sorting of large (15-20 μm) particles from smaller particles (7-10 μm). Once the inertial sorter is fitted into the integrated device, the spiral operating flow rate is decreased to 1200μl min^{-1} to maintain effective CTC sorting. To determine the purity and efficiency of the inertial sorting process, cell line experiments were also performed using cell suspensions that were prepared by spiking pre-stained PANC-1 cells and WBCs into PBS.

Fabrication of PDMS Microfluidic Chip

Microfluidic channel designs were produced and modified using AutoCAD and photoresist masks were generated from these designs. Master molds were fabricated using SU8-100 negative photoresist (Microchem Corp.) following standard photolithography procedures, at the Lurie Nanofabrication Facility (LNF), at the University of Michigan. Specifically, to fabricate these reusable silicon molds for PDMS device fabrication, photoresist was deposited on a preheated, clean 4 inch silicon wafer (UniversityWafer). The wafer was initially spun at 500rpm for 10 seconds for spreading, immediately followed by spinning at 2530rpm for 60 seconds. It was then baked on a hot plate at 65 ^{0}C for 10 minutes followed by baking at 95 ^{0}C for 40 minutes. Then the SU-8 was UV exposed for 30 seconds under UV light in a MJB 45S Mask/Bond Aligner in the Wet Chemistry room of LNF. The exposed wafer was again baked at 65 ^{0}C for 5 minutes followed by baking at 95 ^{0}C for 10 minutes. To develop the photoresist, the wafer was immersed in SU-8 developer for 7 min. The developed SU-8 mold was further baked at 150 ^{0}C for 3

minutes. All molds were fabricated with a thickness of 100µm. The Dektak 6M Surface profilomter was used to measure feature height of the molds. Then to fabricate the PDMS devices, a 10:1 ratio of PDMS polymer : curing agent (Dow-Corning) was mixed and de-bubbled prior to pouring over the SU8 molds. The PDMS was allowed to cure at 65^{0}C overnight.

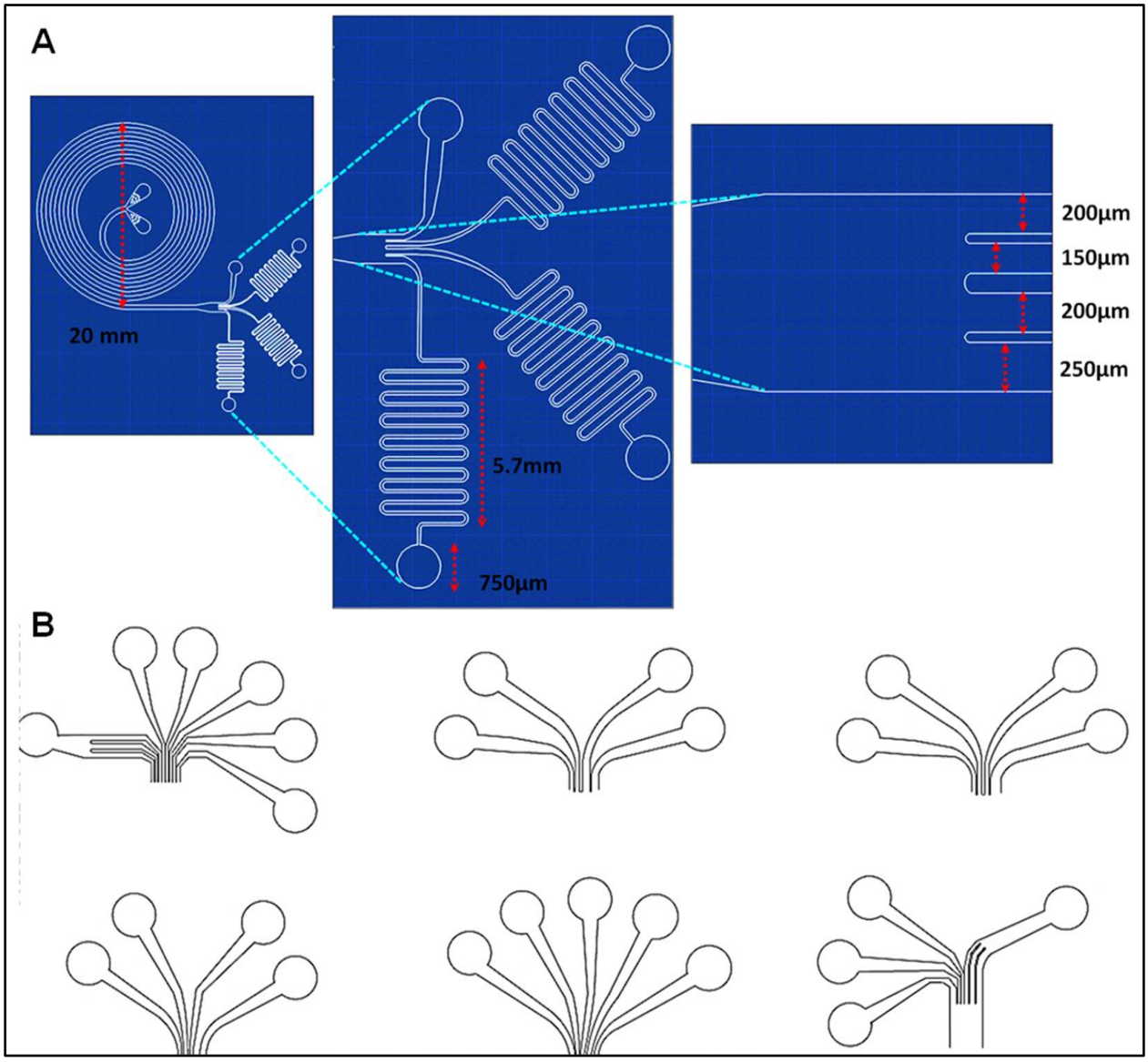

Figure 2.2: Inertial Sorter Optimization: parameters and devices studied during the 2nd generation device optimization to arrive at final spiral design (A) Optimized device dimensions showing resistance matching channels (B) Different outlet designs tested to facilitate optimal inertial cell sorting in stand-alone spiral.

After curing, the PDMS chips were manually cut and peeled from the mold, trimmed to size, and inlet/outlet holes were punched. PDMS chips were bonded by oxygen plasma to cleaned glass

slides. Tygon tubing was inserted to connect device inlets and outlet ports to syringes. Sample flow was driven and controlled using Harvard Apparatus syringe pumps. Prior to running samples, tubing and chips were primed with 0.05% Pluronic F127 solution (Sigma Life Sciences), followed by PBS rinsing to prevent cells from sticking to the PDMS surfaces.

Table 2.1: Parameters and devices studied to arrive at a final spiral design.

Device #	Spiral Radius (mm)	Outlet Widths (µm)				# of Turns	Comments
		1	2	3	4		
1	15	125	125	125	225	6	500µm wide (75,75,250 spacing)
2	15	150	150	150	350	6	Outlets designed by measurement 500µm wide (50, 50, 50 spacing)
3	20	150	150	250	250	3	500µm wide (50, 100, 50 spacing)
4	10	150	150	250	250	5	100µm wide channel (50, 100, 50 spacing)
5	20	150	150	250	250	3	250µm wide Short expansion (50, 100, 50 spacing)
6	20	150	150	250	---	3	250µm wide, 3 outlets, 700 vs 1000µm expansion (50, 100 spacing)
7	20	150	150	250	250	3	250µm wide channel (50, 100, 50 spacing)
8	20	125	125	125	125	3	250µm wide, 575 vs 1000µm expansion (25, 25, 25 spacing)
9	10	150	150	250	250	5	250µm wide channel (50, 100, 50 spacing)
10	10	150	150	250	250	5	500µm wide channel (50, 100, 50 spacing)
11	15	100(x3)	100	100	100(x3)	6	25µm spacing 8 outlets, 3 grouped 5 single
12	15	150	150	250	250	6	50,100,50 spacing
13	15	150	150	150	350	6	50,100,50 spacing
14	15	200	100	125	150(x2)	6	5 outlets , varied spacing
15	15	100	100	100	100(x3)	6	3 single , 3 wastes grouped

Polymer Micro Beads

Device prototypes for the spiral inertial sorter and the passive mixer were first evaluated using fluorescent polymer beads. 20µm (FITC, Polymer Sciences), 15µm (DAPI, Invitrogen), 10µm (Dragon Green, Bangs Lab), and 7µm beads (Sky Blue, Spherotech) were used for flow characterization at concentrations ranging from 10^4-10^5 beads mL^{-1}. Also, magnetic fluorescent polymer beads (8µm, Bangs Lab) were used to characterize the magnetic sorter.

Cancer Cells

A PANC-1 cell line (human pancreatic carcinoma, epithelial-like cell line), obtained from ATCC, was maintained at 37°C with 5% $C0^2$ and 95% relative humidity in DMEM, supplemented with 10% FBS. PANC-1 cells were harvested on the third day after seeding, once they achieved >60% confluence, to exploit optimal cell surface EpCAM expression. Cells were labeled with CellTracker Green dye (Thermo Fisher Scientific) for easy visualization and counting. Human white blood cells, (WBCs), which were used for spiking experiments, were obtained from healthy donor blood using a dextran-mediated, centrifugation technique for WBC isolation.

The cells were then fixed and made permeable with BD CytoPerm/CytoFix to enable nuclear staining with DAPI. All fixed cells were stored at 4°C. For appropriate dilutions, cells were counted using a hemocytometer and then diluted with PBS accordingly. For cell spiking experiments of 1000 cells mL^{-1} or less, 1 mL of cells was prepared at 10^4 cells mL^{-1} concentration and 10-100 μL of the solution was added to a 1 mL blood aliquot for device testing. Two additional samples were plated during recovery experiments to be used as counting controls, to supplement mass balance results.

To arrive at the final spiral design several design parameters were studied such as largest radius of curvature, device footprints, channel width and height, and outlet configuration (Table 2.1). The optimized spiral design that was employed in the integrated chip consists of a 500 μm wide channel that expands to 1000 μm at the outlet that branches into one collection channel (innermost outlet) and three waste channels that have been modified with narrow serpentine channels to account for resistance matching once the spiral is connected to the passive mixer module. The collection channel is 200μm wide. The largest inertial sorter radius is 15 mm and the height of the microfluidic channels is 100 μm (Figure 2.2). Resistance matching allows the modified spiral to perform as if it were not connected to the mixer.

2.3.2 Passive Mixer module design and development

Cancer Cell Labeling Efficiency for Magnetic Cell Sorting

To determine the appropriate bead dilution and incubation time for ensuring sufficient PANC-1 cell immunomagnetic labeling, (~85% of cell with at least 1/3 surface coverage), labeling experiments were carried out in buffer and blood. To test the on-chip mixing and labeling

procedure, cells and diluted beads were flowed through the passive mixer at 100µL min^{-1} for a total volume of 1-1.5 mL. The cells and beads were allowed to incubate for test times of 5, 10, 15 and 30min in the reservoirs, with occasional rocking to prevent cell/bead settling and to enhance bead-cell mixing. As a negative control, equivalent volumes of cell sample and beads were mixed in an Eppendorf tube. The tube was occasionally rocked to prevent cell/bead settling. After each incubation time, a drop of mixed sample was imaged at 20X and cell bead coverage was evaluated. These experiments were performed with 1:10 and 1:5 bead dilutions and cell concentration of approximately 10^5 cells/mL. Since both bead dilutions resulted in comparable cancer cell labeling regardless of reservoir or Eppendorf tube incubation, (Figure 2.7), 1:10 bead dilution was used. Cell labeling was further tested in diluted blood to ensure bead-cell labeling efficiency was maintained even in blood.

Passive Mixer module design

Calculations demonstrate that for a cell to experience a magnetic force sufficient enough to pull it in the direction perpendicular to flow, and therefore allow it to be sorted, a cell of average diameter of 20µm requires less than 1/3 bead coverage to be deflected to the desired magnetic sorter outlet. Therefore, mixer designs were evaluated and compared based on the quality of bead coverage resulting after the bead-cell mixture emerged from the mixer (see Figure 2.3A). For each design simulations of laminar flow were performed with COMSOL finite element fluidic solver to fluid shear rate since high shear rates could impact cell viability (Figure 2.3B). Several different designs were tested for passive mixing which are shown in Figure 2.3C including a planar micromixer,[149] the tesla mixer[150] and various serpentine mixer designs.

The serpentine configuration for the passive mixer was chosen since cell labeling efficiency with this design was deemed adequate, requiring a module footprint that operated in combination with the other modules. The turns in the serpentine channels give rise to centrifugal Dean Forces that allow particles to cross fluid stream lines and become mixed. These forces increase with increasing fluid flow rate to lead to rapid mixing and high mixing efficiencies.[151] Typically, for the microchannel-based passive mixer, flows through the device are primarily laminar with values of Reynolds' number, (Re), in the range of $0.01<Re<100$ (Re~30 in the passive mixer studied)[152]. Because both viscous and inertial forces are appreciable in this range of Re, flow around the serpentine bend generates "secondary flows" in both the axial and radial directions thus increasing the interfacial area over which diffusion and mixing occur. The

serpentine channel has a height of 100µm and a width of 250µm and is capable of mixing particles at flow rates of 50µL min^{-1} or higher. As the flow rate increased, mixing occurred sooner and was primarily dependent on chaotic advection rather than diffusion, which arises at slower flow rates where Dean forces are weak.

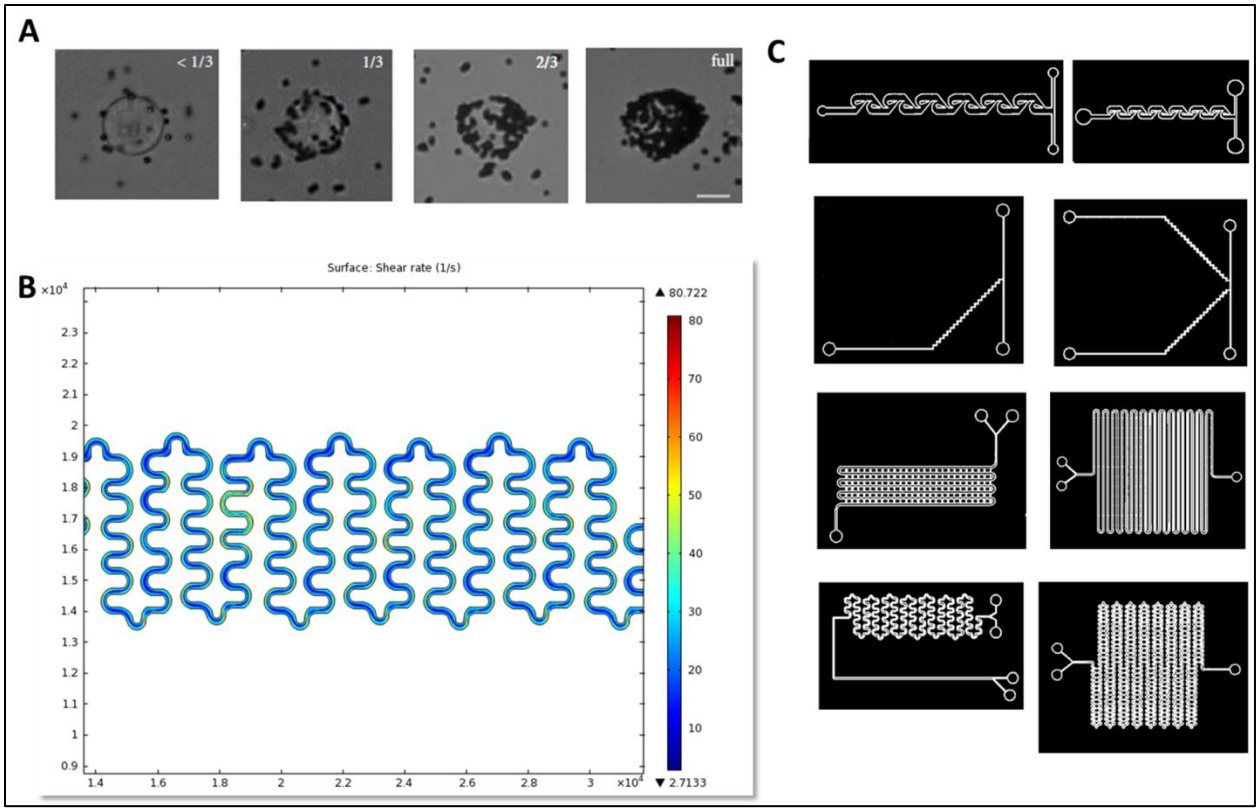

Figure 2.3: Passive Mixer Development. (A) Metric of bead attachment to cells to evaluate passive mixing efficiency (B) COMSOL simulation of fluid shear rate in mixer (C) Different passive mixer designs tested.

Preliminary evaluation of mixing was done by observing the mixing patterns of yellow- and blue- dyed buffer solutions generated in the mixing module. Using flow rates of 10-100µL min^{-1}, the mixing quality was characterized by the distance along the mixer required for the two distinct streams of yellow and blue, to become one well-mixed green stream (Figure 2.4). At a flow rate of 100µLmin^{-1}. The highly compact mixer design enabled fluids to be completely mixed by the third channel segment, at a channel length of ~4cm.

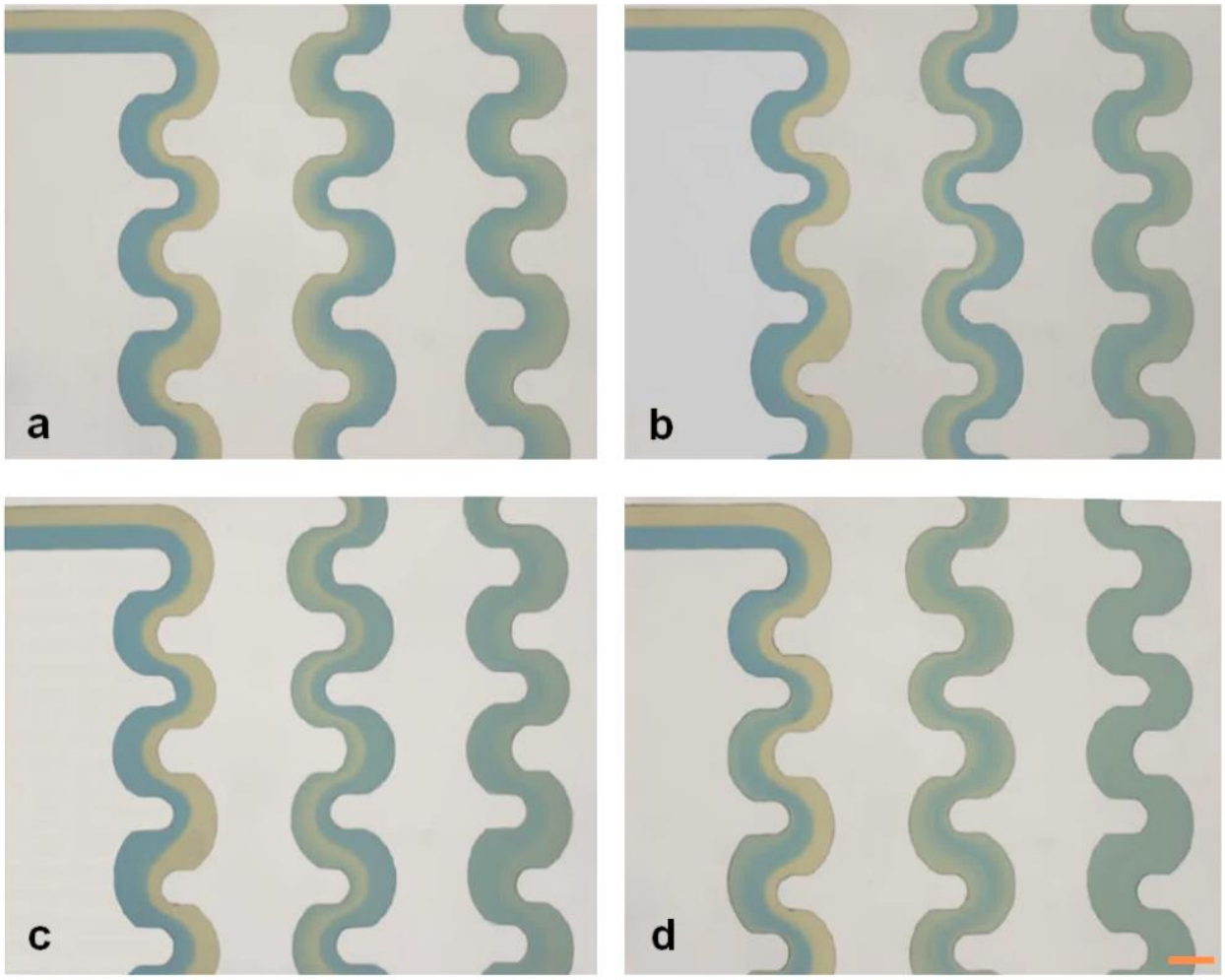

Figure 2.4: Mixing progression through passive mixer. Dyed PBS was used to demonstrate how increasing flow rates lead to mixing occurring closer to the beginning of the channel (a)10 µL min^{-1} (b)40 µL min^{-1} (c)70 µL min^{-1} (d)100 µL min^{-1}. Scale = 250µm.

The efficiency of cancer cell labeling with EpCAM coated magnetic beads was examined through static experiments (PANC-1 cells and EpCAM-labeled beads in an Eppendorf tube) and on-chip experiments (on-chip passive mixing of PANC-1 cells and EpCAM-labeled beads then flowed into reservoirs). The quality of mixing was validated by immediately observing the mixed effluent to quantify the extent to which cells were labeled with magnetic beads for each incubation time point. Since cells demonstrate a range of sizes, and extensive bead-cell attachment made individual bead counting problematic, cells were characterized as having no coverage, 1/3 to 2/3 coverage, and greater than 2/3 coverage, as illustrated in Fig. 2.3A.

2.3.3 Reservoirs design and development

The mixture of magnetic beads and cancer cells that emerges from the passive mixer flows into four reservoirs where the mixture incubates briefly to allow more time for cell labeling. Use of the reservoirs also allow the flow rate of the sample to be decreased since the magnetic sorting process necessitates a lower flow rate than the inertial sorting and mixing processes. Therefore, the function of the reservoirs is twofold. To fabricate the reservoirs, 3D cone-shaped mold designs were generated in AutoCAD and machined in the Mechanical Engineering machine shop at the University of Michigan. Molds were fabricated using brass and Teflon but the Teflon molds were utilized to make the molds. Four of the molds were screwed to a petri dish and PDMS was poured over the molds and allowed to cure overnight at 65^0C. Molds were then unscrewed and the PDMS reservoir device removed from the dish. Holes were punched at the base of the reservoirs before bonding to the rest of the integrated system. Each reservoir is capable of holding 0.5mL of sample in the final fabricated system.

2.3.4 Magnetic Sorter Module design and development

The magnetic sorter channel has three inlets so that the two outer buffer streams flank the sample stream in the center of the 250μm channel. Flow of the buffer streams was biased by using two different size syringes at a fixed syringe drive setting so that the top and bottom streams could simultaneously flow at two different flow rates. Notably, biasing the flow in this manner significantly improved magnetic sorting by establishing a sample distribution pattern in the magnetic sorter channel that directed the non-target cells to the waste outlet. This flow bias also allowed magnetized cells to flow slow enough to maximize magnetic trapping magnetized cancer cells into the collection channel. At the same time, the established design and flow rates used prevents the buildup of magnetic beads in the channel, which could result in blockage of the magnetic sorter. The outlet is split into two channels, with a 35μm collection channel and a 65 μm waste channel. The channel length is 25 mm with a height of 100 μm. Permanent magnets (500 mT, K&J Magnetics) are aligned end-to-end and positioned parallel the channel with a 1mm separation gap between the channel and the magnets. The sample continuously flows through the sorter at a rate of 50μL min^{-1} and cells with as few as one-third surface bead-coverage can be deflected into the collection channel. The sample waste, which consists of unwanted RBCs and WBCs and other blood components, continues along streamlines to the waste outlet.

2.3.5 The Integrated Device operation

Before processing sample in the devices, each module was primed with 0.05% pluronic solution followed by a rinse with PBS buffer. In establishing the proof of concept of the integrated magnetic sorter device, 1mL of whole blood was routinely processed, both for device optimization and for testing patient samples. Once the modules are connected to operate as a continuous system, 1 ml of whole blood can be processed in an approximated 30 minute, which includes a 5-minute on-chip incubation of the blood sample with the antibody-coated magnetic beads. At the inertial sorter inlets, the initial whole blood input flows at approximately 400µL min^{-1}, while the corresponding buffer input flows at 1200 µL min^{-1}. The higher buffer flow rate readily establishes stable flow prior to the blood sample introduction and concurrently dilutes the blood sample. At the inertial sorter outlets, the innermost outlet (where the large cells align) is connected to one of the two passive mixer inlets. The other passive mixing inlet introduces the antibody-coated magnetic beads (1µm, Dynabeads) at a rate of 100µL min^{-1}. Then, the outlet of the passive mixer leads the sample into four reservoirs where beads and cells undergo a brief incubation period to ensure more extensive magnetic bead binding to the cancer cell targets.

After incubation, a syringe filled with air is used to pressurize the reservoirs and drive the flow of the sample through the magnetic sorter. In addition, buffer flows through two of the outer inlets of the magnetic sorter to flank and align the sample stream. The buffer stream closest to the magnet flows at a rate of 75µL min^{-1}, the sample flows at a rate of 50µL min^{-1} and the buffer stream furthest away from the magnet flows at a rate of ~25µL min^{-1}. These flow rates enable efficient magnetic attraction and redirection of the flowing, magnetically labeled cells for collection.

2.3.6 Cell Viability Assay

To ensure cells processed through the integrated magnetic device would be viable for further cellular studies, cell viability was assessed through the MTT assay (Figure 2.5). PANC-1 cells were either seeded directly into a 96-well plate (Control), processed through the integrated device in media without magnetic beads (Test 1), or processed through the integrated device in media with the addition of magnetic beads (Test 2). Magnetic beads were exposed to UV light for 8 hours prior to use in these experiments to promote experimental sterility. After collecting

the output of the integrated device, the processed cells and control cells were plated in 96 well plates at 4000 cells/well. Every 24 hours, cells were subjected to MTT protocol and absorbance at 570nm was recorded. Control cell absorbance on Day 1 was used as the basis to normalize the results. Media was changed on Day 3. This experiment was repeated 3 times and similar growth patterns were observed among the three trials. As seen in Figure 2.5, absorbance among the different tests was comparable for the duration of the assay. This indicated that cells processed through the device were viable, thus resulting in nearly the same growth rate as the control cells and therefore similar levels of dye absorbance.

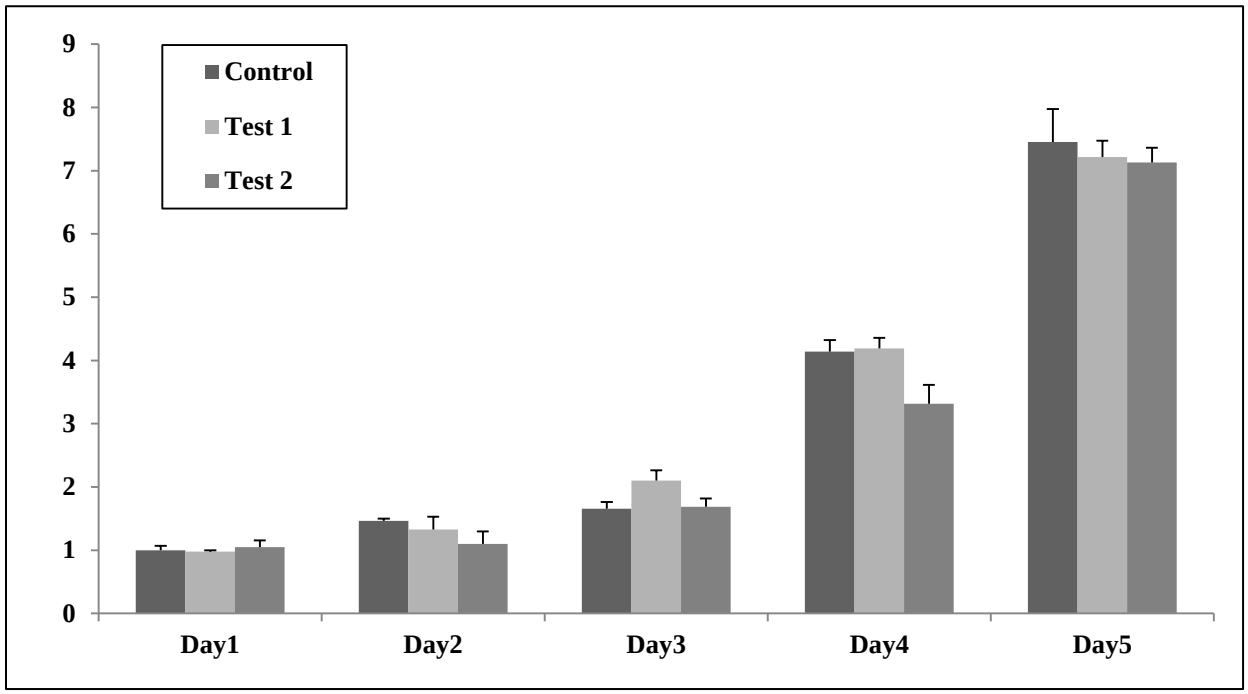

Figure 2.5: MTT assay to determine cell viability. Cells were processed through the integrated device either without magnetic beads (Test 1) or with magnetic beads (Test 2). Control cells were unprocessed. Then cells were plated in 96 well plates and grown for 5 days – with MTT assay performed on one plate per day to assess growth. Growth was normalized to control cells on Day 1. (n=5, bars indicate standard deviation)

Therefore, processing patient samples through the device should not be detrimental to their viability. Furthermore, these results support the use of isolated CTCs for subsequent studies such as molecular profiling and CTC culturing.

2.3.7 Patient Blood Testing with the IMI Device

Blood samples from pancreatic cancer patients were collected using institutional IRB guidelines with informed consent from the patients or the next of kin while blood from healthy donors were collected with informed consent according to standard protocol. The patient samples, (courtesy of the University of Michigan Comprehensive Cancer Center) and the healthy donor samples were collected in EDTA tubes and tested within four hours of blood draw.

Table 2.2: Patient statuses for samples processed and enumerated.

DATE	ID	VOL. (mL)	CTCs /mL	WBCs/ mL	AGE	SEX	DISEASE STAGE
3/3/2014	P1	1.2	938	7	73	F	Metastatic to lymph nodes outside of surgical field
4/14/2014	P2	1.0	80	0	81	F	Locally Advanced/unresectable
4/21/2014	P3	1.0	16	0	75	M	Likely PDA/resectable (pending Pancreatitis)
4/21/2014	P4	1.0	22	0	50	F	Locally PDA
7/29/2014	P5	1.3	141	12	63	M	pT4 N1 MX-Stage III
7/29/2014	P6	1.4	190	25	53	M	PDA Stage IV
8/4/2014	P7	1.2	38	0	58	F	PDAM Stage IB-IV
8/4/2014	P8	1.2	80	35	60	M	PDA Stage IV
8/11/2014	P9	0.7	280	49	66	M	Metastatic Panc Adeno to liver Stage IV
8/11/2014	P10	0.6	58	389	63	M	Locally advanced/borderline resectable
8/12/2014	P11	1.4	20	14	40	M	Resected pT3N1- Stage IIB
8/18/2014	P12	1.2	48	12	81	M	Possible PDA, renal mass
8/18/2014	P13	1.0	14	0	61	M	Metastatic Panc Adeno Stage IV
8/18/2014	P14	1.4	113	51	65	M	Metastatic Panc Adeno Stage IV

To evaluate the ability of the optimized IMI device to isolate CTCs from patient samples, fourteen metastatic or locally advanced PDAC samples and 4 healthy controls were processed through the device. Up to 1.4 mL of whole blood was processed for each patient. CTCs were

identified via fluorescent immunostaining for CK+/DAPI+/CD45-. Additional confirmation of an epithelial cell type was garnered by brightfield images of CTCs, showing bound EpCAM magnetic beads on the cells. WBCs were identified as CK-/DAPI+/CD45+. The corresponding patient clinical data is shown in Table 2.2.

2.3.8 Immunofluorescent Staining for CTC Identification

The resulting CTC suspension from the IMI device was processed using the cytospin technique where 300μL of sample was spun onto a poly-lysine coated glass slide at 600-800rpm for 10min. The sample was then demarcated with the hydrophobic pap-pen and the sample fixed with 4% PFA for 20min. The slide was then rinsed and the sample covered in PBS buffer and refrigerated in 4^0C until immunofluorescence staining was performed. Slides were stained for CTC markers using a primary antibody for anti-cytokeratin-19 (CK-19, epithelial cell marker, (Santa Cruz Biotechnology, rabbit polyclonal IgG) and nuclear stain 4',6-Diamidino-2-Phenylindole, Dihydrochloride (DAPI, Invitrogen). Negative staining with the leukocyte marker anti-CD45 (BD Pharmigen Purified Mouse Anti-Human CD45, HI30 clone, isotype Mouse IgG1, ƙ) was also performed. Samples were then stained using secondary antibodies with fluorescence conjugation namely, AlexaFluor 568 (Life Technologies), for CK-19 detection and AlexaFluor 488 (Life Technologies), for CD45 detection. For the primary antibody stains, overnight incubation was carried out, while for secondary staining, 1hr was allowed. For DAPI staining ProLong Gold anitfade mountant with DAPI, (Life Technologies) was applied overnight. Immunofluorescence imaging for anti-CD45 was performed using a FITC filter while anti-CK was performed with a PE filter and DAPI, a UV filter, all at x20 magnification.

2.3.9 M-RNA Profiling of pancreatic CTCs isolated with the IMI device

To further demonstrate the potential of the integrated device in allowing sensitive CTC molecular interrogation subsequent to CTC isolation, mRNA profiling was carried out on eight additional patient samples. Of these, three were categorized as borderline and two as locally advanced while three were metastatic. To isolate total RNA, after enriching CTCs from 6.5 mL of patient blood, 300μL of the fraction was fixed and stained to enumerate for CTCs and the remaining portion was processed for total RNA isolation. RNA was isolated using the Norgen Single Cell RNA Purification kit (Norgen Biotek Corp.), according to the manufacturer's

protocol with minor modifications. After lysing the cells the CTC lysates were then stored in -80^{0}C until total RNA purification was ready to be carried out. For total RNA purification, samples were thawed on ice and 200µL of 96-100% ethanol was added to the cell lysate and vortex mixed for 10 seconds. At this point the manufacturer's protocol was followed for total RNA extraction. RT was carried out on the purified RNA followed by pre-amplification (18 cycles) using cDNAs corresponding to 96 genes of interest from a CTC-specific panel. The pooled TaqMan Gene Expression Assays and Cell-to-CT Kit (Ambion, Invitrogen) were used. To carry out gene expression profiling of the pre-amplified cDNAs, TaqMan Gene Expression Assays for the 96 genes and the BioMark HD qPCR platform (35 cycles) were used. For genes undetected during qPCR, a cycle number of 40 was assigned for analysis purposes. To normalize CT values among different genes, GAPDH was used as an internal reference. Statistical analysis was performed based on –ΔCT of gene expression.

2.3.10 MicroRNA Profiling of pancreatic CTCs isolated with the IMI device

MiRNAs are important regulators of cancer cell properties however they have been in general, understudied in the context of CTCs. Currently, the relatively low purity rates proffered by most CTC isolation technologies limit specificity in genomic characterizing. The high CTC purities of the integrated device enable CTC-specific miRNA profiling. Accordingly, we profiled 372 miRNAs in CTC enriched samples from 2 locally advanced PDAC patients alongside a healthy control sample.

After enriching for CTCs from 6.5 mL of patient blood, 300µL of the fraction was fixed and stained to enumerate for CTC levels and the remaining portion was processed for total RNA isolation. RNA was isolated using the Norgen Single Cell RNA Purification kit (Norgen Biotek Corp.), according to the manufacturer's protocol with minor modifications. After lysing the cells a mix of 3 synthetic Caenorhabditis elegans, (C. elegans) miRNA oligonucleotides, cel-miR-39, cel-miR-54 and cel-miR-238 was added to the sample to be used for miRNA normalization. The CTC lysates were then stored at -80^{0}C until total RNA purification was ready to be carried out. For total RNA purification, samples were thawed on ice and 200µL of 96-100% ethanol was added to the cell lysate and vortex mixed for 10 seconds. At this point the manufacturer's protocol was followed for total RNA extraction. Once total RNA was extracted, samples were profiled for the abundance of 372 miRNAs. To carry out reverse transcription, 13µL of each

sample was processed using miRCURY LNA Universal RT microRNA PCR kit (Exiqon) according to the manufacturer's protocol. UniSP6 spike-in control was added to each reaction for normalization. Once reverse transcription was completed, the products were diluted and combined with SYBR Green master mix (Exiqon) and ROX reference dye (Applied Biosystems) and loaded into the commercially available, Ready-to Use- PCR, Human panel I, V4.M qRT-PCR arrays (Exiqon). QuantStudio ViiA7 PCR system (Applied Biosystems) was used for carrying out quantitative PCR. CT values were calculated by exporting the data using automatic threshold values. Normalization was carried out across all plates based on the data obtained for the UniSP6 and Inter-Plate Calibrator control assays. The blanks of all the assays were undetectable. Any miRNA assay having a CT value beyond the limit of detection or greater than the blank control array were considered as not detected (ND). All other assays that were reliably detected were median normalized. Based on these CT values, fold change for each miRNA was calculated based on the expression levels in the healthy control. Fold change values were then uploaded to Ingenuity Pathway Analysis (IPA) software (Qiagen), and analysis was carried out using Ingenuity Knowledge base reference set, with filters for Human species alongside an "experimentally observed" confidence.

2.4 Results

2.4.1 Evaluation of the Inertial Spiral sorting module

The spiral design was optimized as a stand-alone device and subsequently, the three waste outlets were re-designed to allow for resistance-matching once it was connected within the fully integrated system (Figure 2.2A). The inertial sorter separates larger particles (15 -20µm) from smaller particles (7-10µm). Figure 2.6A shows the fabricated polydimethylsiloxane (PDMS) device, Figure 2.6B illustrates the arrangement of cancer cells (green) versus WBCs (blue) at the outlet of the sorter and Figure 2.6C demonstrates how the polystyrene particles (20 µm (green), 15 µm (blue), 7 µm (orange)) separate into distinct, focused streams at the outlets of the spiral channel. Similarly, in Figure 2.6D, PANC-1 cancer cells (green streak) focus to the innermost outlet and WBCs (blue streak) focus to the second outlet. Figure 2.6E shows how the larger PANC-1 cells, (indicated by red arrows) spiked into diluted blood focus to the innermost outlet amidst the other blood cells.

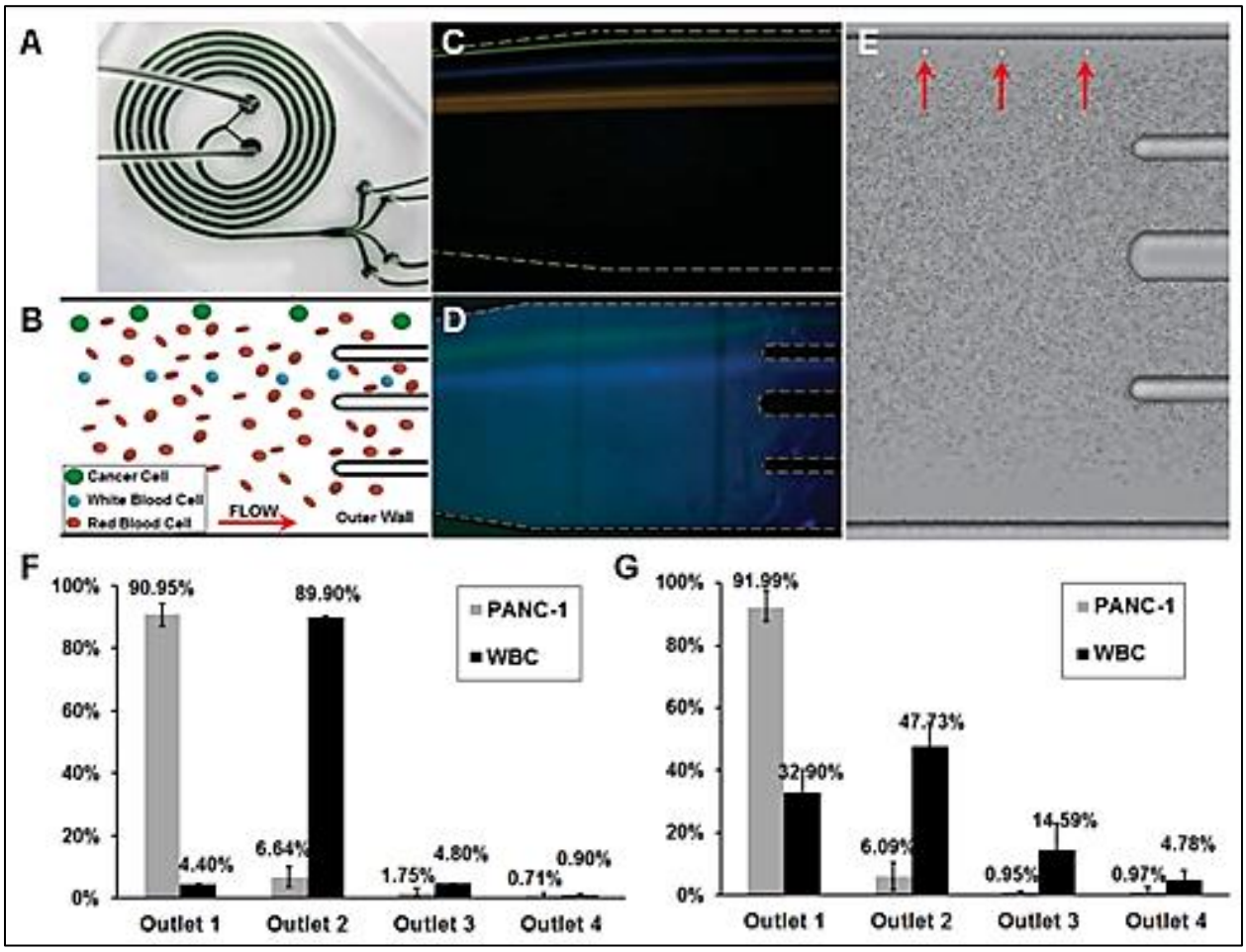

Figure 2.6: Optimized Spiral Module. (A) PDMS device (B) Larger CTCs (green) go to innermost outlet channel. (C) Fluorescent beads, (D) fluorescent cells and (E) high-speed imaging demonstrate cancer cell sorting. Analysis of cell distribution in outlets both in PBS buffer (F) and blood (G).

To quantitatively evaluate inertial sorting PANC-1 cells and WBCs were spiked into PBS and processed through the module. The effluents from each outlet were collected and analyzed for cell counts. Notably, 90.95% ±3.61 of cancer cells spiked in PBS buffer were collected in the desired outlet, as shown in Figure 2.6F. Whole blood was routinely diluted x10 for blood-spiked experiments to facilitate conditions amenable to microscope visualizing. Figure 2.6G shows cell distribution in the four outlets after repeating the experiments in diluted blood. Results consistent with PBS-spiked experiments were achieved such that 91.99% ±4.94 of cancer cells were enriched in the innermost spiral outlet.

The increase in WBC contamination in moving from PBS buffer (4.4%) to diluted blood (32.9%) may be as a result of spiking stained WBCs into the diluted blood for enumeration purposes, even though the original WBCs were still present in the blood sample. The heightened concentration of WBCs may have interfered with focusing of the cells to a distinct position across the channel cross section.

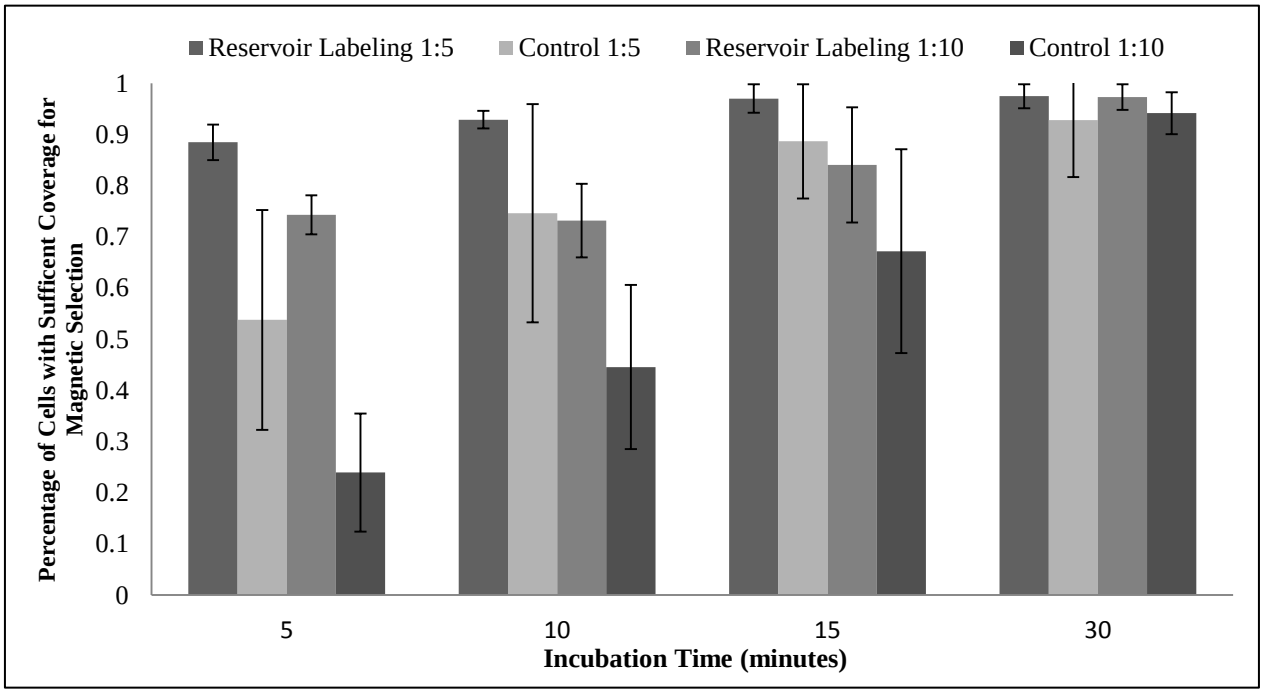

Figure 2.7: Magnetic bead labeling efficiency of PANC-1 cells. Bead concentration and incubation times were varied. Scanned images of cells were used to quantify bead coverage. Each experiment (data point) was repeated in triplicate. Bars indicate standard deviation.

2.4.2 Evaluation of the Passive mixing module

For static incubation tests of PANC-1 labeling with EpCAM beads, time points of 5, 10, 15 and 30 min were evaluated and compared with the use of the passive mixer module, at the same time points. Also, bead dilutions of 1:10 and 1:5 were evaluated. After characterizing cells as having no coverage, 1/3-2/3 coverage, and greater than 2/3 coverage, in static conditions, at least 15 minutes of incubation time was required to achieve at least 1/3 surface coverage on 85% of cells (Figure 2.7). With the use of the passive mixer and reservoir for cancer cell labeling, after only 5min incubation, over 90% of cells have appreciable bead labeling. Moreover, at all the time points, use of the passive mixer and reservoir demonstrate superior cancer bead

attachment. Additionally, Figure 2.8 shows that 92% of cells from the reservoirs have sufficient coverage after only 5 min incubation after repeating the experiment in diluted blood.

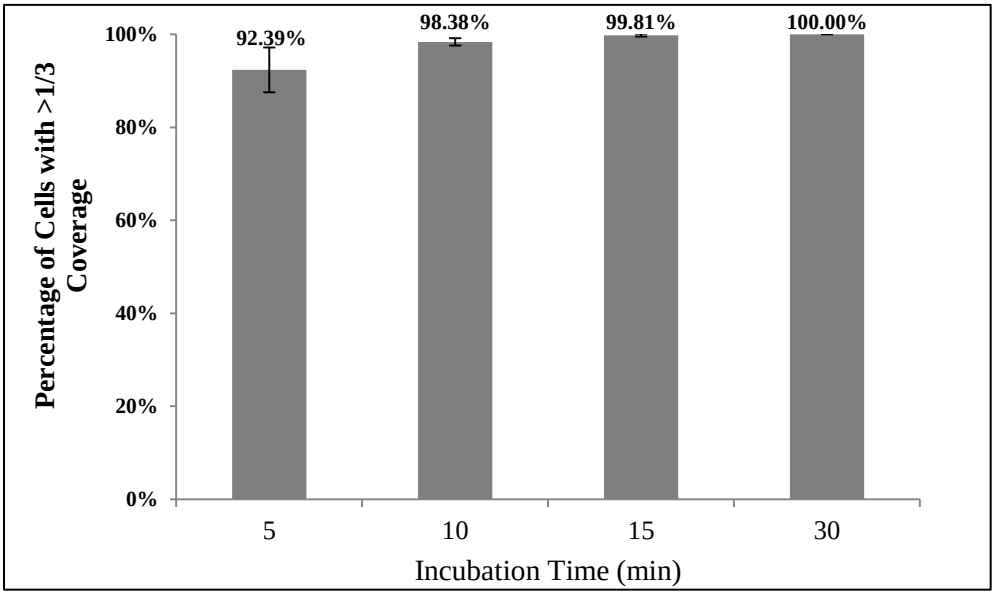

Figure 2.8: Incubation times for bead-cell labeling in diluted blood. Plot showing percentage PANC-1 cells labeled within the reservoirs at times of 5, 10, 15, and 30 minutes. Beads were diluted 1:10 beads to buffer before entering the reservoir. (n=3, bars indicate standard deviation).

2.4.3 Evaluation of Magnetic Sorting Module

After the final designs for the magnetic module were narrowed down, to determine the flow conditions that would facilitate the highest purity rates for cancer cell sorting using the magnetic sorter module, two flow conditions were tested. The conditions included biased buffer stream flows with one at 50µl/min bottom-17 µL min^{-1} top (50 µL min^{-1} bias), and the other at 75 µL min^{-1} bottom-25 µL min^{-1} top (75 µL min^{-1} bias). For the 50 µL min^{-1} bias condition, contamination was 2.35% ± 2.72 and efficiency was 88.39% ± 5.79 in the collection channel. For the 75 µL min^{-1} bias setup, WBC contamination decreased to less than 0.5% but the recovery efficiency was also reduced (Figure 2.9). However, since the purity was higher using the 75 µl/min bias conditions this setup was implemented. Using 75 µL min^{-1}- bottom, 25 µL min^{-1}-top buffer and 50 µL min^{-1} flow rate for the sample, results show that for blood spiked tests, WBC contamination was 2.28% ±0.68 and recovery efficiency was 94.60% ± 1.48. Of note, the few PANC-1 cells in the waste were poorly labeled and so not expected to be magnetically sorted.

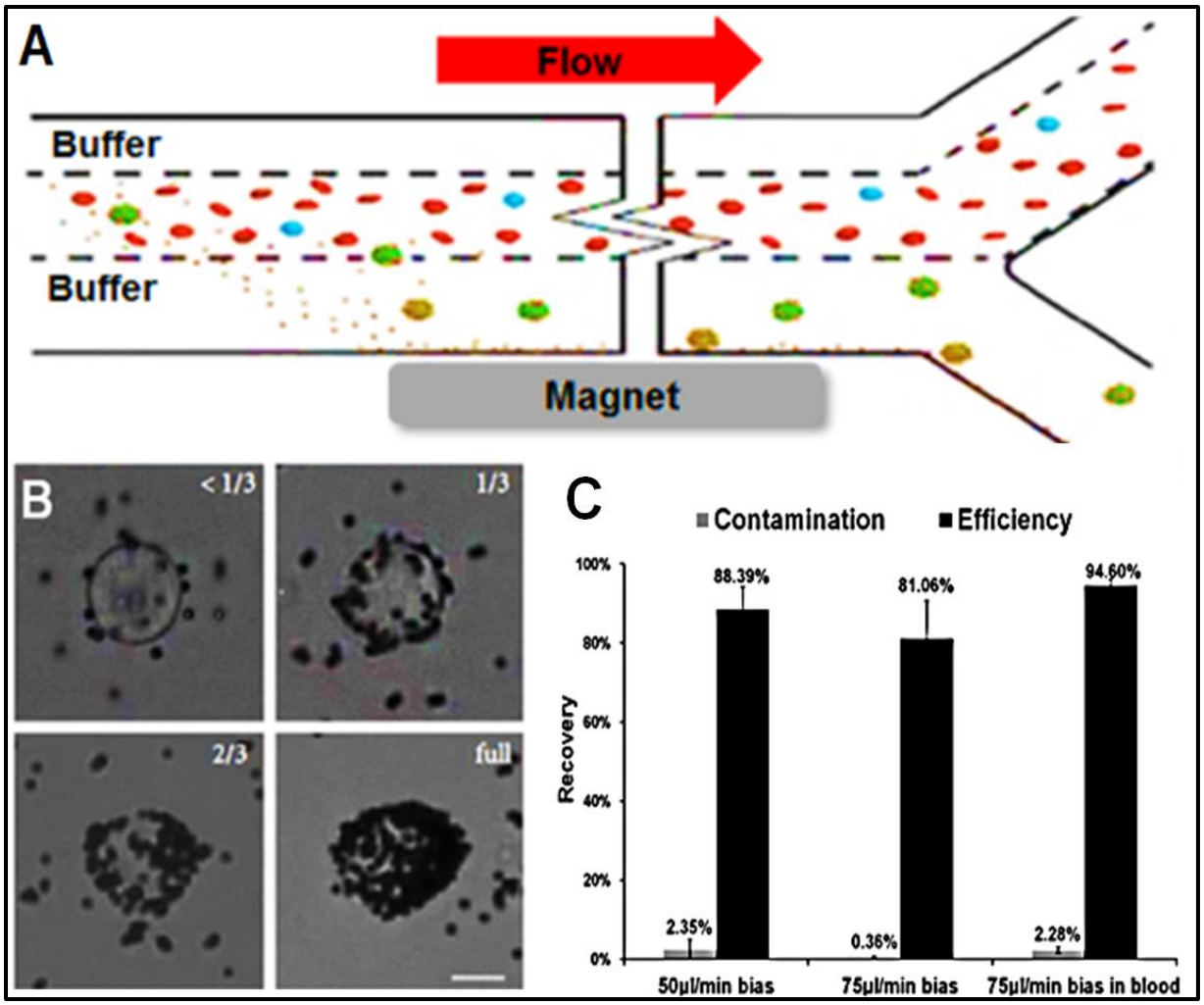

Figure 2.9: Magnetic Sorter Operation. (A) Schematic of device operation. Only magnetically labeled cancer cells get attracted and flow to the collection outlet. (B) Representative images of the categories of bead coverage used to characterize labeling of cells collected (C) Graph showing the recovery and contamination rates of PANC-1 cells and WBCs spiked in buffer for 50 and 75µL min^{-1} bias conditions and diluted blood for 75µL min^{-1} bias condition.

2.4.4 Evaluation of the IMI Device

Once the individual modules of the integrated device were fully optimized, the next step involved optimizing the connected, integrated device. Device performance was evaluated with simulated patient samples. Specifically, whole blood was spiked with PANC-1 cells and pre-isolated WBCs. Buffer and the blood sample were driven through the inertial sorter at an initial flow rate of 1200 µL/min for the buffer stream and 400 µL/min for the blood through. Magnetic beads at a 1:5 buffer dilution were flowed into the passive mixer at 100 µl/min, along with the cell suspension that emerged from the innermost outlet of the inertial sorter. The beads and cells

traveled to the reservoirs and were incubated for 5 min. After 5min, the reservoir inlet was connected to air flow to pressurize the reservoirs and then the reservoir outlet was opened for draining into the magnetic sorter to processed. The output from the collection channel of the magnetic sorter, which presumably contained a majority of magnetically labeled cancer cells, was then analyzed. The integrated device was tested with both 1000 and 100 PANC-1 cell spikes in whole blood.

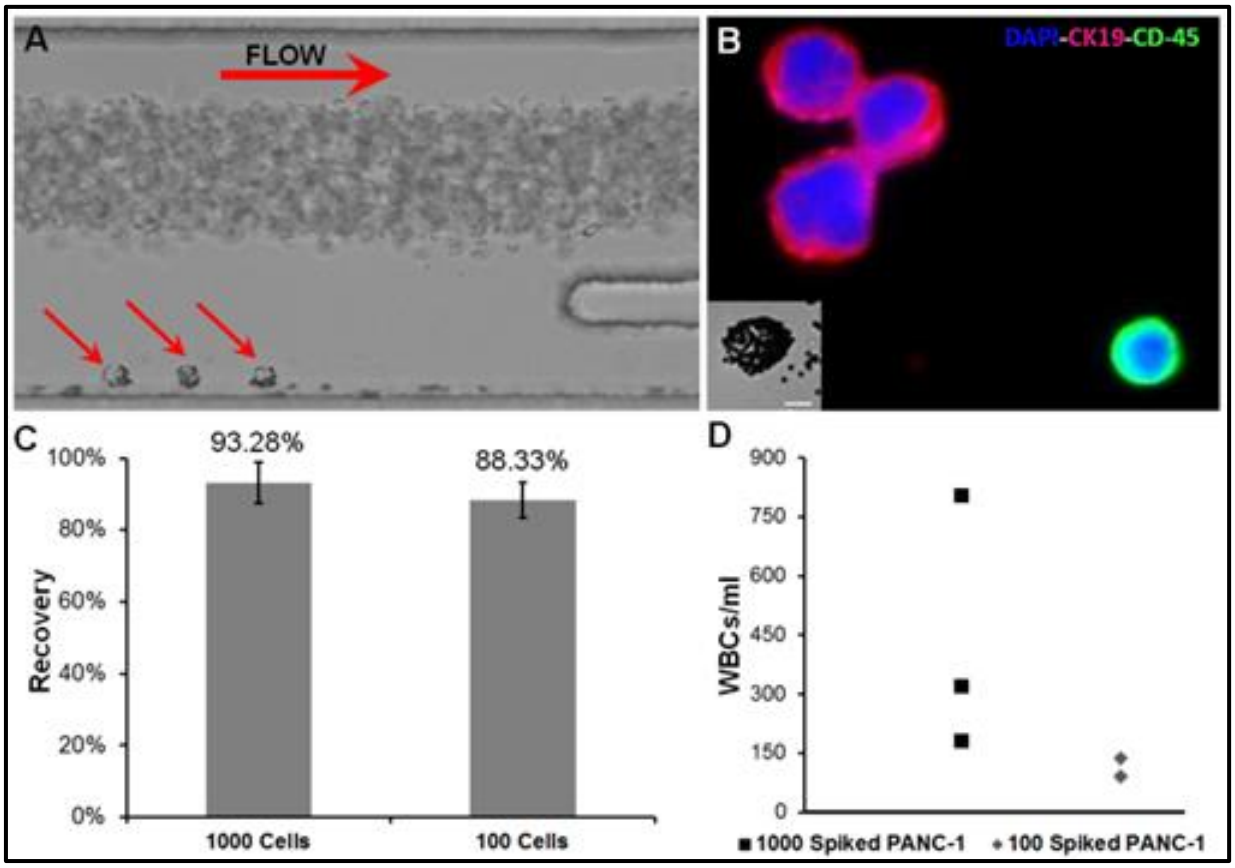

Figure 2.10: Integrated Device Operation (A) Magnetic Sorter outlets show highly enriched cancer cells separating from waste cells (B) Immunofluorescence staining used in identifying cancer cells (PANC-1) and WBCs with inset of magnetically labeled cancer cell (10 µm scale bar) (C) Recovery of PANC-1 cells spiked into whole blood at 100 and 1000 cells mL^{-1}. (D) Number of contaminating WBCs for 100 and 1000 PANC-1 cells spiked into whole blood.

As seen in Fig. 2.10 the efficiency of PANC-1 collection was nearly 90% after accounting for PANC-1 cells in all outlets. For both the 1000 and 100 PANC-1 cell spikes, WBC contamination ranged from 82-801 WBCs/ml, resulting in purities of up to 75% (Fig. 2.10D). Additionally, as previously described, cell viability of the isolated PANC-1 cells was assessed

through MTT assays and was comparable to unprocessed control cells (Fig. 2.5) ensuring culture of collected cells is feasible.

Overall, the rate limiting step of the integrated device is the magnetic sorting of the samples however this process can be sped up by multiplexing the magnetic sorters. Using the commercially available 10-syringe holder for the Harvard Apparatus syringe pumps, up to 5 magnetic sorters are easily operated simultaneously. Moreover, the combined purity and viability of the isolated PANC-1 cells makes it possible to complete sensitive downstream assays subsequent to enriching the cancer cells in the integrated device. In addition, the unprecedented purity rate achieved by the device facilitates RNA profiling at the single cell level. The purity will also contribute to successful culture of isolated cancer cells without the inconvenience of blood cells that can potentially interfere with cancer cell growth and cell imaging. The purity demonstrated by the integrated magnetic sorter is comparable to some of the other reported technologies including GEDI (68%), herringbone (14%), Ichip (1500WBCs/mL), and the CTC chip(9%) platforms for CTC enrichment. [30, 61, 153, 154]

2.4.5 Pancreatic patient CTC Isolation with the IMI Device

The patient samples (n=14) and healthy controls (n=5) were enumerated and CTC purity percentages are as reported in Figure 2.11. For all 14 patients, CTCs were isolated with counts ranging from 14-938 CTCs mL^{-1}, which was higher than the average 3 CTCs mL^{-1} for healthy controls. Notably, CTCs have been recovered from patient blood with significant depletion, on the order of 10^6 WBCs, with average CTC purity being 82.5% ±23.5. Figure 2.11A shows representative images, both of a fluorescently labeled CTC and a WBC.

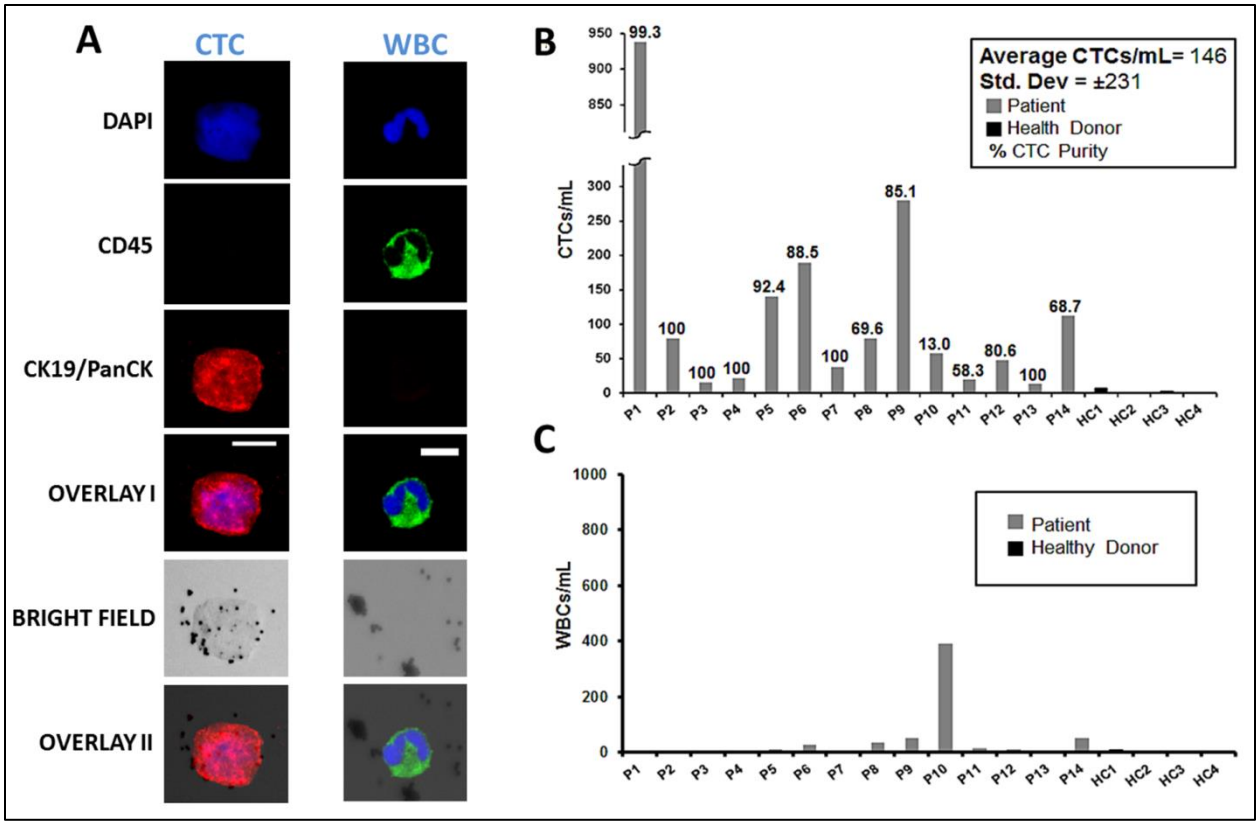

Figure 2.11: Processing PDAC patient samples (A) Fluorescent and brightfield image of a CTC (20 µm scale bar) and a WBC (10 µm scale bar) identified through immunofluorescent staining (B) Cell counts of CTCs in 1mL of patient blood. (Percent purities are indicated) (C) Corresponding WBCs for the same samples.

Table 2.3: Patient statuses for samples processed, enumerated and RNA profiled.

micro RNA Profiling					
Date	**ID**	**Vol. (mL)**	**CTCs/mL**	**WBCs/mL**	**Stage**
02/09/15	P1	5	7	2	Borderline resectable-Resected
02/09/15	P2	5	15	1	Borderline resectable

05/19/15	HC1	5.5	0	0	N/A- Healthy Control
mRNA Profiling					
Date	**ID**	**Vol. (mL)**	**CTCs/mL**	**WBCs/mL**	**Stage**
1/12/15	M1	6.5	11	0	Metastatic PDAC-deceased Aug 2015
1/26/15	L1	6.5	1	3	Locally advanced PDAC
12/15/14	B1	12	9	0	Borderline resectable
1/12/15	B2	5	161	27	Borderline resectable-Resected
12/15/14	B3	12	6	0	Borderline – Eventually developed metastasis
12/15/14	M2	12	9	0	Metastatic PDAC- Showed Progression
01/20/15	L2	5.5	12	0	Locally advanced PDAC concerning for metastasis
12/8/14	M3	7	62	1061	Metastatic- Resected – deceased Mar 2015

2.4.6 Comparing CTC mRNA profiles of metastatic versus other stages

Patient statuses for CTC samples that were molecularly profiled are reported in Table 2.3. As seen in Figure 2.12A, hierarchical clustering of mRNA expression levels from patients CTC samples resulted in all borderline profiles (B1-B3) clustering closely while two of three metastatic cases clustered apart from all other profiles. Moreover, seven mRNAs Zeb1, KLF4, cMYC, BRCA1, HER2, CD3D, and HPRT1 expression levels (indicated by the green box in

Figure 2.12A) were able to distinguish metastatic sample profiles from the other borderline or locally advanced CTC sample profiles. SPARC was also higher-expressed in the metastatic group (LogFC=4.7, p=0.037). Specifically, Zeb1 (LogFC=11.6, p=0.037) has shown to be an independent predictor of mortality in pancreatic cancer while overexpression of cMYC (LogFC=9.9, p=0.037) in pancreatic cancers was previously studied.[155, 156] The role of KLF4 (LogFC=11.6, p=0.037) as both as a tumor suppressor and an oncogene in cancer progression was previously reported.[157] Interestingly, BRCA1 (LogFC=10.9, p=0.037) was reported to be down regulated in cases of pancreatitis and sporadic PDAC.[158] Additionally previous reports have speculated on the potential of targeting HER2 amplification (LogFC=10.1, p=0.037) among PDAC patients for therapeutic purposes.[159] Aberrantly high expression of SPARC (LogFC=4.7, p=0.037) in pancreatic CTCs was also observed in both mouse and human samples.[100] Even among a small patient cohort, corroboration of reported studies by the results of CTC molecular profiling enriched by the described device shows promise in its use to ascertain information that may be specific to pancreatic CTCs.

2.4.7 Analyzing microRNA profiles of CTC samples versus healthy control samples

Of the 372 miRNAs profiled, 106 miRs demonstrated abundance in expression in both samples compared to the healthy control. 81 miRs had low expression and were categorized as not reliably detected (NRD). Interestingly, several miRs previously reported as PDAC associated, including, miR-221-3p, 210, -23a-3p, -143-3p and -21-5p were among those highly expressed in the CTC samples (Figure 2.13A).[160-163] Additionally, based on pathway analysis, the top network functions enriched in the profiles were for cancer and organismal injury and abnormalities. Pathways involving Smad2/3 and MAP2K1/2 were implicated in PDAC CTC biology (see Figure 2.13B). Moreover, for the first time we report that PDAC CTC miRNA profiling revealed a trend towards high expression of miRs 17-5p, 19b-3p, 320b and let7a-5p. Also, miR-96-3p, 216b, 155-5p, 212-3p and -31-5p which demonstrated decreased expression have been previously reported to exhibit down regulation in pancreatic cancer.[160, 161]

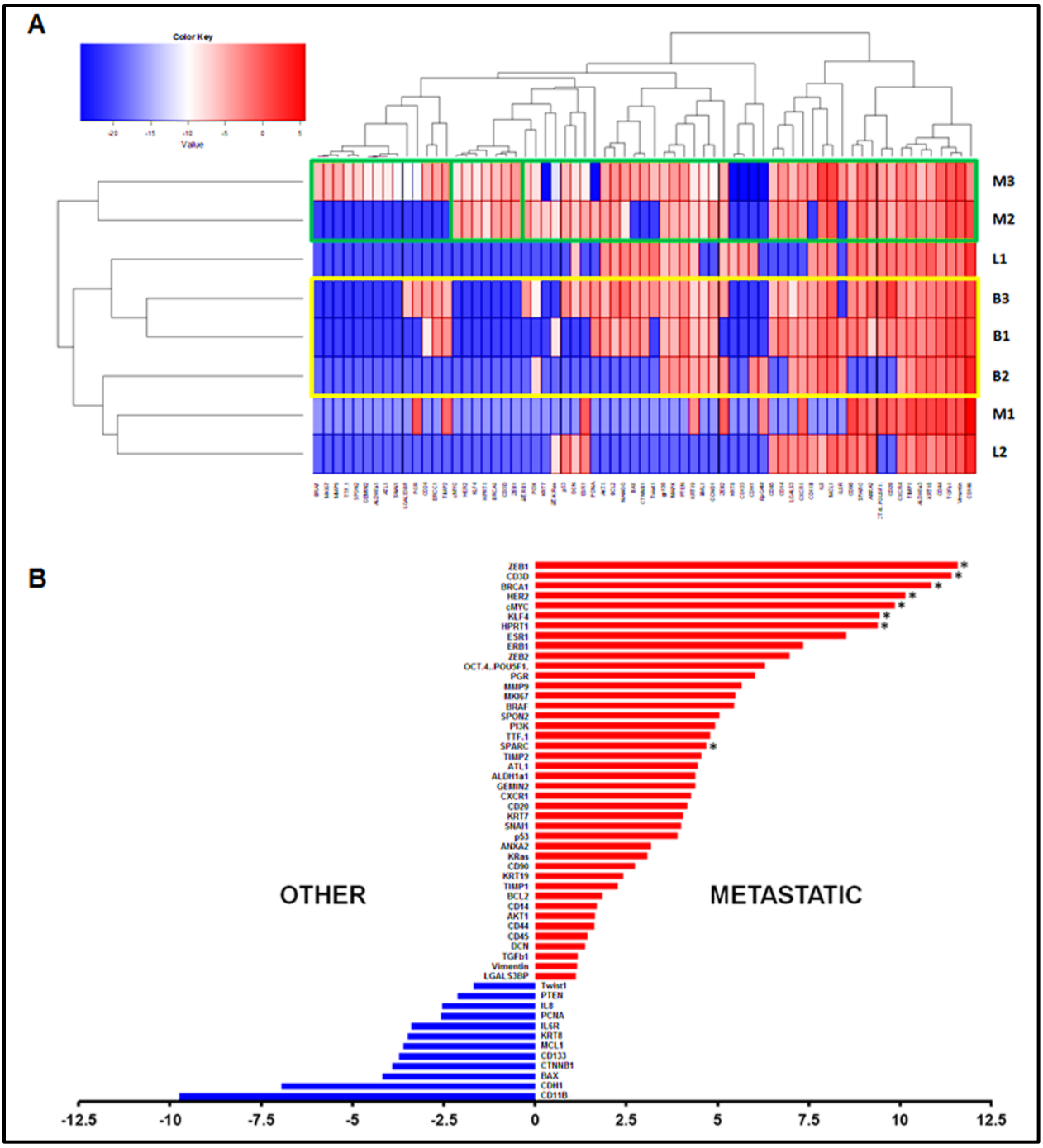

Figure 2.12: Messenger RNA profiling of CTCs enriched from PDAC samples from 3 borderline (B), 2 locally advanced (L) and 3 metastatic (M) patients p (A) Heat map plot reveal that 2 of 3 M profiles cluster together separately from others. Seven genes (green box) distinguish between the two groups. (B) Log fold increase plot of mRNAs increased in metastatic versus borderline patients. (* indicates samples with p=0.036).

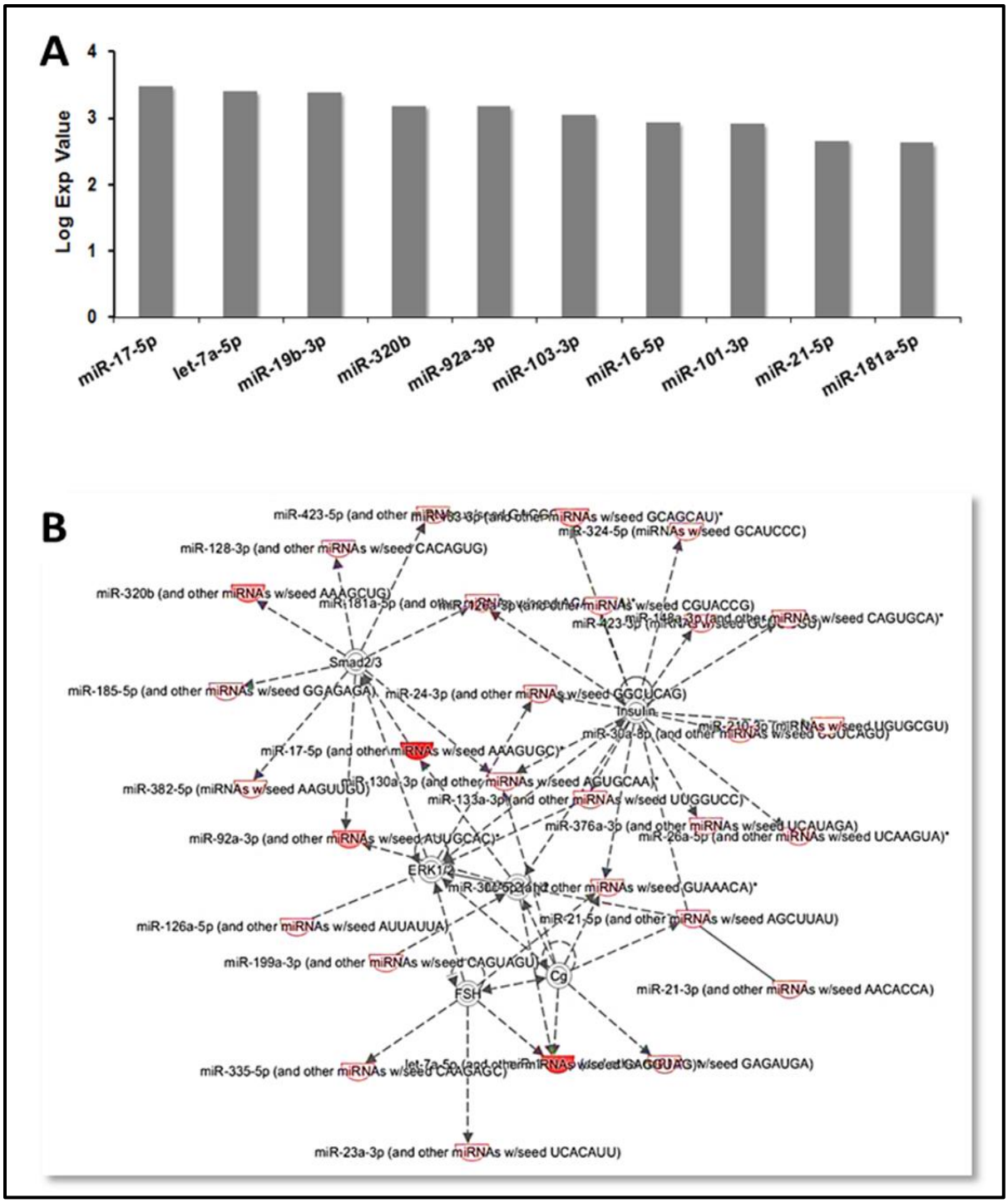

Figure 2.13: MiRNA profiling (A) Log Exp values for 10 highest expressed miRs (B) network generated in IPA that infers relationships among miRNAs with highest levels of expression. Lines, referred to as "edges" indicate inferred relationships between molecules. MAP2K1/2 and Smad2/3 pathways appear to be impacted based on the miRNA expression profile of the PDAC CTCs.

2.5 Discussion

The integrated microfluidic device described is capable of isolating significantly enriched cancer cells that are viable. The capability of collecting highly pure populations of CTCs in suspension is advantageous for subsequent cell studies including DNA or RNA analysis, gene expression profiling, or even CTC culturing and expansion. Moreover, single-cell analysis and efforts geared towards understanding the implications of tumor cell heterogeneity are gaining significant prominence. CTCs isolated in suspension are ideal for single cell analysis and related CTC studies. The device reported uses inertial sorting to perform rapid pre-sorting and de-bulking of the original sample. De-bulking the sample significantly reduces the volume to be further processed, and thus reduces the overall sample processing time required. On-chip magnetic labeling not only allows very sensitive cancer cell tagging in the absence of the majority of blood cells, but also allows for specificity, and presents an opportunity to reduce the required quantity of antibodies. Moreover, the antibodies used for on-chip labeling can be modified to select for specific populations of CTCs through use of epithelial markers, stem cell markers, or other biomarkers. Finally, with the magnetic sorter module, multiplexing the device can significantly reduce the time taken to process large sample volumes.

Since the integrated system provides the opportunity to isolate and enrich for CTCs from patient samples, we were able to perform CTC-specific mRNA and miRNA profiling for patient samples to study expression patterns unique to PDAC CTCs. The analysis of the profiling results recapitulated patterns of miRNA expression obtained from biomaterial specific to pancreatic cancer such as tumor tissue, whole blood, as well as blood plasma. Moreover, miRNAs previously reported to be dysregulated in pancreatic cancer, such as 221-3p, 23a-3p, 143-3p, 21-5p, 103 and let-7a, among others, demonstrated abundance in expression in the patient CTC samples compared to the healthy control.[163-165] Additionally, mRNA profiling revealed that mRNAs Zeb1, KLF4, cMYC, BRCA1, HER2, CD3D, and HPRT1 in were highly expressed among metastatic PDAC derived CTCs. The platform presented enables senstive studies of CTC RNA expression which, in turn, can help to identify their putative roles in cancer metastasis.

Chapter 3

Microfluidic Continuum Sorting of Sub-Populations of Tumor Cells *via* Surface Antibody Expression Levels

3.1 Abstract

The extent of inter- and intra- tumor cell heterogeneity observed in a patient's tumors appear to be directly associated with the patient's prognosis. Moreover, studies indicate that targeting distinct subpopulations of tumor cells may be more relevant to successfully managing cancer metastasis. The ability to distinguish and characterize unique tumor cell subpopulations within a given sample is thus exigent. Existing platforms separate cells based on some threshold level of phenotypic characteristics without consideration of the continuum levels of biomarker expression and the associated implications. Herein we describe how specific tumor cell groups have been immunomagnetically enriched according to a continuum of EpCAM surface marker expression levels. Even among a relatively homogenous group of cells such as the PANC-1 cell line, cells could be separated according to their EpCAM levels into low, moderate and high expression. To functionally assess each subpopulation, a wound healing assay was performed which revealed distinct invasive potentials among each subset. Furthermore, the clinical relevance of the approach was demonstrated by isolating pancreatic cancer CTCs from the same patient sample based on their EpCAM levels. We demonstrate a robust method of isolating CTCs based on varied levels of EpCAM expression, which enables studies of tumor cell heterogeneity. Interestingly, 5 of 6 patient samples had CTCs that could be recovered at all three levels of EpCAM expression, though the majority of CTCs were recovered as low expression events.

Preliminary studies that compare tumor cell subpopulations in this continuum manner can potentially increase our understanding of the dynamic nature of tumor cell heterogeneity and how it relates to patient outcomes. Furthermore investigations as such may reveal therapeutic targets among the different tumor cell subpopulations.

3.2 Introduction

The clinical ramifications of tumor heterogeneity have been demonstrated in a number of studies that investigate the levels of heterogeneity among patients and how these levels correlate with patient outcomes.[166-168] It is believed that genetically distinct subclones that comprise tumors cooperate to facilitate tumor growth and progression and as such, tumor heterogeneity is thought to be necessary for sustained tumor growth progression.[169, 170] Identifying the heterogeneous populations of cells that comprise tumors has influenced decisions in patient treatment as interpatient tumor heterogeneity provides a platform for molecular biomarker testing and predictions of patient response.[171] Moreover observations that such biomarkers may evolve over the clinical course, has led to increased focus on the impact of intratumor heterogeneity in patients.[171] In light of the significance that tumor heterogeneity plays, whether among different patients or within a single tumor from a patient, the need to sensitively and reproducibly interrogate tumor heterogeneity is imminent.

Furthermore, a small subset of tumor cells is thought to be responsible for the metastatic cascade in many solid tumors.[172, 173] These cells acquire the ability to disseminate from the tumor and travel through the vasculature before initiating a secondary tumor at another site, demonstrating biological properties that are distinct and crucial to metastasis. Circulating tumor cells, (CTCs) represent prime targets in the fight against metastasis. Therefore the ability to isolate and interrogate different subtypes of CTCs can potentially open many clinically beneficial avenues towards cancer management. [15, 100]

One approach that adopted for tumor cell sorting is fluorescently activated cell sorting (FACS) with tumor cells that have been digested from tumor tissue or tumor derived cell lines.[174, 175] FACS has been universally employed for sorting cell subpopulations as it conveniently allows rapid cell measurement readouts of 10^4 cells s^{-1}. Additionally the limit of detection of 1 fluorescent cell is 10^{-6} and multiple cell surface markers can be analyzed simultaneously. Typically cells are sorted according to high and low levels of surface markers of

interest based on their fluorescence intensity where most studies so far, gate and separate cell subpopulations based on very high (positive) and very low (negative) expression of proteins of interest. Thus cell sorting is carried out without considering the continuum levels of phenotypic characteristics and the associated implications with respect to tumor cell heterogeneity. Apart from its costliness, FACS sorting becomes less advantageous when small numbers of cells are considered, as is often the case with rare CTCs from patient samples. Using FACS to sort the few CTC events that occur among billions of other blood cells represents a less sensitive approach that can potentially become time consuming and impractical.[173, 176, 177]

To sort cells according to their varying levels of surface marker expression one study reported development of a nanoparticle mediated microfluidic cell sorting approach that used velocity valleys to slow and trap cells.[178] Purities were 19% when target cells were trapped from blood and overall throughput was 2mL hr^{-1}.[178] Currently, the majority of molecular assays that are performed subsequent to CTC isolation necessitate high purities so that molecular profiling and analysis that is specific to CTCs can be obtained. Previously, the integrated magnetic system demonstrated highly sensitive and robust CTC isolation through inertial presorting of whole blood, followed by immunomagnetic CTC labeling and magnetic CTC sorting.[148]

By implementing simple alterations and a strategic workflow to the magnetic sorter module, we demonstrate the ability to isolate distinct groups of tumor cells immunomagnetically, according to their levels of surface protein expression. Essentially the magnetic field strength experienced by magnetic particles under flow in the microfluidic channel was manipulated by adjusting the distance of the external magnet from magnetic particles flowing in the sorter. As a result, cancer cells that were immunomagnetically labeled with 1μm magnetic beads were sorted based on the different levels of magnetic bead attachment among them. In addition, the clinical utility of the device was demonstrated by processing pancreatic ductal adenocarcinoma (PDAC) blood samples from 6 patients and characterizing the isolated CTCs from these samples. Tumor cells were isolated based on low, moderate and high EpCAM levels and were studied and compared to determine any detectable differences such as detection rate, and morphological features. Thus, we demonstrated that even with cells that occur at a low frequency among non-target cells, this approach can be applied in their isolation.

3.3 Methods

3.3.1 Evaluating Cancer Cell EpCAM protein levels

The feasibility of the immunomagnetic continuum sorting concept is predicated on heterogeneity in surface protein expression levels among the target cell. Thus we evaluated the differences in surface protein expression levels of cells within the same cell line passage to establish the practicality of the approach. EpCAM protein expression was studied since EpCAM is widely expressed among CTCs and is extensively used as the CTC capture antibody.[179] Additionally, the pancreas adenocarcinoma PANC-1 cell line was selected as a relevant reference alongside the PDAC patient samples that were included in the study. To characterize the levels of EpCAM on PANC-1 cells, it was assumed that for viable cancer cells that are mixed and allowed to incubate with antibody-coated, magnetic microbeads, the quantity of magnetic bead attachment to a cell indicates the available protein on the cell surface, provided that neither incubation time nor bead availability are limiting factors. To determine the distribution of EpCAM protein level among PANC-1 cells, cells were incubated with magnetic beads for 5, 10, 15 and 30min and then immediately imaged for the level of bead coverage on the cells. After 30min, there was negligible increase in cell bead coverage with beads compared to the 15min incubation period which supported the idea that incubation time was not a limiting factor. Each cell was categorized as having a surface coverage level of magnetic beads of either none, <1/3 (low), 1/3 to 2/3 (moderate) or >2/3, (high) coverage (see Figure 3.1A).

The magnetic sorting module is part of the previously reported integrated immunomagnetic microfluidic device shown in Figure 3.1B.[148] The device was previously implemented to isolate rare CTCs from whole blood at a throughput of 24 mL h^{-1}. The blood sample is first presorted to reduce erythrocyte and leucocyte contaminants, after which the sample mixes with magnetic beads on chip, followed by immunomagnetic sorting of magnetically labeled CTCs. Typically, the resulting sample is a significantly enriched suspension of CTCs.[148] Based on the continuum of protein expression levels displayed by cells from the same passage, the next step was to determine whether the magnetic sorter module (outlined in Figure 3.1B) could be leveraged to effectively separate cell subpopulations based on incremental differences in protein expression. Figure 3.1C shows that for a cell suspension under flow in the magnetic sorter, an external magnet which is placed parallel to the main sorter channel attracts only magnetized cells to the collection outlet with high purities by separating them away from unlabeled cells.

We hypothesized that by adjusting the separation distance between the flowing cell suspension and the magnet at the micron scale, the magnetic field strength experienced by the magnetized cancer cells could be tuned. In so doing, the magnetic force experienced by cells could be tuned so that subsets of cells could be isolated based on their varying levels of magnetic bead coverage and thus, according to their levels of protein expression. Figure 3.1D illustrates the approach we hypothesized to separate cells from the same cell suspension according to low, moderate and high levels of EpCAM expression. For a wide separation gap only cells with very high magnetic bead attachment would experience a magnetic force strong enough to separate them from the flowing cell suspension. The effluent waste of the first magnetic sorter, now depleted of cells with high magnetic bead coverage would then be processed through a magnetic sorter with a narrower separation gap so that cells having moderate bead attachment would be separated from the rest of cells into the collection stream. Ideally, the effluent waste of the second magnetic sorter, now depleted of cells with moderate bead coverage would contain cells having low to no bead attachment. Therefore cells from the same population would be separated according to low, moderate and high EpCAM levels.

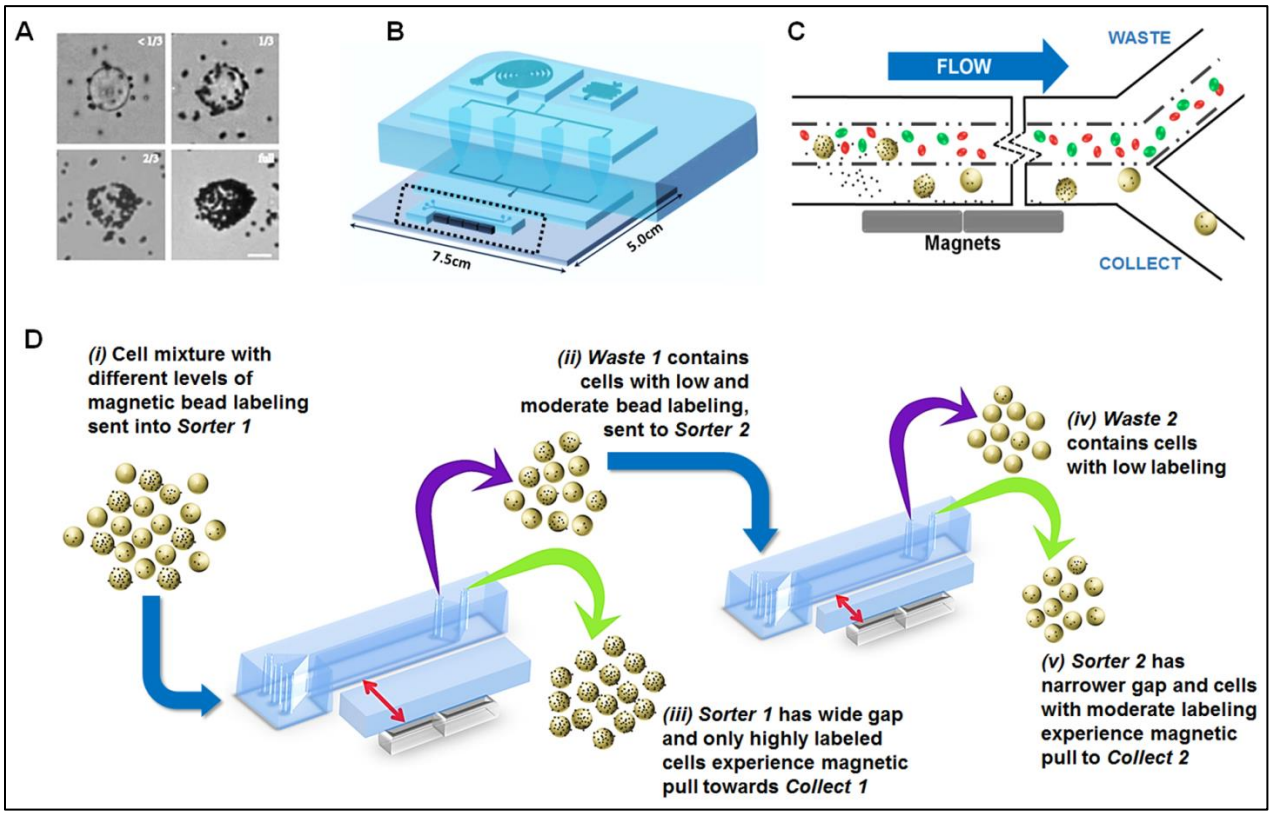

Figure 3.1: Implementing Magnetic Sorter module for continuum sorting (A) Sorter outlined in illustration of the integrated magnetic cell sorting platform (B) Schematic of magnetic sorter outlets used to collect magnetized cancer cells (Scale bar represents 10μm). (C) Categories used to evaluate cell-magnetic bead coverage (D) Schematic of 2-tier magnetic sorter process used to isolate 3 cell populations based on low, moderate and high levels of protein expression.

3.3.2 Tuning Magnetic Flux density to isolate cell subpopulations

The magnetic flux profile in Figure 3.3A, generated in COMSOL, shows the variation of magnetic flux densities developed by a magnetic bead in the microfluidic channel, positioned at either the near edge (blue line) or far edge (black line) of the magnetic sorter where "near" and "far" represent distances from the magnet. Since the magnetic flux density decreases with increasing distance from the magnetic source, adjusting the distance between the magnetic particle and the external magnetic source alters the strength of the magnetic force experienced by the magnetized particle. Additionally, the intensity of the magnetic force is dependent on the magnetization of the magnetic particle, which correlates with the number of beads attached to each cell. By tuning the strength of the magnetic force developed via adjustment of the gap distance, cell subsets having low, moderate and high magnetic bead coverage and therefore expressing low, moderate and high EpCAM levels, respectively, could be individually isolated.

Figure 3.3B shows the distribution of flowing cells in the magnetic sorter. As indicated by the rightmost arrow, the largest vertical distance a magnetized cell needs to traverse to be pulled into the collection channel, L_y, is 150μm. In the absence of beads or a magnet, and with sample input flow at set at 50 $\mu L min^{-1}$cells were tracked under a high speed camera in laminar flow through the microchannel and the cell linear velocity in the x-direction (u_x) was determined to be 125mm s^{-1}. So for a channel length, L_x=25mm in the direction of flow, the time that a cell is exposed to the magnetic field, or its residence time, t_r was determined to be 0.2s. Based on these calculations, it is implied that a cell needs to travel a vertical distance, L_y, of 150μm in 0.2s. Consequently, for t_r= 0.2s and L_y= 150μm, the minimum vertical traversing velocity, u_y, of the cell to successfully enter the collection channel is 750μm s^{-1}. Achieving this velocity is dependent on cells having sufficient magnetic bead attachment to experience a sufficient magnetic force, F_M, to magnetically pull them towards the collection channel. The minimum required bead attachment for a cell in turn, is dependent on the separation width, such that as distance increases, the minimum number of beads required increases.

To determine how the magnetic sorter separator width affected the minimum bead coverage required for a cell to be deflected and separated into the collection channel, four different separator widths, (400, 1200, 2300 and 3400μm) were studied. For a superparamagnetic microparticle exposed to a magnetic field range that saturates its magnetization, velocities are proportional to the magnetic field gradient. Assuming electrostatic and van der Waals forces are negligible and the magnetic force F_M dominates, the drag force acting on the particle balances F_M and so Stokes law can be applied.[180, 181] Thus, under laminar flow, the magnetic force can be approximated such that,

$$3\pi\eta u_t D_{bead} = F_{D\,bead} = F_{M\,bead} \qquad (1)$$

where η is the fluid viscosity, u_t is the terminal velocity in the direction perpendicular to flow (which was approximated by tracking bead movement across the channel), D_{bead} is particle diameter, and F_D is the drag force.[180, 181]

By the same token, for a magnetized cell,

$$3\pi\eta u_t D_{cell} = F_{D\,cell} = F_{M\,cell} \qquad (2)$$

Given that each bead attached to a cell contributes equally to the total $F_{M\,cell}$, F_M of the total number of beads is taken to be equal in magnitude to cell magnetic force and thus the cell drag force, $F_{D\,cell}$. Moreover, the minimum magnetic bead attachment required by a magnetized cell for it to be deflected to the collection channel was determined by the magnetic force required to achieve a cell velocity of 750μm s^{-1}.

For the magnetic beads, the only unknown, u_t was estimated by tracking and measuring the movement of a single magnetic bead in the microfluidic channel as demonstrated in Figure 3.3C. In Figure 3.3C (i), y_0, t_0 corresponds to initial bead position at time 0s while y_1 and t_1 correspond to positions 1 at time t_1, and y_2 corresponds to position 2 at time 2. For each width, to determine the velocities of the particles, magnetic beads were placed into the microfluidic channel and initially directed, magnetically to the channel edge further away from the designated position of the permanent magnet, at y_0, t_0. Then the permanent magnet was positioned at the designated gap distance and the movement of particles towards the permanent magnet, from y_1 at time t_1 to y_2 at t_2 was video recorded using a predefined frames-per-second (fps) rate. For each

gap width, the velocity of a single magnetic bead, $u_t=u_{y(bead)}$ was determined based on these values.

For *N* number of beads attached to a cell,

$$F_{M\ cell} = [N \bullet F_{M\ bead}] \qquad (3)$$

By Stokes law,

$$[D_{cell} \bullet u_{y\ cell}] = [N \bullet D_{bead} \bullet u_{y\ bead}] \qquad (4)$$

Recalling that the minimum required bead velocity for successful deflection is 750µm s^{-1} and taking cell diameter as 20µm, for 1µm beads,

$$N = [20\mu m \bullet 750\mu m\ s^{-1}] / u_{y\ bead} \qquad (5)$$

Using this approach, the minimum number of beads required for a cell to be isolated at each different separator width can be determined. In turn, this shows how cells from the same sample could be separated according to levels of low, medium and high protein expression, using the system.

3.3.3 Establishing a workflow for continuum magnetic sorting of cells

Considering the proposed workflow for separating cells according to their continuum level of EpCAM expression (Figure 3.1D), two different magnetic sorter gap widths, one narrower and one wider, were required for continuum cell sorting. To determine the most effective 2-sorter combination of widths that would facilitate isolation of relatively low, moderate and high EpCAM expressing cells, the four magnetic sorters of different gap sizes were each tested with magnetic bead-labeled cancer cells. This range of widths (400-3400µm) was specifically selected to avoid magnetic bead buildup in the channel. Bead buildup occurs with gaps that are too narrow, which leads to beads becoming entirely immobilized within the channel. Additionally, the range was selected to avoid too weak a magnetic field strength with gaps so wide that no magnetic particles or cells get magnetically deflected to the collection outlet. Firstly, each sorter was tested individually to evaluate the bead attachment on the cells isolated in both its waste and collection channels. A cell suspension was prepared at a spiking

rate of 10^3 cells mL^{-1} from PANC-1 cells that were labeled with EpCAM conjugated magnetic beads. Based on previous flow rate optimization with the magnetic sorter module, 1mL of the suspension was driven through the sorter at 50 µL min^{-1} with the upper and lower buffer streams flowing at 25 and 75 µL min^{-1} respectively.[148] To evaluate and compare the ability of the devices to effectively sort magnetically labeled cells, the bead attachment of cells in the collection and waste outlets were analyzed.

Then, to evaluate the effectiveness of the different 2-sorter combinations to sort cells according to low, moderate and high EpCAM levels, labeled cancer cells (10^4 cells mL^{-1}) were processed using the decided workflow. Then FACS analysis was performed to determine the level of EpCAM on the magnetically separated cell subsets. Once cells were sorted based on low, moderate and high EpCAM levels, the samples were analyzed using the MoFlo Astrios EQ flow cytometer. The samples were gated based on the relative EpCAM fluorescence intensity of the unstained, negative control using Summit 6.3 software. FACS dot plots of particle size (FSC-1 Height) versus particle fluorescence intensity (EpCAM log FL10 height) for control unstained cells, and for cells sorted according to low, moderate and high protein expression levels are shown in Figure 3.3C. To better quantitate and compare the relative levels of EpCAM in each of the magnetically sorted populations, FACS readouts of cell fluorescence intensities were analyzed by converting the FSC files to CSV files using Flowjo software.

3.3.4 Scratch Assay of Cell Subpopulations

Traditionally scratch assays have been carried out to investigate the relative proliferation and migration rates of mammalian cells, which in turn, could be indicative of the invasive potential of cells.[182, 183] To investigate whether the samples sorted according to varied EpCAM protein levels would display unique physiological differences beyond surface EpCAM expression, a scratch assay was carried out on cell subsets sorted according to low, moderate and high EpCAM levels. A control population that was not processed through the magnetic sorters was also investigated for comparison. To conduct the scratch assay, 3mL of a sample containing viable, EpCAM-bead labeled PANC-1 cells was processed through the 2300µm magnetic sorter gap. The cells emerging from the collection channel of this wider sorter was designated as high expression. Then the waste effluent was processed through the 1200µm magnetic sorter so that the cells emerging from the collection channel was plated and designated moderate expression

while the waste channel was designated low expressing cells (see Figure 3.6A). Once low, moderate and high expressing cells were plated, the cell count in each well was adjusted by resuspending the cells so that cell densities would be comparable among the four samples.

Additionally, EpCAM-bead labeled cells from the same cell line passage, that were not magnetically sorted, were plated at a comparable cell density to use as a control. To perform the scratch, for each well, once ~80% confluence was achieved in the well, a scratch was performed using a micropipette tip on day 0 and the healing rate of the scratch was monitored by capturing images of each well on day 1 and then each day until the scratch healed or up to day 13. By measuring the rate at which the scratch was repopulated with new cell growth over the cleared surface for each sample, the invasive potential among the samples could be compared. For each scratch, on each day three measures of the scratch width were taken and the average width was recorded. The rate of scratch healing was determined for each condition by plotting the average scratch width (μm) as a function of time (days).

In determining the healing rate for each sample, normalization was conducted based on cell density recorded immediately after plating each sample. The change in scratch width was divided by cell density for each condition, each day and plotted as a function of time. Figure 3.4C is an example of a plot obtained for the control condition. As an estimate of the scratch healing rate, the negative slope of the scratch healing rate was compared among the four conditions. Additionally to investigate whether cells would maintain these relative EpCAM expression levels after sorting, cells sorted according to the continuum approach of low, moderate and high EpCAM expression were cultured for six days. On day six cells were relabeled with EpCAM beads and incubated for 20min. Images of cells from each group were immediately taken and bead attachment on cells was quantified.

3.3.5 Continuum isolation of PDAC derived CTCs

To determine whether a continuum isolation approach could be useful in the context of patient derived CTCs, six PDAC patient samples processed using the established sorting method. The goal was to determine whether subsets of CTCs in the patient samples could be isolated based on the level of their EpCAM expression. For each sample, 5mL of patient blood was presorted using the inertial spiral sorter of the previously reported integrated microfluidic system.[148] The effluent of the spiral was then directly mixed with EpCAM magnetic beads on

chip via the passive mixer and the mixture was allowed to incubate for 20 minutes. The sample was then processed using the established workflow to sort the CTCs according to low, moderate and high levels of EpCAM. CTCs were identified as cells staining positive for nuclear content with DAPI, being panCK+ or CK19+ and CD45-. In most instances, EpCAM bead labeling served as an additional means of identifying epithelial derived CTCs.

3.4 Results

3.4.1 Cancer Cell EpCAM protein levels

Results of cancer cell line labeling with magnetic beads are as shown in Figure 3.2. Even after 30min of incubation, almost 3% of PANC-1 cells still maintained <1/3 bead coverage, thus indicating a relatively negligible EpCAM expression among those cells. 8% of cells had >2/3 bead coverage, indicating high expression levels of EpCAM in this subset of cells. MiaPACA-2 cells, which are known to express low EpCAM levels, were tested as a control, using the same procedure. For MiAPaca-2 cells, as much as 64% of cells showed <1/3 EpCAM bead coverage after 30min of incubation. Based on these results from magnetic bead attachment, PANC-1 cancer cells from the same passage, which are relatively homogenous compared to tumor cells in circulation, demonstrate different levels of protein expression. In turn, this supports the heterogeneity that exists among cells within the same tumor and points to the possibility of sorting cells according to some continuum of surface-protein expression levels.

3.4.2 PANC-1 isolation according to low, moderate and high EpCAM levels.

Figure 3.3D shows how bead velocity u_y varies with gap widths where, as the gap width increases, u_y appears to decrease linearly. This relationship affects the number of beads required for cells to be sorted successfully given the sorter dimensions and sample flow rate of 50µL min^{-1}. For instance, based on such calculations, with a gap size increase from 400 to 1200µm, the minimum number of beads required increases 1.2 fold while an increase to 3400µm requires a 7 fold increase in the minimum number of beads required (see Figure 3.4A). Overall, it can be seen that at sufficiently large of a gap size, only cells having relatively high bead attachment can be magnetically deflected and collected, while cells having fewer beads remain in the waste stream. Based on these results, this approach enables cells from the same sample to be separated according to levels of low, medium and high protein expression.

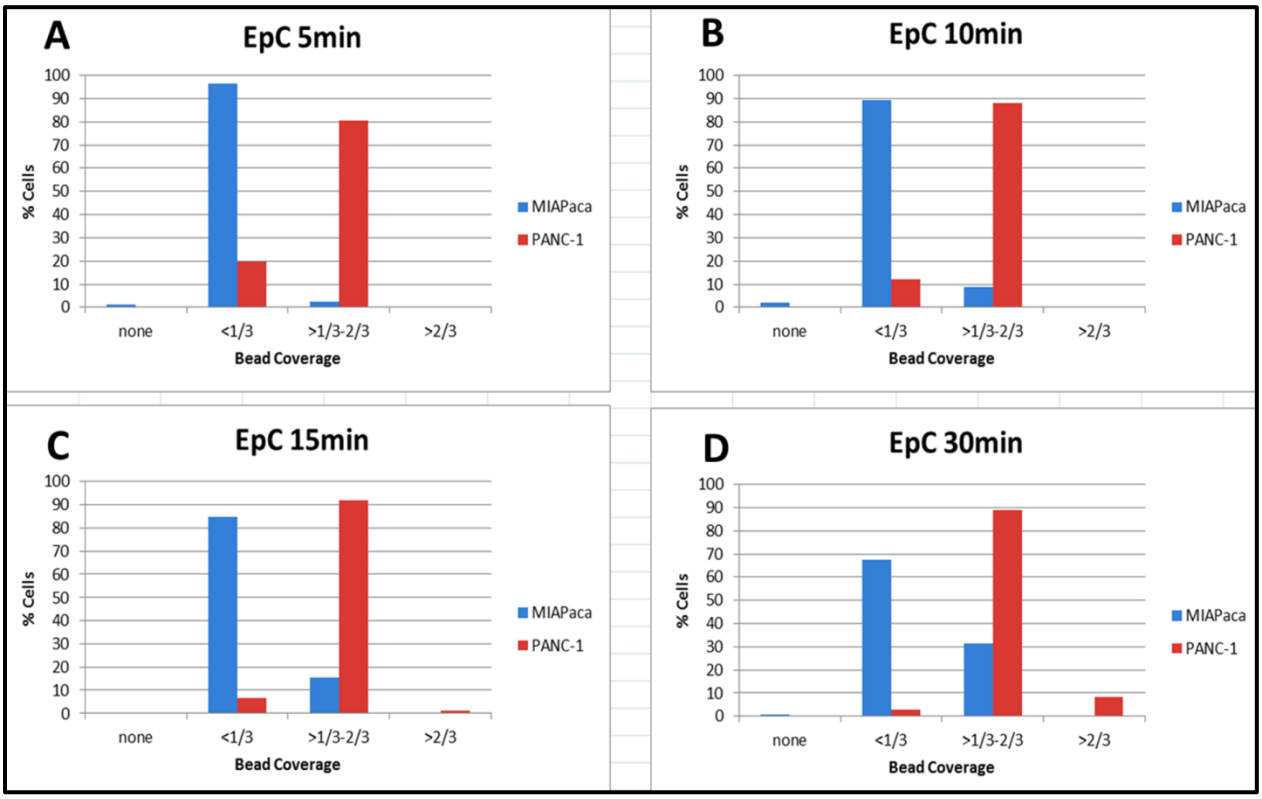

Figure 3.2: PANC-1 and MIAPaCa-2 EpCAM bead labeling. Cells and beads undergo static incubation for 5-30min resulting in ~3% of PANC-1 cells and >65% MIAPaca-2 cells with <1/3 bead coverage after 30min incubation.

Among the four sorters, as the gap size increased there was an increase in the percentage of cells that have full bead coverage in the collection samples (Figure 3.4B). Interestingly, as the gap size increased the percentage of cells having entirely full bead coverage increased, yet the overall recoveries of cells with >2/3 bead coverage decreased. This indicated that cell isolation in the 3400µm sorter required extremely high (full) bead attachment to be successfully isolated. As such, gap widths of 1200µm and 2300µm were selected for the 2-sorter separation workflow where there is a significant increase in the fraction of cells having extremely high EpCAM expression sorted from the 2300µm sorter compared to the 1200µm sorter. The procedure adopted to sort cells in a continuum manner involved initial cell sorting through a sorter with 2300µm gap to collect high EpCAM expressing cells. This is followed by cell sorting of the waste outlet through a sorter with 1200µm gap to collect moderate EpCAM expressing cells from the collection outlet and low EpCAM expressing cells from the waste outlet.

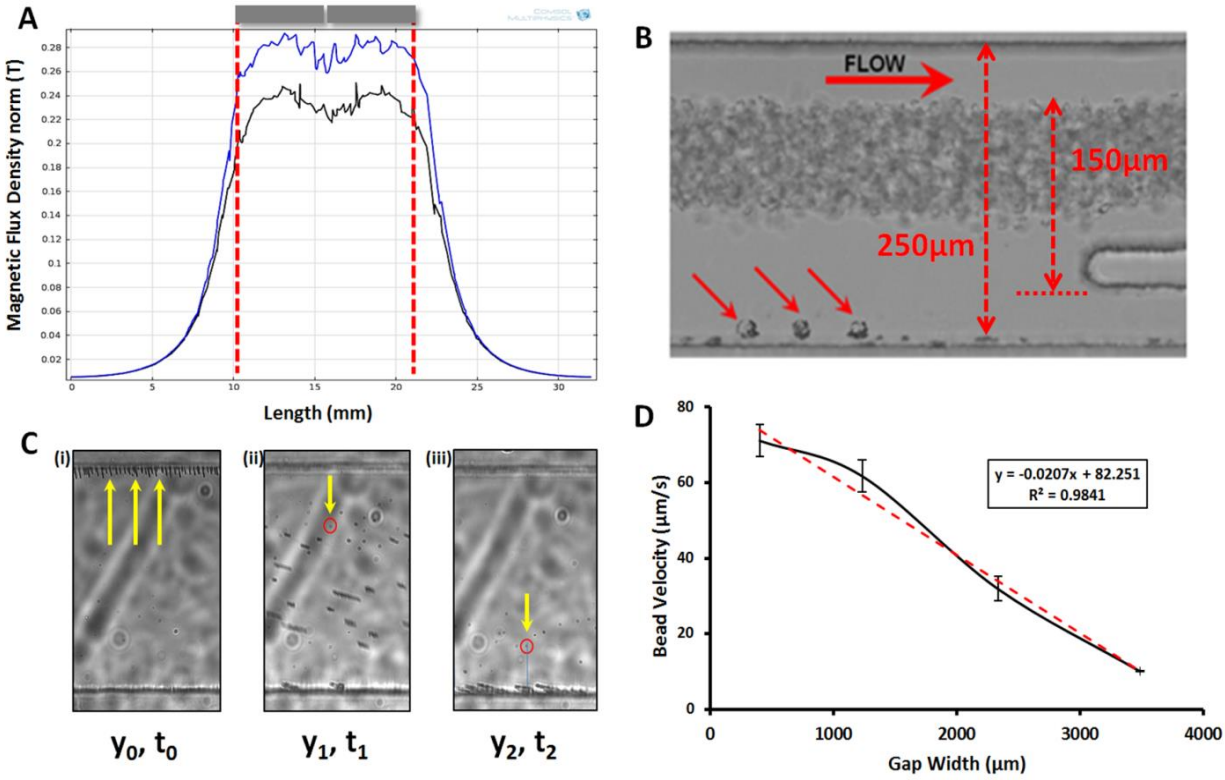

Figure 3.3: Controlling Particle Magnetic Force (A) COMSOL simulation of magnetic flux density at the near edge (blue line) and far edge (black line) of the channel in relation to the external magnets. (B) The sample is confined to middle of magnetic sorter channel with only magnetic labeled cells deflected and separated (C) Tracking a single magnetic bead to determine bead velocity dependence on (D) Plot shows how bead velocity varies as a function of gap distance between magnet and channel.

Analysis of the FACS data gave detailed information about the level of EpCAM expressed within each cell subset, beyond what was immediately observable with the FACS dot plots. As seen in the histogram plot in Figure 3.4D, the fraction of cells expressing the highest EpCAM fluorescence of logFL10 height of ≥4 increased in moving from low to moderate to high EpCAM expression. Additionally, in moving from low to moderate to high EpCAM expression, there was a progressive decrease in the fraction of cells with lowest EpCAM expression. Therefore these FACS results are in agreement with results obtained from brightfield imaging analysis of bead coverage on cells from the three samples.

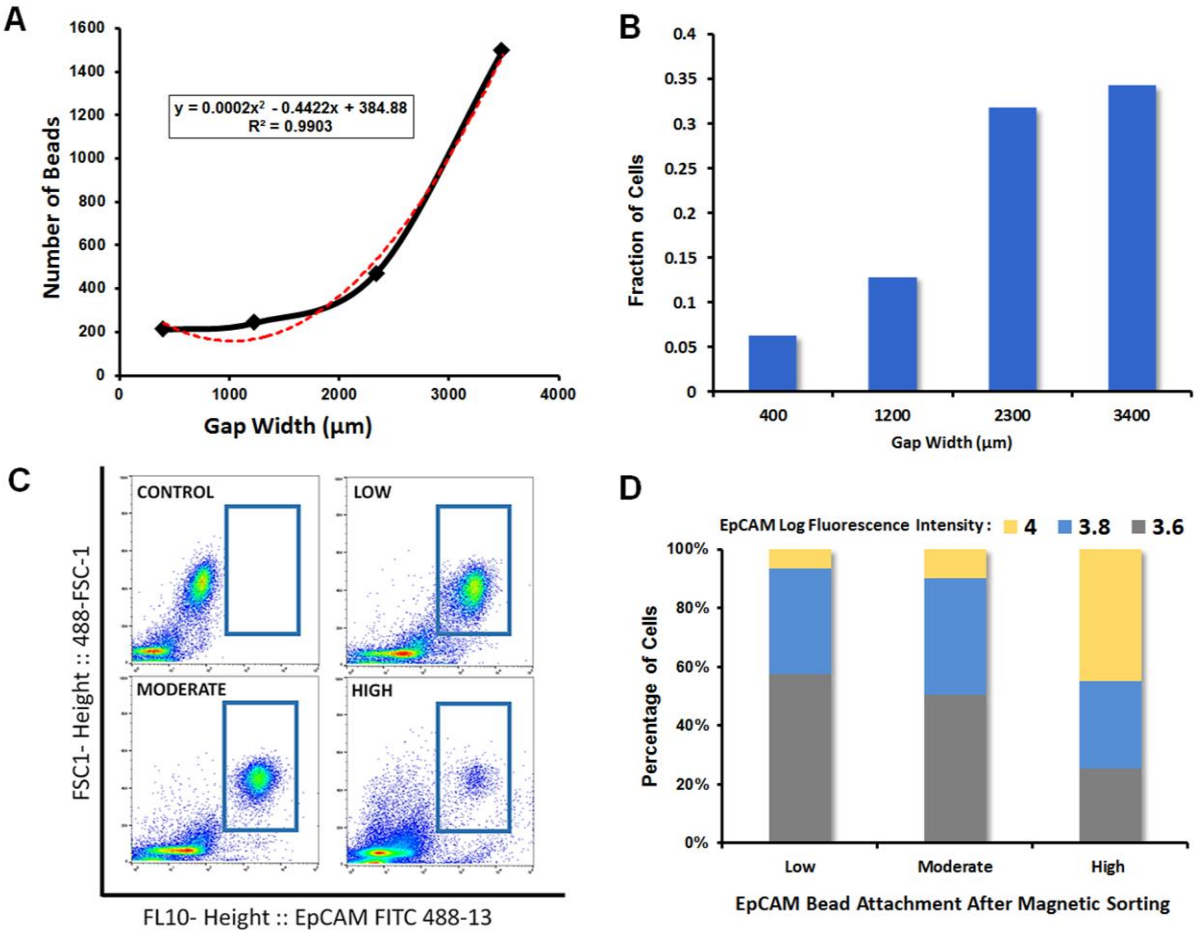

Figure 3.4: Tuning Magnetic Force to sensitively isolate cell subpopulations (A) Effect of magnetic sorter gap width on amount of cell-magnetic bead coverage required for cell isolation (B) Effect of gap width on isolation of cells with full magnetic bead coverage and on recovery of cells with >2/3 bead coverage. (C) FACS dot plots and (D) FACS histogram of EpCAM protein detected from PANC-1 cells isolated according to low, moderate and high EpCAM protein expression.

Figure 3.5 shows that even after six days of culturing, cells that were sorted according to low, moderate and high EpCAM expression appear to maintain the same relative EpCAM expression levels. Cells originally sorted according to low EpCAM expression showed 43% of cells with <1/3 coverage compared to 40% and 8% among moderate and high expressing cells respectively. Conversely, cells expressing high EpCAM levels had 64% of cells showing full surface coverage of cells compared to ~40% of cells in both low and moderate expressing subsets. Overall, the cells that were originally sorted as high EpCAM expressing cells maintain the highest percentage of cells with full bead coverage while the group of cells isolated as low EpCAM expressing cells demonstrate the highest percentage of cells with <1/3 bead coverage.

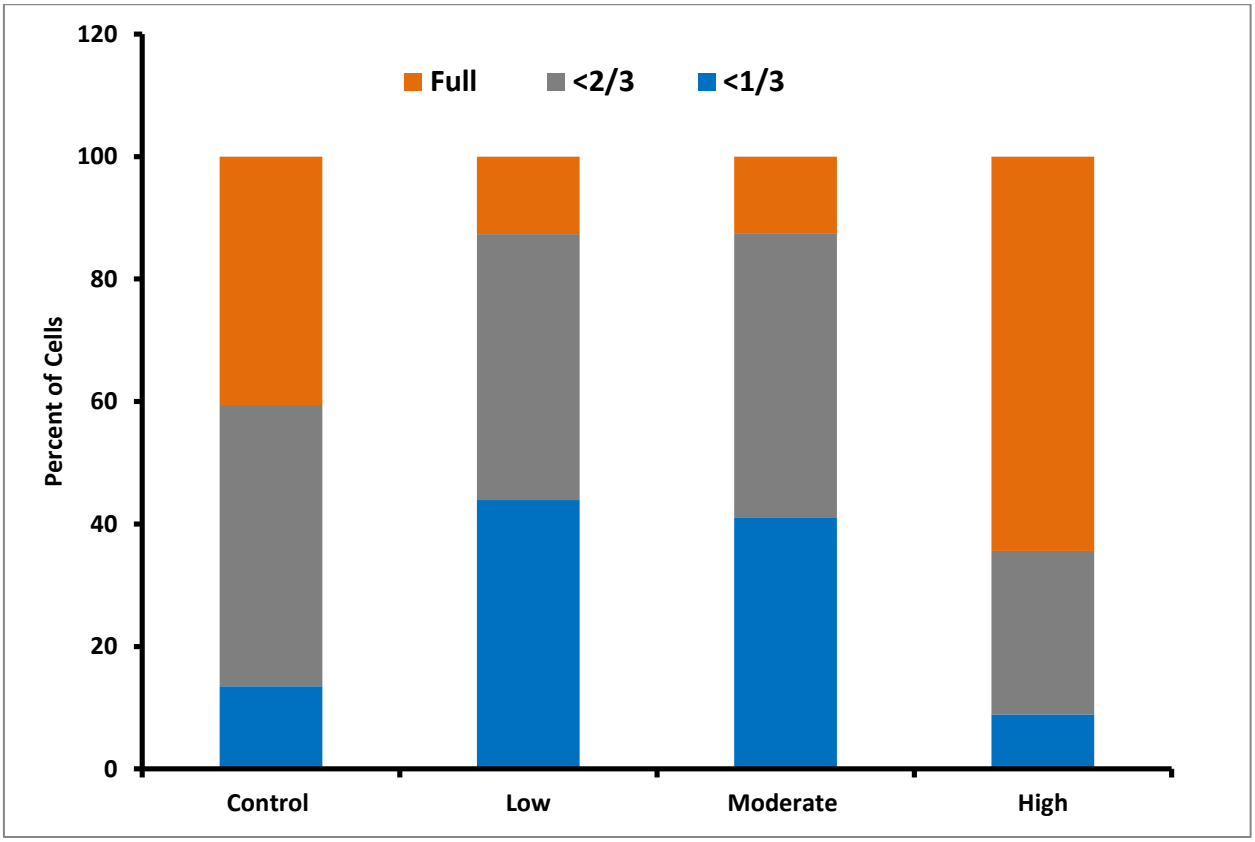

Figure 3.5: Evaluation of EpCAM bead binding to sorted and cultured PANC-1 cells. Cells were sorted according to low, moderate and high EpCAM expression then cultured for 6 days and relabeled with EpCAM beads.

3.4.3 Comparing scratch-healing rates among cell subpopulations

The procedure carried out for the scratch healing assay is illustrated in figure 3.6A where healing rates for cells sorted according to low, moderate and high EpCAM expression were monitored. Figure 3.6B is an example of the scratch healing rate plot obtained for the control condition showing an initial scratch width of ~1mm on day 1, which decreases to 500μm by day 5. Figure 3.6C shows the relative scratch healing rates for each condition, which factored in the initial cell seeding density recorded for each well. As seen in Figure 3.6C the level of EpCAM expression on cell subpopulations appears to directly correlate with the scratch healing rate such that, as the level of EpCAM increases, the scratch healing rate also increases. The control population of cells appears to heal more rapidly than cells isolated according to low protein levels. While the bio-physiological basis for these results needs to be further investigated, results demonstrate that the continuum sorting approach was able to separate cell subpopulations that

display unique phenotypic qualities after being cultured. This was reflected in the different scratch healing rates of the unique cell populations.

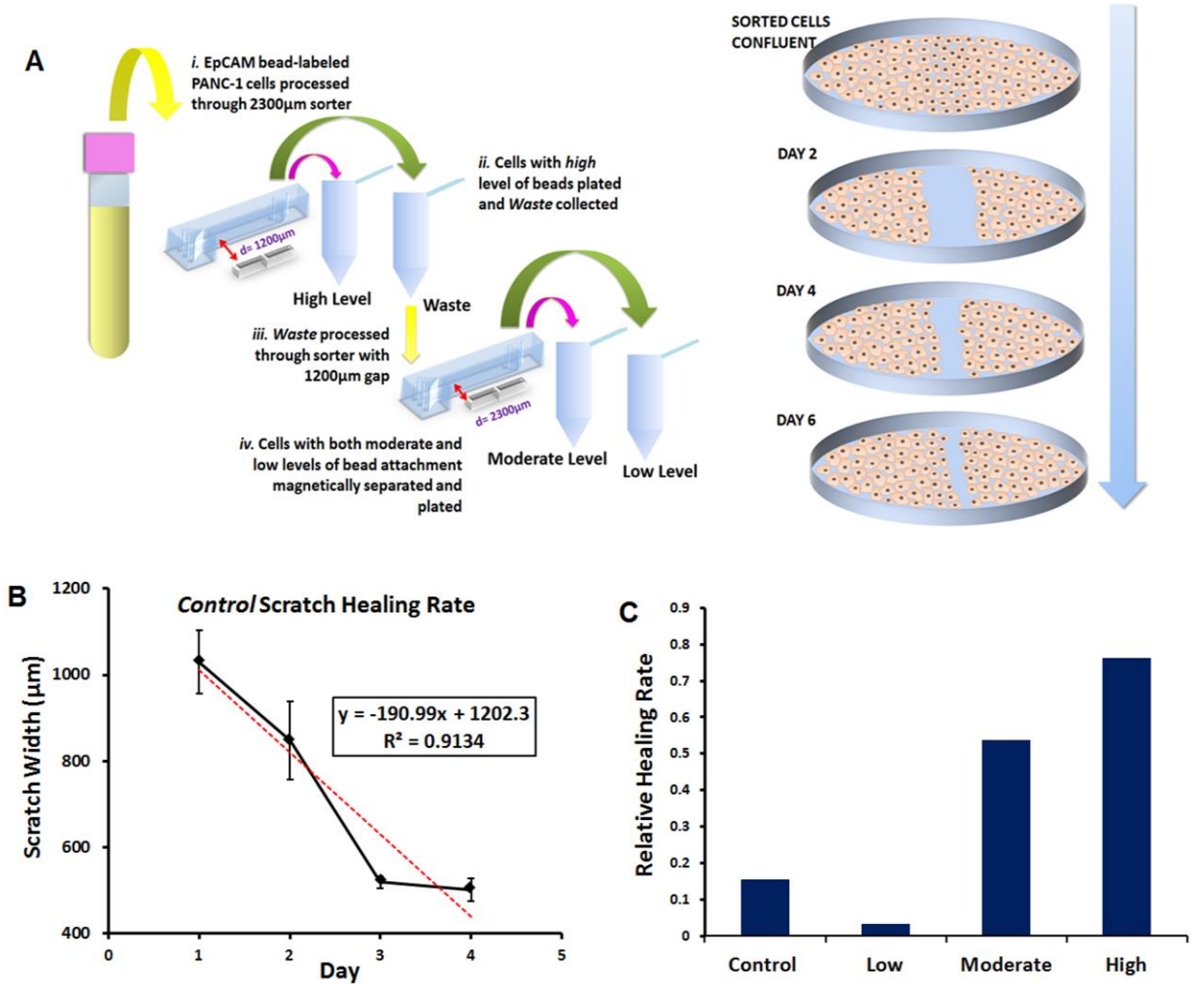

Figure 3.6: Tumor Cell Scratch Assay of low, moderate and high EpCAM levels (A) Schematic of process used for isolating cells according to 3 varying levels of EpCAM and performing scratch assay with isolated cells (Arrow indicates time progression from day 0 to time of scratch healing). (B) Example of plot of scratch healing rate for control sample (C) Normalized growth rates for cell subpopulations based on EpCAM expression levels

3.4.4 CTC isolation according to low, moderate and high EpCAM levels

Results for the six PDAC patient samples that were sorted according to the established EpCAM based continuum sorting approach are shown in Figure 3.7A. Among the 6 patients, the majority of CTCs appear to express low levels of EpCAM (mean = 66.2% ±23.45) compared to

moderate (mean = 12.9% ±11.87) or high (mean = 20.9% ±20.23) expression levels. Figure 3.7B shows brightfield and immunofluorescent images of CTCs isolated based on low, moderate and high EpCAM expression levels. Especially with brightfield capture, the heterogeneity among CTC EpCAM expression can be readily observed. In turn, this points to the potential to discriminate among different CTC subpopulations according to their surface protein levels using the approach described.

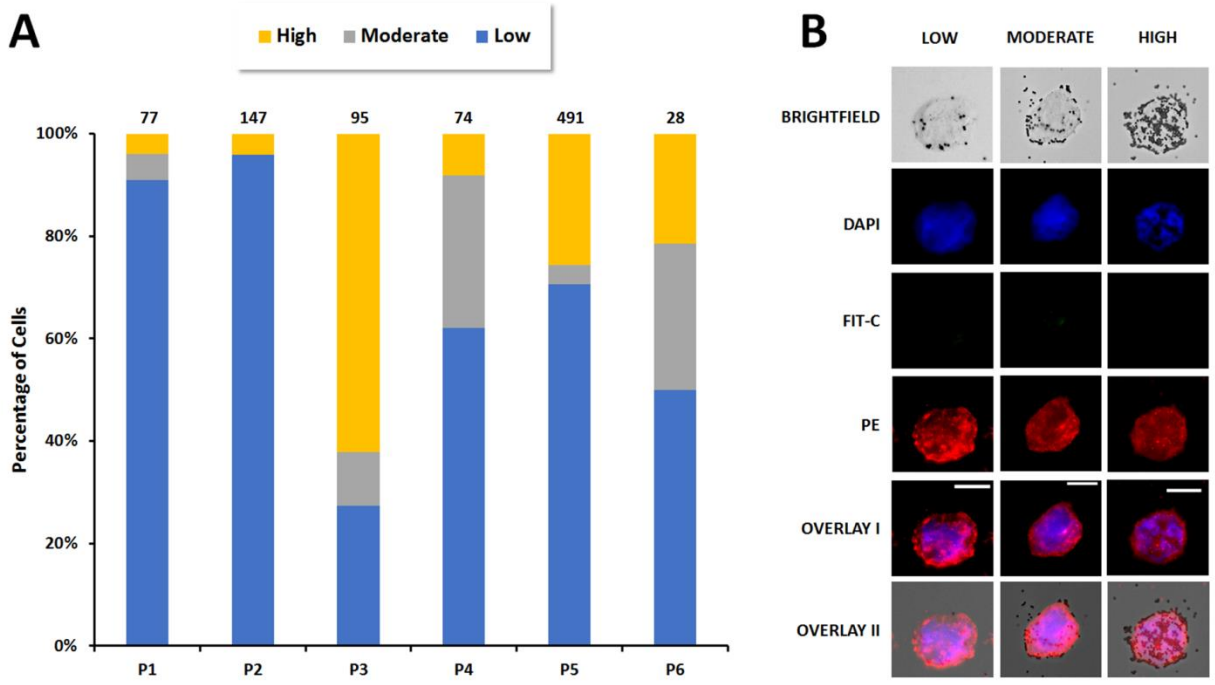

Figure 3.7: Continuum isolation of PDAC CTC (A) Percentage of CTCs isolated according to low, moderate and high EpCAM levels. CTCs/mL for each patient is indicated above bar. (B) Brightfield and immunofluorescent images of CTCs isolated based on low, moderate and high EpCAM expression levels (Scale bars represent 20μm).

3.5 Discussion

Numerous reports so far have described probable mechanisms of cancer metastasis, and how distinct cell subpopulations that comprise the tumor may uniquely contribute to the invasive metastasis cascade. Therefore, platforms to separate tumor cells according to their different subpopulations are crucial. Most studies characterize tumor cells according to positive and negative expression of proteins of interest without consideration of moderate expression of

protein levels. Here we report isolation of PANC-1 tumor cells according to low moderate and high levels of EpCAM protein. FACS analysis on the samples corroborated the ability of the described approach to sort cells according to EpCAM expression levels. Additionally, characterization of tumor cells according to such categories revealed notable differences among the three groups based on invasive properties. Furthermore, processing PDAC patient samples according to the continuum sorting approach revealed that the majority of PDAC samples contain CTCs that were categorized at all three expression levels. We have demonstrated a sensitive and reproducible approach to isolate cancer cell populations according to a continuum of surface protein expression levels and demonstrated the clinical relevance of the system via CTC isolation. The work represents a step towards studying the complexities of tumor cell heterogeneity, as evidenced by a detectable continuum of surface protein expression among cell lines as well as circulating tumor cells.

Chapter 4

Dual-Marker Isolation and Characterization of Pancreatic Ductal Adenocarcinoma Circulating Tumor Cells *via* EpCAM- and CD44- based Immunomagnetism

4.1 Abstract

While the significance of epithelial-to-mesenchymal transition (EMT) programs to tumor cell heterogeneity and the invasive metastasis cascade are currently being elucidated, their anticipated roles have led to increased efforts to identify and characterize different tumor cells subpopulations. Moreover, characterization of circulating tumor cells (CTCs) based on their stemness or cancer-initiating potential has buttressed some proposed mechanisms of metastasis that implicate the concept of cancer stem cells. Apart from the established epithelial marker EpCAM, expression of the stem cell marker CD44, among pancreatic cancer CTCs has taken on particular importance since these cells demonstrate an enhanced metastatic potential. To study whether CD44-based CTC isolation would contribute to any immediate differences among CTCs enriched from pancreatic cancer samples, we analyzed CTCs from ten patient samples isolated via an immunomagnetic approach. Magnetic beads conjugated with anti-EpCAM as a standalone antibody or in combination with anti-CD44 conjugated beads were used. Results show that within this patient cohort there was no significant difference ($p=0.328$) in detection rates between EpCAM+CD44 dual isolation (average CTCs/mL=64±63) compared to EpCAM only isolation (average CTCs/mL=42±33). Additionally, among the 8 samples in which CTCs appeared in clusters, their detection was independent of whether standalone EpCAM or EpCAM-CD44

combination was used (p=0.593). Of note, CDKN1A (p=0.0140, logFC=11.586) as well as HSP27 (p=0.0044, logFC=10.139) were more highly expressed in samples with >50% CTCs in clusters, to a significant degree. In contrast, ERCC1 (p=0.0140, logFC=-2.856), CTNNB1 (p=0.0460, logFC=-13.473), PARP1 (p=0.0068, logFC=-7.231), as well as FBXW7 (p=0.0350, logFC=-7.231) were all expressed more highly in samples with <50% CTCs in clusters, to a significantly extent. Interestingly, among patients with borderline resectable/resected disease, CTC mRNA profiles for EpCAM-CD44 isolation clustered distinctly from those isolated solely with EpCAM (n=5). This distinction was not observed among patients with borderline unresectable/unresected disease (n=3). Though preliminary, studies as such can be used in further characterization of pancreatic cancer metastatic advance.

4.2 Introduction

The putative role of circulating tumor cells (CTCs) in cancer metastasis has led to rapidly increasing interest in these rare, blood-borne cells as they hold the potential to understand how cancer thrives and spreads in a facile, clinically relevant manner.[184] Furthermore, the epithelial-to-mesenchymal transition (EMT) of primary tumor cells, where cells evolve from an epithelial state to become more motile and intravasate into the circulation, is thought to be the first stage of the invasion metastasis cascade.[185, 186] After these cells extravasate from the circulation to a distant site, they are thought to regain their epithelial characteristics in order to seed micrometastases at a distant location, in the reverse process, termed mesenchymal to epithelial transition (MET).[187] More recent studies support the existence of a hybrid epithelial/mesenchymal phenotype wherein cells have undergone a partial or incomplete EMT. These cells are believed to exhibit stemness and are thought to be a major target in fighting disease relapse and metastasis.[185, 186, 188]

Cancer stem cells (CSCs) represent a subset of CTCs thought to have self-renewal capacity with the ability to regenerate the distinct subpopulations of cells that comprise the original tumor.[189, 190, 191] Studies in breast cancer have demonstrated how progressive overexpression of EMT markers in carcinomas is associated with acquisition of the stem cell marker CD44, in addition to demonstrating that CTCs display an enhanced EMT program.[104, 192]

So far several studies have reported on CSC expression of CD44 and ultimately on the important role CD44 plays in the progression of many tumor types including pancreatic cancer.[193, 194] While these cells account for a small percentage of all tumor cells, they are highly resistant to apoptosis and have been implicated in metastasis even after extended periods of dormancy. They are believed to be directly responsible for the persistence and spread of cancer in many solid tumor cancers, including pancreatic cancer.[191 190] Identification of a highly tumorigenic subpopulation of pancreatic cancer stem cells was reported that expressed the markers CD44, CD24 and ESA.[27] One report described how a CD44+ subpopulation of pancreatic cancer cells was able to reproliferate and regenerate a gemcitabine resistant cell subpopulation after high dosage exposure to the chemotherapy.[195] In fact findings from initial preclinical trials support the idea that CSC functioning can be ablated by therapeutic targeting of CD44.[194] Understanding the role of CD44 in the functioning of these cells in metastasis is becoming more relevant to current efforts aimed at treating and monitoring patients.

Additionally, the detection of CTCs grouped in cell clusters, also described as circulating tumor microemboli (CTMs), has been the topic of interest of more recent CTC studies [196-198 173, 177] These cells co-express epithelial and mesenchymal markers.[186] Studies involving cancer patients as well as animal models indicate that CTC clusters have an enhanced ability to mediate cancer metastasis compared to single CTCs.[173, 177] The presence of multicellular clusters in one breast cancer patient accompanied an increase in mesenchymal CTCs. Interestingly, such clusters appeared to be absent from samples in which the majority of CTCs had an epithelial phenotype.[104] Detection of CTC clusters was also reported in patients with varying stages of non-small cell lung cancer (NSCLC).[196-198] So far few studies have described the isolation and characterization of clusters derived from pancreatic ductal adenocarcinoma (PDAC). One report described the detection of clusters in 4 out of 18 pancreatic cancer patients through the use of an enrichment free immunofluorescence approach.[199] Another study which employed the commercially available ISET platform, reported cluster detection in 3 of 10 pancreatic cancer patients as well as the presence of both epithelial and mesenchymal markers on cells comprising the clusters.[115] A recent study reported on detection of CTMs in 81% of PDAC patients, demonstrating that CTM detection could be an independent prognostic factor of overall survival.[177] Taken together, focus on the clinical significance of cluster appearance in cancer patients can potentially shed more light on metastasis.

The integrated microfluidic magnetic cell sorter is amenable both to single CTC isolation and CTMs in an enriched manner, so that the cells are made available in suspension for subsequent analyses.[148] The platform first presorts cancer cells using size based inertial sorting, allows the enriched CTCs to be labeled with CTC-specific antibody coated magnetic beads, then further sorts the cells using immunomagnetism to obtain a highly enriched CTC suspension. Previously EpCAM was used as a standalone antibody for CTC isolation with this platform. Given the importance of CD44+ tumor cells in circulation and driven by the concern that standalone EpCAM CTC isolation could potentially preclude detection of this important subset of CTCs, we adapted the platform to allow CD44 based CTC isolation. Following we report on comparison of CTCs and CTMs isolated using both EpCAM and/or CD44 from pancreatic cancer patients. Molecular characterization of CTCs was also performed to determine whether patterns associated with the different isolation approaches could be observed.

4.3 Methods

4.3.1 Evaluation of cancer cell immunomagnetic isolation using cells lines

To evaluate the dual marker immunomagnetic isolation approach with EpCAM and CD44 in the integrated device, cell line experiments were carried out using MIA PaCa2 and PANC-1 pancreatic cancer cell lines. Anti-EpCAM- and anti-CD44- antibody coated magnetic beads were used to magnetically isolate cells during testing. Firstly, as a control experiment each cells line was incubated with a mixture of both types of beads to evaluate bead-cell labeling. As seen in Figures 4.1A and 4.1B, different size beads were used to distinguish between antibodies. 1μm beads are coated with anti-CD44 antibody while 2.85μm beads are coated with anti-EpCAM antibody. Figures 4.1A and 4.1B are representative images of the extent of magnetic bead labeling of PANC-1 and MIAPaca2 cells respectively. Overall, MIAPaca2 showed negligible labeling with EpCAM beads with more significant labeling with CD44 beads. PANC-1 cells experienced a significant extent of labeling with EpCAM coated beads while labeling with CD44 beads appeared relatively low. Therefore PANC1 and MIAPaca2 cells demonstrated preferential antibody-based bead labeling with EpCAM and CD44 respectively.

Given these results of preferential bead labeling, further experiments were carried out to characterize magnetic sorting and isolation of a mixture of the magnetically labeled cancer cells using each marker. Specifically, PANC-1 cells (dyed with CellTracker Red) and MIAPaca-2

cells (dyed with Cell Tracker Green) were separately incubated with 1μm EpCAM beads for 40min and then fixed. The same procedure was carried out with each cell line using 1μm CD44 beads. Then for each marker, a cell suspension was prepared by evenly spiking PANC-1 and MIAPaca2 cells at 10^4 cells mL^{-1} in buffer. The sample was then processed through the magnetic sorter module of the integrated device, using either anti-EpCAM or anti-CD44 coated beads separately for magnetic sorting. For each marker, experiments were repeated x3. Cells emerging from the collection channel of the magnetic sorter were scanned and analyzed for the number of PANC-1 cells (red) and MIAPaca-2 cells (green) successfully sorted.

4.3.2 EpCAM- versus CD44- based CTC isolation

Ultimately the ability to isolate and compare CTCs using dual marker isolation can potentially reveal tumor cell biology pertinent to EMT and metastasis.[148] The previously reported integrated microfluidic immunomagnetic approach for CTC isolation was optimized to isolate CTCs expressing both EpCAM and CD44 surface proteins (see Figure 4.1D).With the whole blood samples obtained from patients, the blood was first processed through the inertial sorter to presort CTCs from other blood cell contaminants. The CTC enriched sample was then mixed and incubated for 20min with 1μm magnetic beads coated with either anti-EpCAM or anti-CD44, or a combination of the two types of beads. Then the sample was processed through the magnetic sorter to isolate CTCs labeled with magnetic beads. To directly compare EpCAM and CD44 CTC detection rates , in one patient cohort (n=8), 5mL of sample was divided into 2, with half of the sample processed using EpCAM beads while the other half was processed using CD44 beads. The final samples that emerged from the magnetic sorter were then centrifuged to reduce the volume for immunofluorescence staining. The samples were then cytospinned and fixed to do immunofluorescence staining for CTC identification and enumeration.

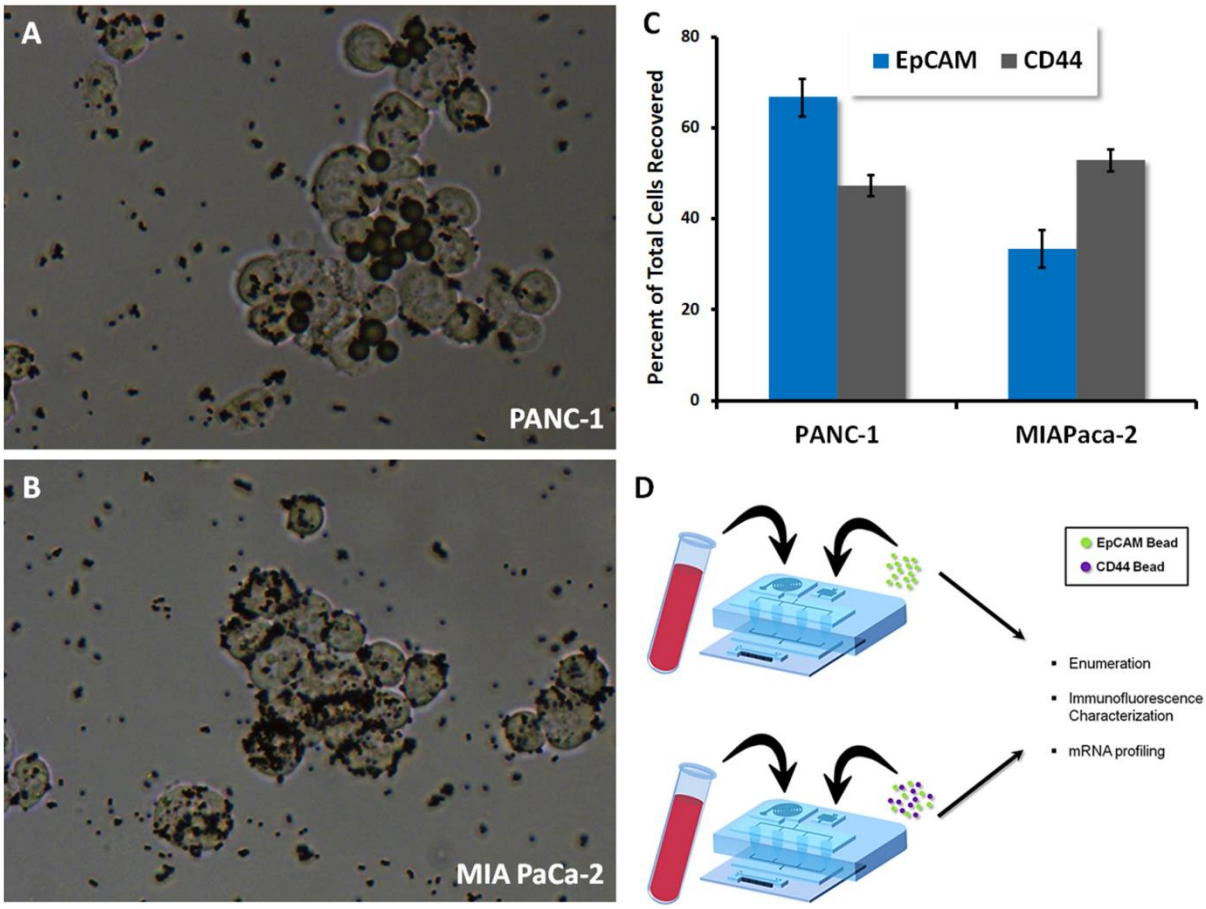

Figure 4.1: Dual Isolation of CTCs. (A) PANC-1 cells shows significant extent of labeling with 2.85µm EpCAM coated magnetic beads 1µm magnetic beads coated with CD44 compared to 2.85µm EpCAM coated magnetic beads. (B) MIAPaca-2 cells shows preferential labeling with 1µm magnetic beads coated with CD44 but negligible labeling with 2.85µm EpCAM coated magnetic beads (C) Magnetic Sorting results of cancer cell line experiments using 1µm EpCAM and CD44 coated beads (D) Schematic depicting dual isolation workflow for CTCs using EpCAM and CD44.

4.3.3 Comparing Vimentin expression among EpCAM- versus CD44- isolated CTCs

Studies show that the more aggressive CSCs that are responsible for cancer relapse express markers that are relevant to the EMT process. One such EMT marker is Vimentin which is expressed by mesenchymal cells.[200] Additionally, in this patient cohort, Vimentin staining was carried out with 6 of the 8 patient samples to determine if there were any correlations with Vimentin expression and the isolation antibody used. To identify four markers with immunofluorescence staining, specifically cytokeratins, CD45, Vimentin and DAPI, the CTC staining protocol was modified. Samples were stained for cytokeratin-19, panCK, and Vimentin

as positive stains while the leucocyte marker CD45 was used as a negative stain. DAPI was used to identify nuclear content. AlexaFluor 647 (Life Technologies) was used for immunofluorescence labeling of Vimentin.

4.3.4 Dual Marker Isolation for molecular profiling studies

Recent studies support the existence of a hybrid epithelial/mesenchymal phenotype wherein cells have undergone a partial or incomplete EMT implicit of which is the continued expression of epithelial markers such as EpCAM. It is these cells that are believed to exhibit stemness and are thought to be a major target in fighting disease relapse and metastasis. Given this possibility of a sustained expression of EpCAM among the more stem-like CTCs, we isolated and compared CTCs among patients using EpCAM and a combination of EpCAM+CD44. Apart from CTC enumeration studies, CTCs were also molecular profiled for mRNA expression levels. In this patient cohort (n=10), half of the 5mL sample was processed using a suspension of EpCAM beads while the other half was processed using a combination of EpCAM and CD44 beads. Samples were processed as previously described. In order to determine CTC detection rates as well as leucocyte contamination, a small volume of the resulting cell suspension for each type of isolation approach was immunofluorescently stained for cytokeratin-19 and panCK as positive stains while the leucocyte marker CD45 was used as a negative stain. DAPI was used to identify nuclear content. For the remaining volume of the resulting cell suspension, total RNA extraction was performed in order to do mRNA profiling for each sample.

4.3.5 Immunofluorescent staining of patient samples

Samples were stained for CTC markers using a primary antibody for anti-cytokeratin-19 (CK-19), epithelial cell marker, (Santa Cruz Biotechnology, rabbit polyclonal IgG), panCK (Santa Cruz Biotechnology, rabbit polyclonal IgG), and nuclear stain 4',6-Diamidino-2-Phenylindole, Dihydrochloride (DAPI, Invitrogen). Negative staining with the leukocyte marker anti-CD45 (BD Pharmigen Purified Mouse Anti-Human CD45, HI30 clone, isotype Mouse IgG1, ƙ) was also performed. Samples were then stained using secondary antibodies with fluorescence conjugation namely, AlexaFluor 568 (Life Technologies), for CK-19 detection and AlexaFluor 488 (Life Technologies), for CD45 detection. For the samples that were stained for

Vimentin, the primary antibody anti-vimentin (BD purified mouse anti-vimentin, RV202 clone, isotype IgG1) and the secondary antibody AlexaFluor 647 (Life Technologies) were used. Negative staining was done with the leukocyte marker anti-CD45 (BIO-RAD mouse anti human CD45, clone F10-89-4) and the secondary antibody AlexaFluor 488 (Life Technologies). For the primary antibody stains, an overnight incubation period was carried out, while for secondary staining, 1hr was allowed. For DAPI staining ProLong Gold anitfade mountant with DAPI, (Life Technologies) was applied overnight. Immunofluorescence imaging for anti-CD45 was performed using a FITC filter while anti-CK was performed with a PE filter and DAPI, a UV filter at x20 magnification.

4.3.6 Messenger RNA profiling of CTC samples isolated using EpCAM and CD44

To isolate total RNA, after enriching CTCs from 5 mL of patient blood, RNA was isolated using the Norgen Single Cell RNA Purification kit (Norgen Biotek Corp.), according to the manufacturer's protocol, with minor modifications. After lysing the cells the CTC lysates were then stored in -80^{0}C until total RNA purification was ready to be carried out. For total RNA purification, samples were thawed on ice and 200µL of 96-100% ethanol was added to the cell lysate and vortex mixed for 10 seconds. RT was carried out on the purified RNA followed by pre-amplification (18 cycles) using cDNAs corresponding to 96 genes of interest from a CTC-specific panel. The pooled TaqMan Gene Expression Assays and Cell-to-CT Kit (Ambion, Invitrogen) was used. TaqMan Gene Expression Assays for the 96 genes and the BioMark HD qPCR platform (35 cycles) was used to carry out gene expression profiling of the pre-amplified cDNAs. For genes undetected during qPCR, a cycle number of 40 was assigned for analysis purposes. To normalize Ct values among different genes, GAPDH was used as an internal reference. Statistical analysis was performed based on –ΔCt of gene expression.

4. 4 Results

4.4.1 EpCAM- and CD44- based immunomagnetic isolation of cells lines

For experiments done to evaluate immunomagnetic isolation of cells lines, cells emerging from the collection channel of the magnetic sorter were scanned and analyzed for the number of PANC-1 cells (red) and MIAPaca-2 cells (green) successfully sorted. Upon quantifying the

magnetic sorting process, Figure 4.1C shows that for each marker, magnetic sorting was able to recover comparable quantities of each type of cell, especially among MIAPaca-2 cells. For EpCAM isolation, a larger fraction of PANC-1 cells (67% versus 33%) were isolated probably because these cells showed preferential EpCAM labeling, compared to the negligible EpCAM bead attachment shown among MIAPaca2 cells. Likewise with CD44 isolation, MIAPaca-2 cells had slightly higher isolation efficiency (53% versus 47%) since MIAPaca-2 cells showed preferential CD44 labeling. Overall, the magnetic sorting process demonstrated the ability to isolate cells expressing a range of magnetic bead attachment, regardless of the marker used for immunomagnetic attachment of beads to cells.

4.4.2 EpCAM- versus CD44- based CTC isolation

After processing the 8 patient samples for EpCAM- and CD44- based CTC isolation, samples were analyzed for their CTC counts. CTC detection rates for the two sets of CTCs isolated using either EpCAM or CD44 are as seen in the boxplot in Figure 4.2A. While there was no significant difference in CTC detection rates ($p=0.722$) between the two groups, the average CTC detection rate was higher in CD44 isolation (average CTC/mL=5.5±4.09) compared to EpCAM isolation (average CTC/mL=3.7±2.80). Notably, CTC counts appear lower than counts among the other patient cohort later discussed possibly due to centrifugation process for volume reduction that was carried out with all samples.

4.4.3 Vimentin expression among EpCAM- versus CD44- isolated CTCs

For samples processed with EpCAM- and CD44 based CTC isolation, Vimentin staining was carried out with 6 of the 8 patient samples. The fraction of CTCs staining positive for Vimentin was calculated as a percentage of all detected CTCs for each sample. Figure 4.2D shows to sets of cells that stain positive for Vimentin. Results show that across the six patient samples analyzed Vimentin expression among CTCs isolated with the two markers did not yield any significant difference. While there was no significant difference in CTC detection rates between the two groups ($p=0.465$), the average percent of Vimentin+ CTCs detected was slightly higher with CD44 isolation (average % vim+ CTCs=39.2±33.2) compared to EpCAM isolation (average % vim+ CTCs=34.4±33.6).

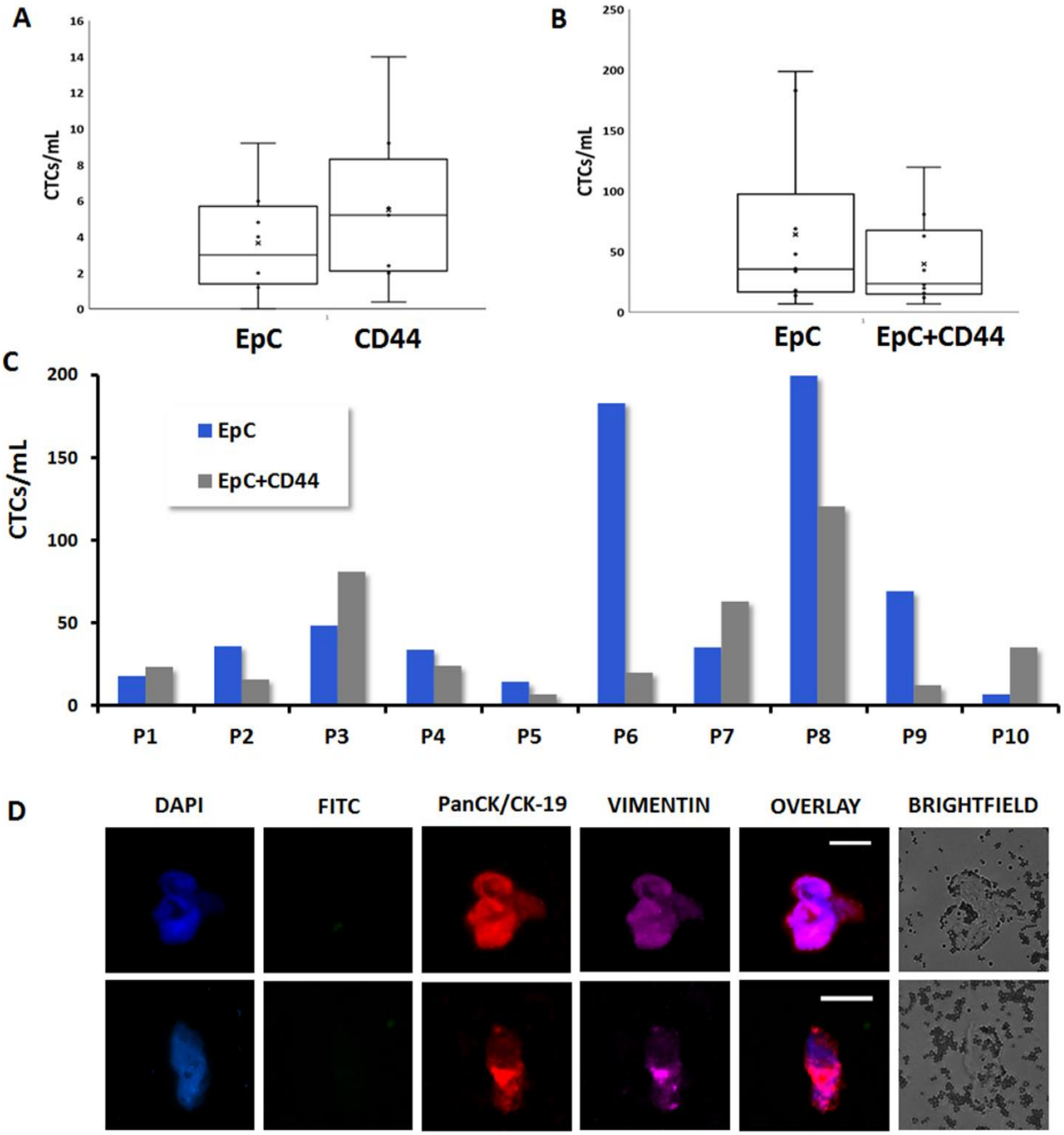

Figure 4.2: Patient CTC Analysis isolated using EpCAM and/or CD44. (A) Box plot of CTC enumeration using EpCAM isolation versus CD44 isolation. (B) Box plot of CTC enumeration using EpCAM isolation versus EpC+CD44 dual marker isolation. (C) Detailed CTC enumeration among 10 patients using EpCAM isolation versus EpC+CD44 dual marker isolation. (D) CTCs staining positive for the mesenchymal marker Vimentin.

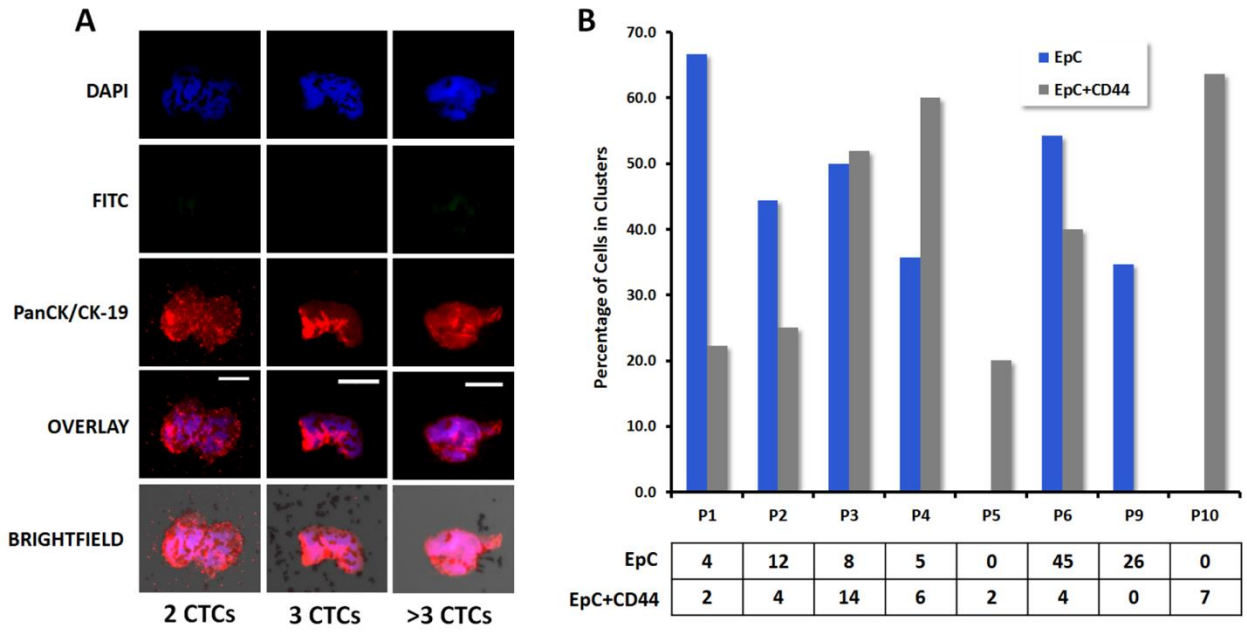

Figure 4.3: Analyzing CTC clusters. (A) CTC clusters detected in patients showing two, three and greater than three CTCs (scale bar =20μm). (B) Percentage of cells in clusters isolated using either EpCAM or EpCAM+CD44 isolation. Table shows numbers of cells in clusters.

4.4.4 Analysis of CTC clusters

Detection of CTCs grouped in cell clusters, have demonstrated co-expression epithelial and mesenchymal markers.[186] Studies involving cancer patients as well as animal models indicate that CTC clusters have an enhanced ability to mediate cancer metastasis compared to single CTCs.[173, 177] Of the 10 patient samples that were analyzed, eight of them had CTCs grouped in cell clusters which ranged from as least two grouped CTCs to greater than 7 grouped CTCs. Specifically, clusters were detected in seven of the eight patients isolated with EpCAM+CD44 compared to six of eight samples processed with EpCAM standalone. Figure 4.3A shows isolated CTCs that appear clustered together, consisting of two, three and greater than 3 CTCs. A comparison of the percentage of cells occurring in clusters between cells isolated with EpCAM only and cells isolated with EpCAM+CD44 revealed that here was no significant difference (p=0.593) with both methods of isolation. Moreover results demonstrated that very similar percentages of cells appeared in clusters, with EpCAM having on average 35.7%±22.7 and CD44 having 35.3% ±20.8 cell in clusters.

4.4.5 EpCAM versus EpC+CD44 CTC enumeration and molecular profiling

For the 10 samples processed using both EpCAM and EpC+CD44 CTC isolation, Figure 4.2B shows CTC detection rates across all samples. Moreover, Figure 4.2C gives detailed CTC enumeration among these 10 patients using EpCAM isolation versus EpC+CD44 dual marker isolation. While there was no significant difference (p=0.328) in CTC detection rates between the two method of isolation, overall EpCAM based isolation appeared to have a higher detection rate with an average of 64.3 ± 65.6 CTCs/mL compared to EpCAM in combination with CD44 which had an average of 40.1±34.7 CTCs/mL.

Also, mRNA profiling was conducted on CTCs samples obtained from this 10-patient cohort. RNA samples were stored at -80^0C until was carried out on the samples. For mRNA profiling a CTC-specific array of 96 genes was used. Of the twenty samples profiled from the ten patients, only nine pairs were considered since the RNA quality from one pair was deemed unfit for profiling. Interestingly, unsupervised hierarchical clustering showed that CTC profiles clustered independent of the marker(s) of isolation used such that EpCAM isolated CTC profiles grouped with EpCAM+CD44 profiles (see Figure 4.4A). Moreover, among the eighteen sample profiles 2 resected pancreatic ductal adenocarcinoma patients, 2 borderline patients that were resected but later showed suspicious pathologies, and 2 resected patients with recurrence or metastases clustered together. These pairs occurred regardless of the isolation method used. A log fold change (logFC) comparison of mRNA expression was carried between EpCAM and EpCAM+CD44 samples. As seen in Figure 4.4B, this analysis revealed that some genes such as MMP6, CDA, DCK, CTNNB1 and ALDH1A3, that were more highly expressed in the EpCAM only group compared to the EpCAM+CD44 group, having logFC of >2. Several genes such as CD20, BAX, JUN and ABL1, among others, were lower expressed in the EpCAM only group, having logFC of <-2. Specifically, ANXA2 (p=0.0400) was significantly lower in EpCAM samples compared to EpCAM+CD44 samples, having a logFC of -1.08.

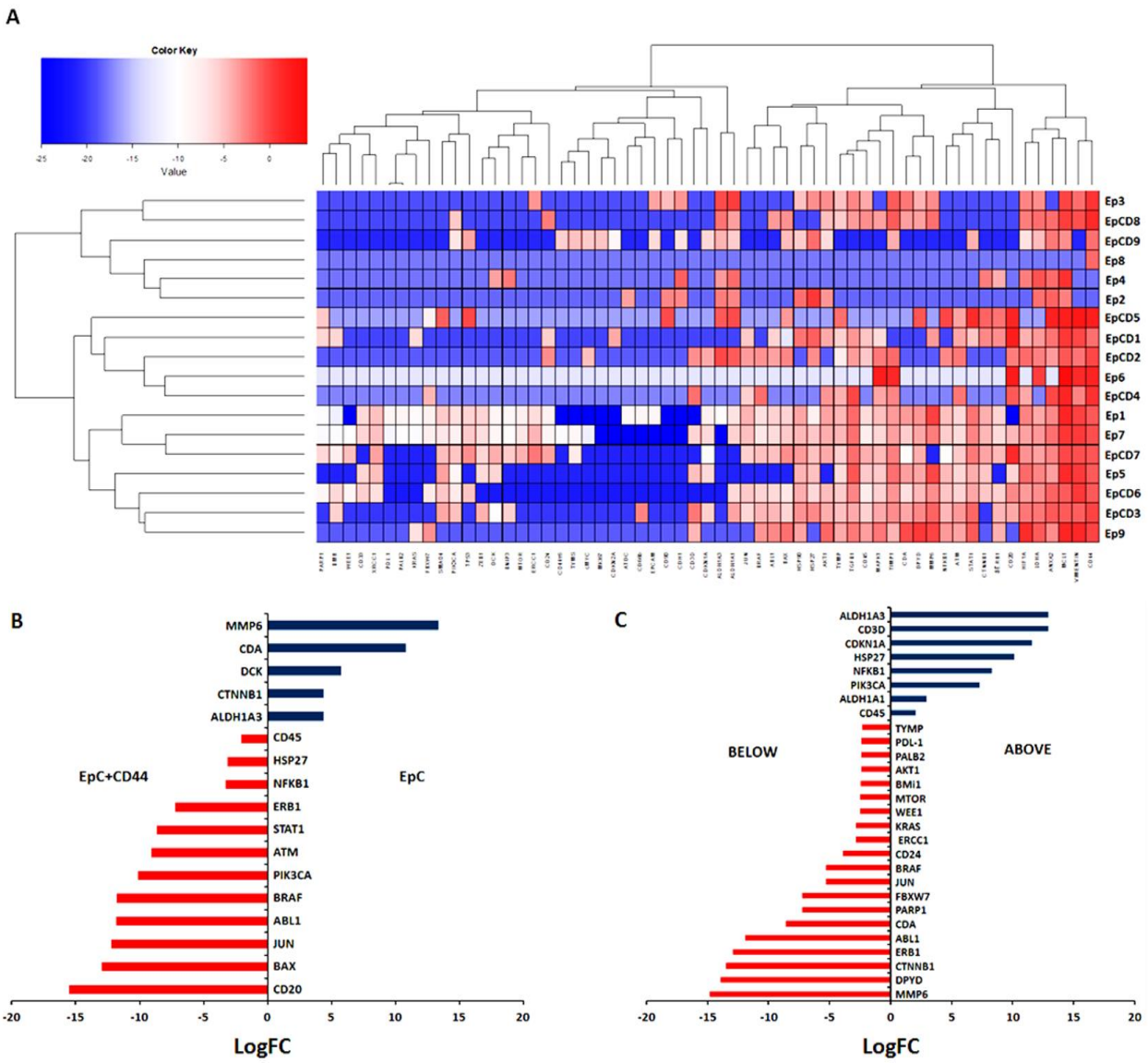

Figure 4.4: Molecular Profiling of CTCs isolated using EpCAM and or CD44 (A) Heat map showing hierarchical clustering among all patient samples (B) LogFC in gene expression among EpCAM isolated CTCs compared to EpC+CD44 isolated CTCs (C) LogFC in gene expression among samples with >50% of cells in clusters compared to samples with <50% of cells in clusters.

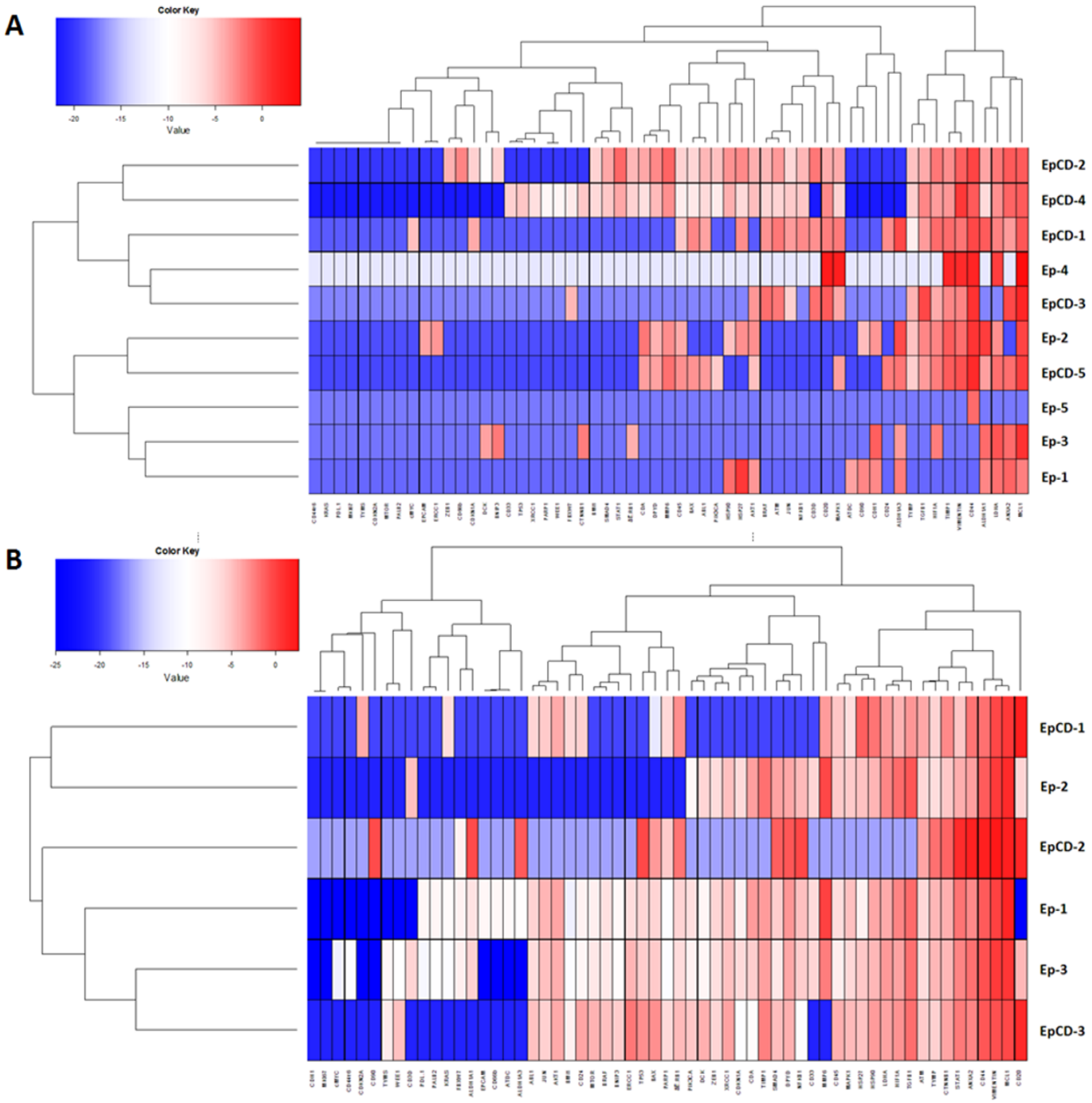

Figure 4.5: mRNA expression profile comparison among Borderline patients: (A) Heat map showing clustering of CTC mRNA profile among resectable/resected patient (B) Heat map showing clustering of CTC mRNA profile among unresectable patients.

Another interesting result was seen in the comparison of samples in which >50% of cells appeared in clusters versus samples in which <50% of cells appeared in clusters, regardless of the isolation approach employed. Specifically, 5 out of 18 samples showed >50% of cells in clusters while the remaining 13 samples had <50% of cells in clusters. Figure 4.4C shows genes that were more highly expressed in samples with >50% CTCs in clusters, having logFC >2 as

well as genes that were lower expressed having logFC <-2. Of note, CDKN1A (p=0.0140, logFC=11.586) as well as HSP27 (p=0.0044, logFC=10.139) were more highly expressed in samples with >50% CTCs in clusters, to a significant degree. In contrast, ERCC1 (p=0.0140, logFC=-2.856), CTNNB1 (p=0.0460, logFC=-13.473), PARP1 (p=0.0068, logFC=-7.231), as well as FBXW7 (p=0.0350, logFC=-7.231) were all expressed more highly in samples with <50% CTCs in clusters, to a significantly extent.

4.4.6 Comparison among Borderline patient profiles

As previously shown, unsupervised hierarchical clustering of all 18 samples revealed a tendency of CTC profiles pairing according to patient pathological conditions, irrespective of the CTC isolation approach used. Given this preliminary finding, we investigated whether there were trends among CTC profiles of patients with similar disease presentation. Since the majority of patients were deemed borderline resected/resectable or borderline unresectable, CTC mRNA profiles were grouped accordingly and unsupervised hierarchical clustering was performed with these two groups. Of all 8 borderline patients, 5 of them were borderline resected/resectable while the remaining 3 were borderline unresectable. Interestingly, among the 10 CTC mRNA profiles generated from EpCAM and EpCAM+CD44 isolation from the 5 borderline resected/resectable patients, 4 out of 5 EpCAM profiles clustered together while, as well as for EpCAM+CD44 mRNA profiles as seen in Figure 4.5. In contrast, among the 3 unresectable patients, the mRNA profiles grouped irrespective of the CTC isolation approach used. These preliminary results possibly support the idea that at the molecular level, CTCs among patients with a less advanced disease can be distinguished according to epithelial phenotype (EpCAM) versus a more stem-like phenotype (EpC+CD44). Additionally, at a more advanced disease stage, this distinction is not immediate.

4.5 Discussion

The implicit role of tumor cells that express CD44, among other proteins, in rendering an enhanced tumor initiating capacity has been reported among several studies. Furthermore, mounting evidence suggests that cells displaying biphenotypic epithelial/mesenchymal expression may be more appropriate targets for abrogating cancer metastasis than cells displaying an exclusively mesenchymal phenotype.[185, 186, 188] In an effort to enhance CTC yields

through immunomagnetic labeling and isolation of CTCs that express CD44 more significantly compared to EpCAM, a dual EpCAM-CD44 CTC isolation approach was implemented versus standalone EpCAM. Interestingly among the pancreatic cancer patients studied, the dual marker isolation approach did not result in increased CTC yields or CTC cluster yields. Additionally, there was no significant difference in Vimentin expression between CTCs isolated with EpCAM and CTCs isolated with CD44. These findings suggest that among these patients EpCAM is expressed by the majority of CTCs such that the addition of CD44 as an isolation antibody is unable to significantly increase CTC yields. Moreover, the population of cells that exclusively express CD44, without EpCAM expression may be negligible to none. At the molecular level, there appeared to be a level of distinction among CTCs isolated with EpCAM and those isolated with EpCAM+CD44. Specifically, among patients with a less advanced pathology, EpCAM+CD44 isolated CTCs were distinguishable from CTCs isolated with only EpCAM such that the mRNA profiles of dual isolation clustered separately from CTC profiles obtained via standalone EpCAM isolation. In patients with more advanced disease, this distinction was not made such that patient CTC profiles clustered together regardless of the isolation approach used. These preliminary results possibly support the idea that at the molecular level, CTCs have the potential to discriminate disease pathology. Moreover, among patients with a less advanced disease CTCs can be distinguished according to a more epithelial phenotype (EpCAM) versus a more stem-like phenotype (EpC+CD44). While these studies are preliminary, at the molecular level, they support the idea that EpCAM expression may not be lost entirely as the disease progresses, yet tumor cells evolve to become more stem-like. Finally, while acquisition of more patient data will be required to validate such findings, the initial results point to the practicality of the reported CTC isolation studies to help in answering important questions about tumor biology and metastasis.

Chapter 5

Inertial Sorting of polymer particles based on particle shape and porosity

5.1 Abstract

The notion that a fraction of CTCs is responsible for driving metastasis has led to increased efforts to distinguish among different CTC subtypes. One primary motivation behind such efforts is the idea that targeted analysis of CTC subpopulations will progressively uncover important characteristics of their unique roles in metastasis. In most instances, cells of interest are expected to express multiple surface proteins, the extents and combinations of which may vary. Moreover, with evidence to suggest that particle shape at the micron-scale enhances antibody specificity and avidity to antigens, use of a variety of particle shapes can be leveraged in multiple-marker immunolabeling of these CTCs. For instance, shapes that allow enhanced avidity can be coated with antibodies against less abundant surface proteins while other particle shapes can be used for immunolabeling involving more abundantly expressed CTC surface markers. This shape-based labeling approach can potentially reduce the amount of sample post-processing via immunofluorescence labeling if each particle shape specifically labels a unique CTC marker of interest. Moreover, the possibility of hydrodynamically sorting particles based on their construct opens up the prospect for rapid and high-throughput cell sorting according to unique expression of surface markers. Apart from particle shape as a factor to hydrodynamically separate and sort

particles, we set out to investigate whether particle porosity would facilitate enhanced particle sorting. The motivation is that separating subsets of CTC labeled with distinct micron particles through inertial microfluidic particle sorting, enables large sample volumes to be processed in a high-throughput, manner. Here we report our initial findings associated with particle synthesis and subsequent sorting of particles using microfluidic inertial sorting.

5.2 Introduction

In a study that compared how shapes of nano- and micro- rods, spheres and discs influenced antibody specificity and avidity, Barua et al reported that particle shape does influence the binding of these antibody-coated submicron particles to target cells. They demonstrated the utility of this increased, shape dependent specificity to attach nanorods coated with trastuzumab, an anticancer therapy, to target breast cancer Her2+ cells.[201] Furthermore, in another study Hur et al showed how non-spherical particles, each categorized using a certain characteristic diameter, were able to attain focused equilibrium positions along microfluidic channels during flow as a result of inertial forces described earlier (chapter 2). They proposed the possibility for use of such asymmetrically shaped particles for high throughput multiplex bioassays.[202] With the understanding that the shape of particles influences the extent to which they interact and attach to target cell, and the evidence that differently shaped particles are able to adopt unique equilibrium positions, we proposed the use of this shape dependent specificity to identify and isolate subpopulations of CTCs.

Moreover, evidence to support the existence of a subset of cells that behave like pancreatic cancer stem cells, (CSCs), was furnished by Li et al, where they showed that these CD44+CD24+ESA+ pancreatic cancer cells demonstrated properties of high turmorigenicity, self-renewal and the ability to produce differentiated progeny.[27] Since these cells demonstrate resistance to both chemotherapy and radiation therapy, they have been heavily implicated in the metastatic process, treatment failure and disease recurrence. Therefore they hold great interest to clinicians and researchers alike. Moreover, isolation of CTCs with similar protein expression to this population of stem cells, and elucidation of the signaling pathways through which their growth and survival are regulated will have important implications, especially for pancreatic cancer, which demonstrates the most robust resistance to standard therapies.[203]

With detailed information about the specific surface markers that are expressed by certain subsets of circulating cancer cells, we proposed synthesizing asymmetric particles and coating them uniquely, with antibodies against these markers of interest. Ideally, the goal would be to design and optimize asymmetric particles, to achieve unique particle focusing positions along curved microchannels. Additionally, we explored whether particle porosity or size, in combination with shape, would enhance particle sorting and separation efficiency using this high throughput approach. Once a set of particles that uniquely separate from each other along the channel cross-section was identified, a combination of these particles would be selected for antibody labeling tests. Ultimately, the goal was to evaluate and optimize cancer cells sorting according to proteins of interest, using this combination of particles to label and then separate cancer cells. To this end, our collaborators synthesized both dextran and poly(lactide-co-glycolide) (PLGA) particles based on variable porosities, shapes and sizes. Previously they demonstrated the ability to synthesize particles that are compartmentalized with different sections demonstrating unique porosities.[204]

For the antibody labeling tests involving the combination of micro particles, the idea was that each type of particle would be surface functionalized with a particular antibody arrayed against a CTC surface markers. To initially test and validate the system, particles would be screened with pancreatic cancer cell lines to determine which combinations of particle-antibody functionalization proffered the most effective antigen-antibody binding with cancer cell. Specifically, anti-CD44, anti-CD133 and anti-EpCAM, which are all relevant surface markers in pancreatic cancer CTCs were considered for testing with the synthesized microparticles. Thus far, the behavior of micron sized discs, cylinders and rods have been tested in curved channels to determine particles focusing behavior in the microfluidic channel. Additionally, we report on initial particle surface functionalization with EpCAM.

5.3 Methods

5.3.1 Polymer particle fabrication

PLGA and dextran particles were synthesized by collaborators in the Lahann lab at the University of Michigan. Briefly, these particles are synthesized by co-jetting organic polymer solutions through a side-by-side capillary system under laminar flow. The application of an

electric potential on the pendant droplet causes it to be distorted. The particles can also be stretched to result in elongated shapes. Subsequent to particle distortion and reshaping, rapid solvent evaporation from the structures results in well-defined particles.[204] To alter the porosity of particles, PLGA was co-jetted with another polymer and upon incubation at pH 5, the polymer would degrade and become porous. After synthesis, particles were filtered to enrich for those of interest and then enumerated and analyzed to determine particle size standard deviation. Particles were then fluorescently labeled to allow them to be distinguished during microscope visualization for device optimization. Flat discs, rods and biconcave discs (termed RBCs) were synthesized for analysis. Spheres were also synthesized and made porous to test the effect of particle porosity on particle focusing. Once particles were counted they were stored in 1% Tween solution at 4^0C to prevent clumping until they were ready to be sorted.

5.3.2 Particle preparation for inertial sorting

To prepare polymer particles before inertial sorting experiments, stored particles were sonicated to disrupt any aggregation of particles which would potentially interrupt microfluidic flow, or result in particle flow behavior artifacts. Next particles were pre-sorted twice using a spiral inertial sorter to enrich them based on size, so that the overall size range of the particle suspension would be narower. Presorting also facilitated removal of debris and any persistnet clumps from the sample that remained after sonication. Particles were collected from the spiral outlet from which the majority of particles emerged, and then re-processed through the sorter, to further enrich the target particles. Once the entire sample was presorted, particles were enumerated and the particle size distribution was determined. To obtain porous particles, after presorting the orignal non-porous dextran particles, the resulting suspension was incubated at pH 5 to enable compartments of the polymer particles to become porous. Particles were again stored in 1% Tween at 4^0C until ready for use.

5.3.3 Particle sorting using inertial sorter module

Polymer particles of differnent physical make up were uniquely dyed with fluorescnce to identify them if and when a mixture of particles were tested and to facilitate fluorescence imaging of the particles under flow in the microfluidic device. Once particles were pre sorted and enumerated they were sonicated and resuspended to comparable concentrations (~10^6

particles/mL). The inertial spiral sorter was primed with 0.05% pluronic solution before sample processing. The design used has a 25mm outer diameter with four outlets of 200, 150, 200 and 250μm widths. To determine how shape affected particle focusing in the inertial sorter, biconcave shaped particles (termed RBCs), and flat discs were tested at flow rates ranging from 500-2000μL/min. Both type of particles had diameters ranging from ~8-10μm. To test the effect of porosity on particle focusing, nonporous and porous particles of the same effective diameter were also tested at flow rates ranging from 500-2000μL/min. Particle flow in the inertial sorter outlets was visualized with fluorescence microscopy and images of the outlets were take. From these images the relative fluorescene intensity across the channel outlets was analyzed as a measure of the particle focusing. The point of maximum fluroescence intensity was taken as the the postion of focusing of the particles while the width of streaks was taken as a measure of the spread of particles. For particles of different shape or posrosity, a larger distance between particle focus points, and a narrower spread of particles allow more effcient sorting of particles.

5.3.4 PANC-1 Cell labelling with porous particles

To determine the labeling effciency of anti-EpCAM coated porous particles with the EpCAM expressing PANC-1 cell lines, the porous particles were first coupled with anti-EpCAM antibody. PLGA/dextran/acytylene/PLA-Alkyne particles were surface modified with an azide-PEG-Biotin group using copper click chemistry over a 10 hour period. Then 50mg/mL of Neutravidin was mixed with the biotinylated particles for 3 hours, after which 10μg/mL of biotinylated-EpCAM was incubated with the particles for 1 hour. To fluorescently label the particles, they were incubated with 1 μg/mL of Alexa Fluor 568 donkey anti-goat secondary antibody for 1 hour. As a labeling control for cell EpCAM expression, cells were incubated with 1μm anti-EpCAM coated magnetic beads. Another control was to incubate cells with polymer spheres that were not surface functionalized with EpCAM. PANC-1 cells were incubated with the polymer particles for periods of 5, 10 and 15min at a 1:2 cell: particle ratio, after which the labelling efficiency was quantified.

5.4 Results

5.4.1 Pre-sorting particles using inertial separation

After polymer particles were presorted to get rid of debris and to enrich particles over a narrower range of sizes, the sample was assessed and compared to the original sample distribution before presorting. Figure 5.1 shows results obtained directly after jetting particles (black bars), and after using a commercially available particle filter (yellow bars). In addition, particle distribution was evaluated after combining commercial filtering with 1 pass of inertial sorting from the first outlet (green bars) and second outlet (lilac bars), to enrich particles based on their size are shown.

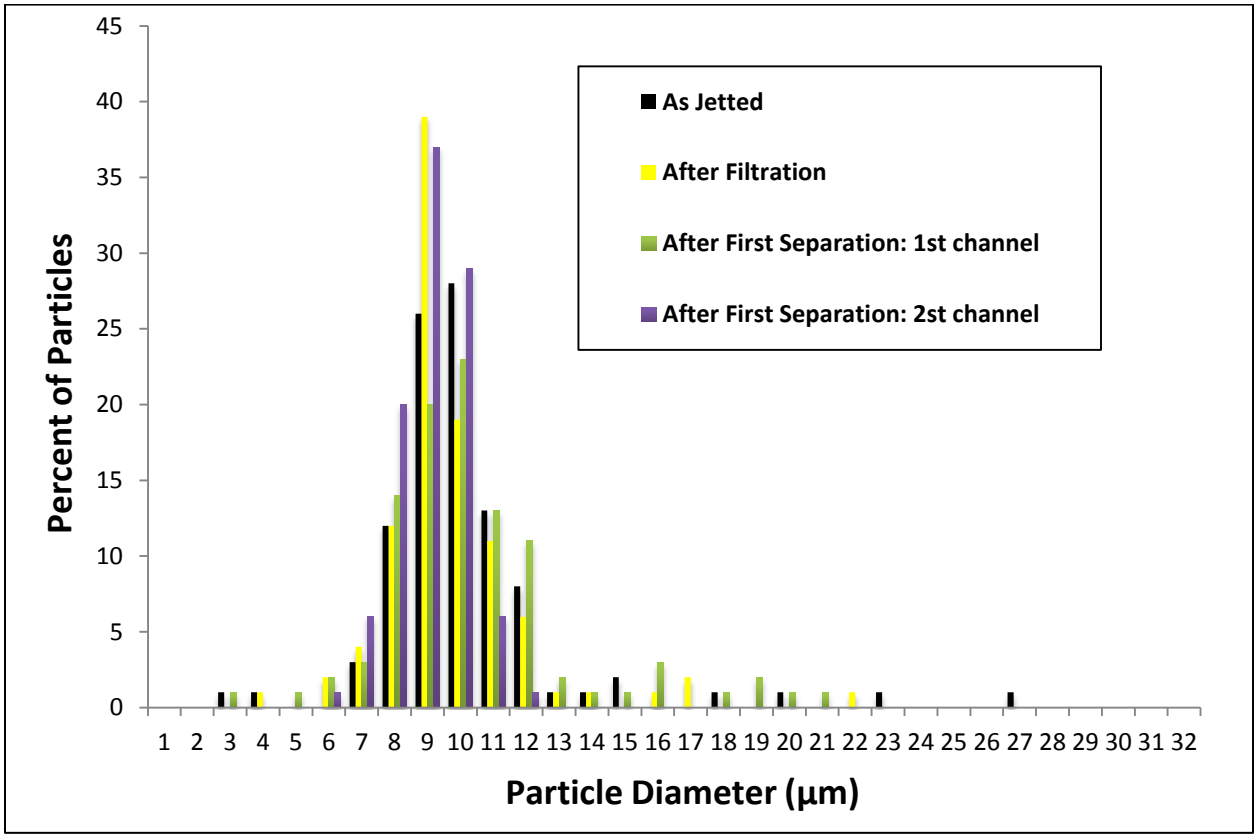

Figure 5.1: Polymer particle distribution before and after sorting. Plot shows distribution of particles sizes directly after jetting, after filtering, and after inertial sorting, both in first and second outlets of inertial sorter device.

Results show that compared to filtering, 1-pass of inertial sorting was able to remove outlier particles and therefore narrow the range of particle size. A similar analysis was carried out on the particles after they were presorted in the inertial sorter and made porous. Once sorted the sample of porous particles was assessed and compared to the original sample distribution before presorting. As seen in Figure 5.2, once particles were made porous, further inertial sorting

resulted in increased enrichment of particles, both porous and nonporous, at 8μm. The number of outlier particles though negligible, did increase.

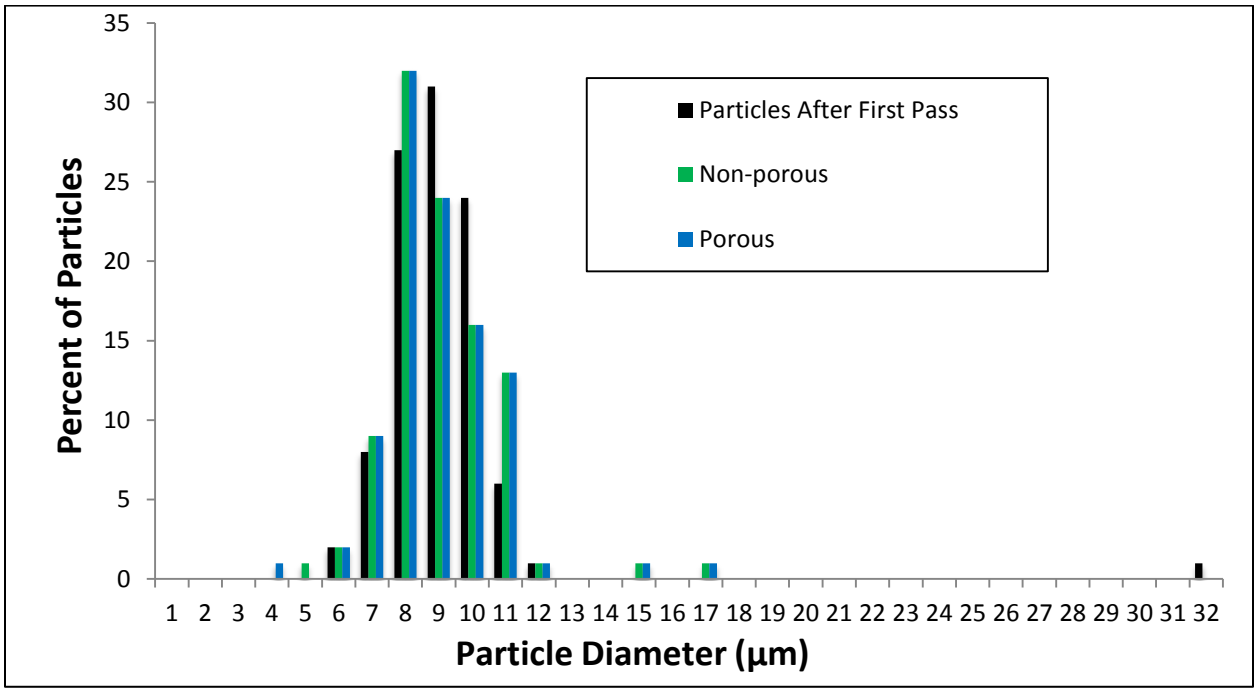

Figure 5.2: Porous particle distribution before and after inertial sorting. Plot shows distribution of porous particles sizes directly after filtering, and after making porous followed by inertial sorting and collection from the second outlet of inertial sorter device.

5.4.2 Separating Particles based on shape

After presorting the particles synthesized as biconcave discs (RBCs), and flat discs, particles were reconstituted to the same concentration (10^6 particles/mL) and processed as separate samples through the inertial sorter. Figure 5.3 shows fluorescence overlays of the flow behavior of flat discs (dyed green) and RBCs (dyed blue) at the inertial sorter outlets, which appear as streaks of green and blue. As seen in Figure 5.4A, across the range of fluid flow rates tested, the focusing positions of flat discs (dyed green) and RBCs (dyed blue) in the device were almost indistinguishable across the flow rate range tested.

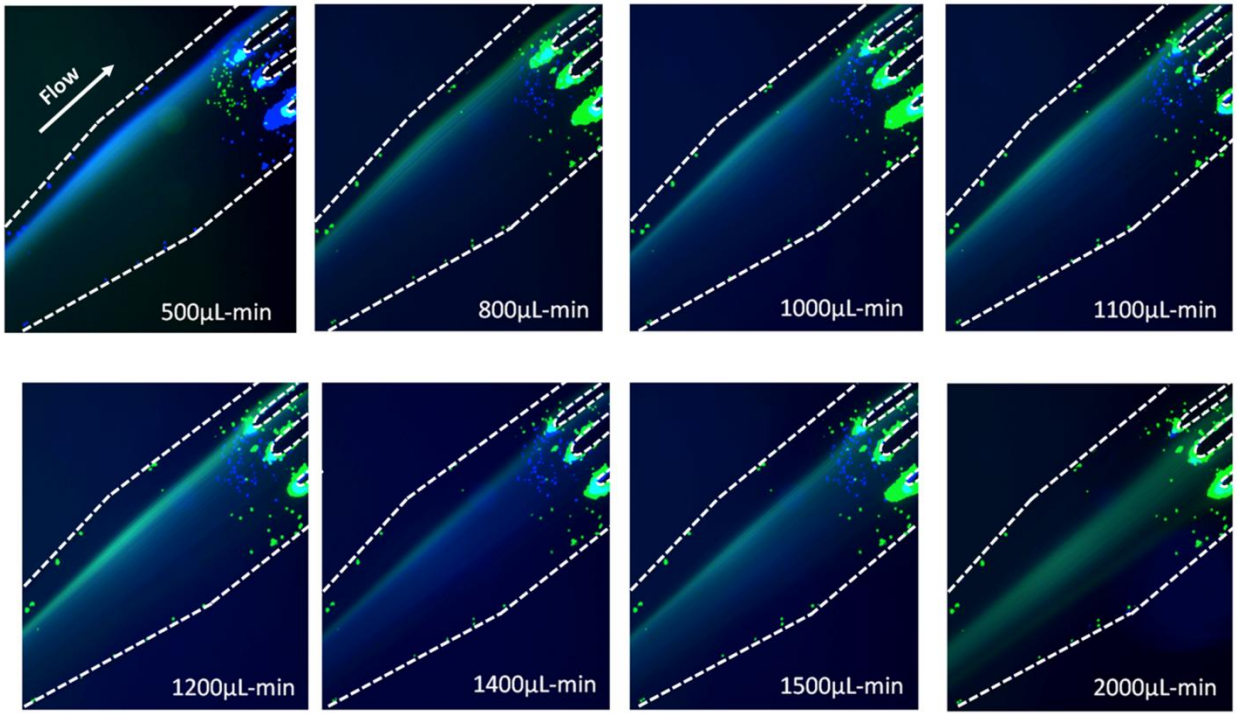

Figure 5.3: Fluorescence imaging of differently shaped particles under flow. Behavior of flat disc (dyed green) and RBC (dyed blue) microparticles was captured at different flow rates.

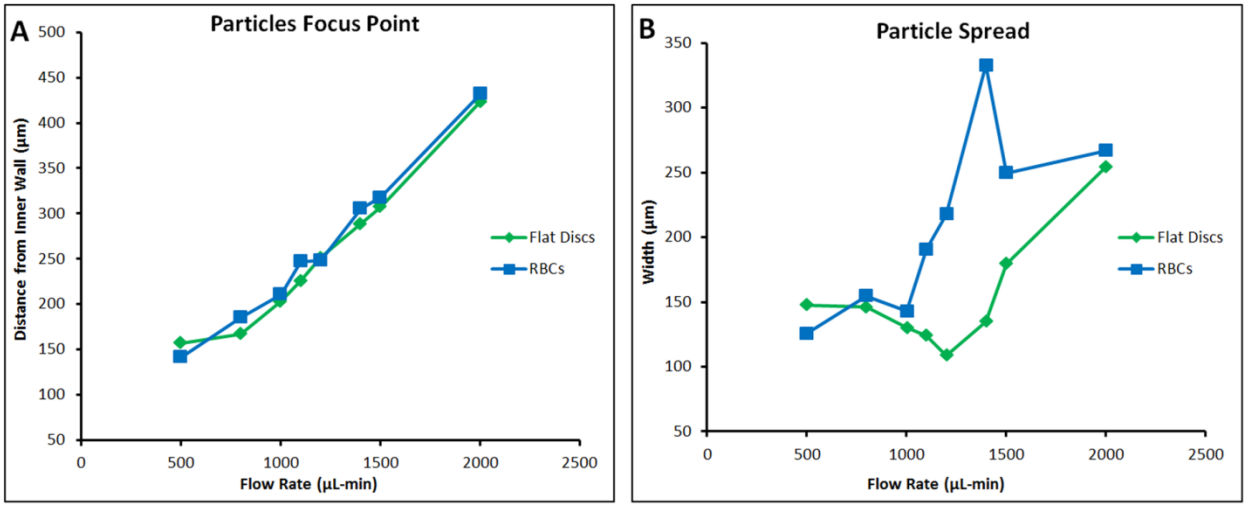

Figure 5.4: Flow rate effect on focusing point and spread of different particle. (A) Focusing positions of flat discs and RBCs and (B) particle spread of flat discs and RBCs as functions of flow rate of suspension.

This reflected what appears to be the primary role of particle size in determining focusing position of particles and the limitation of the specific device design to sort these particles, since both types had comparable effective diameters. Additionally, based on the measures of particle

spread in Figure 5.4B, it appears that flat discs were more effectively focused across this flowrate range compared to the RBC discs, though at higher flow rates the difference in particle spread between flat discs and RBCs becomes less evident.

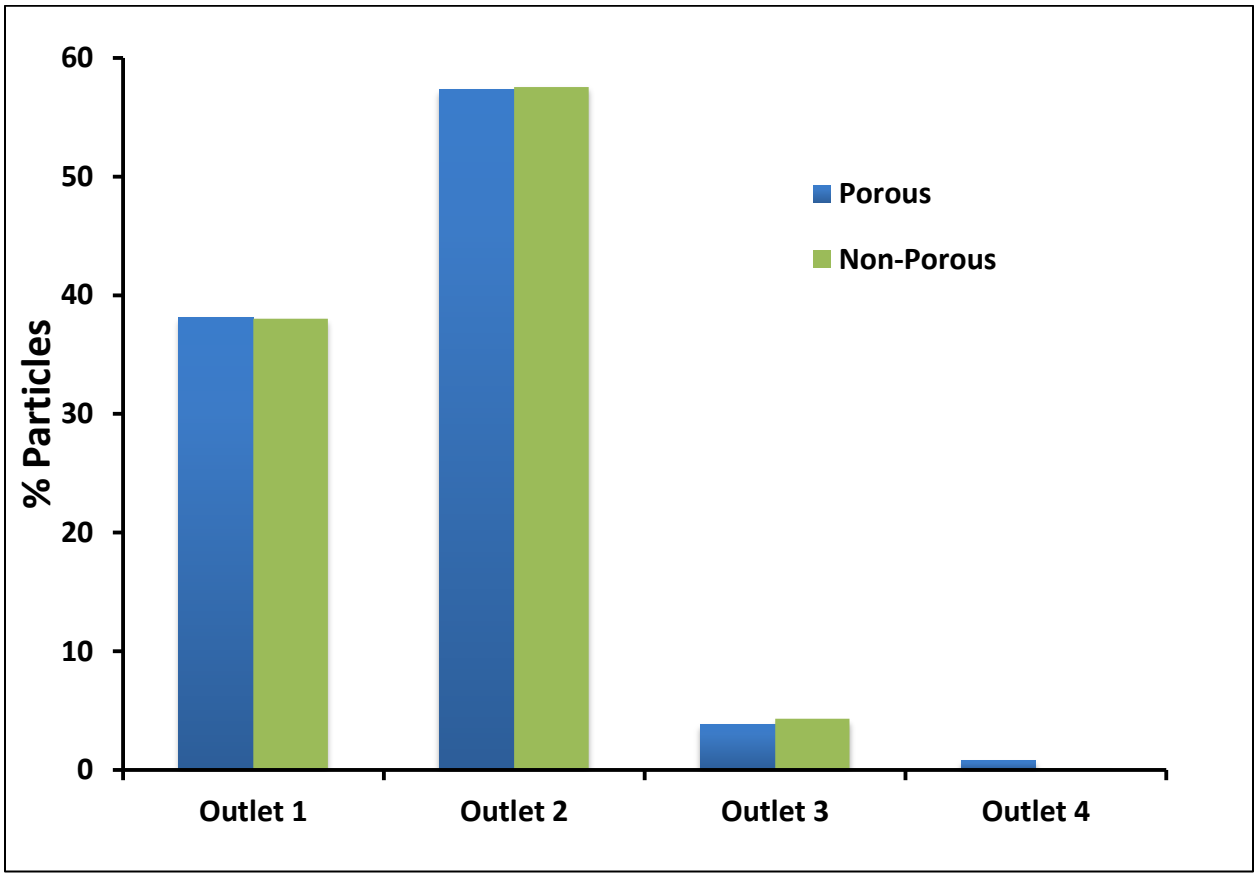

Figure 5.5: Quantification of particle inertial sorting based on porosity. Plot showing distribution of porous and nonporous particles emerging from the four outlets of the inertial sorter.

5.4.3 Separating Particles based on porosity

Once polymer particles were presorted and made porous, they were processed through the inertial sorter and analyzed for particle distribution from the four outlets of the device. Figure 5.5 shows that with the inertial sorter design tested, particle distribution in the four outlets is largely independent of particle porosity. Particle distribution in all four outlets is the same, irrespective of particle porosity. Once again, particle effective diameter appears to be the dominant factor in determining particle distribution in the device. Finally, upon comparison of particle behavior of all four sets of particles at the flowrate range of 500-2000μL/min, it was seen

that polymer spheres, whether porous or not, focused separately from both types of discs (see Figure 5.5). Flat discs and RBC discs focused together in the second outlet while spheres focused in the first outlet. Since discs and spheres showed separation, the next step is to test separation of nonporous spheres and flat discs since both types of particles display higher size and shape uniformity compared to their counterparts.

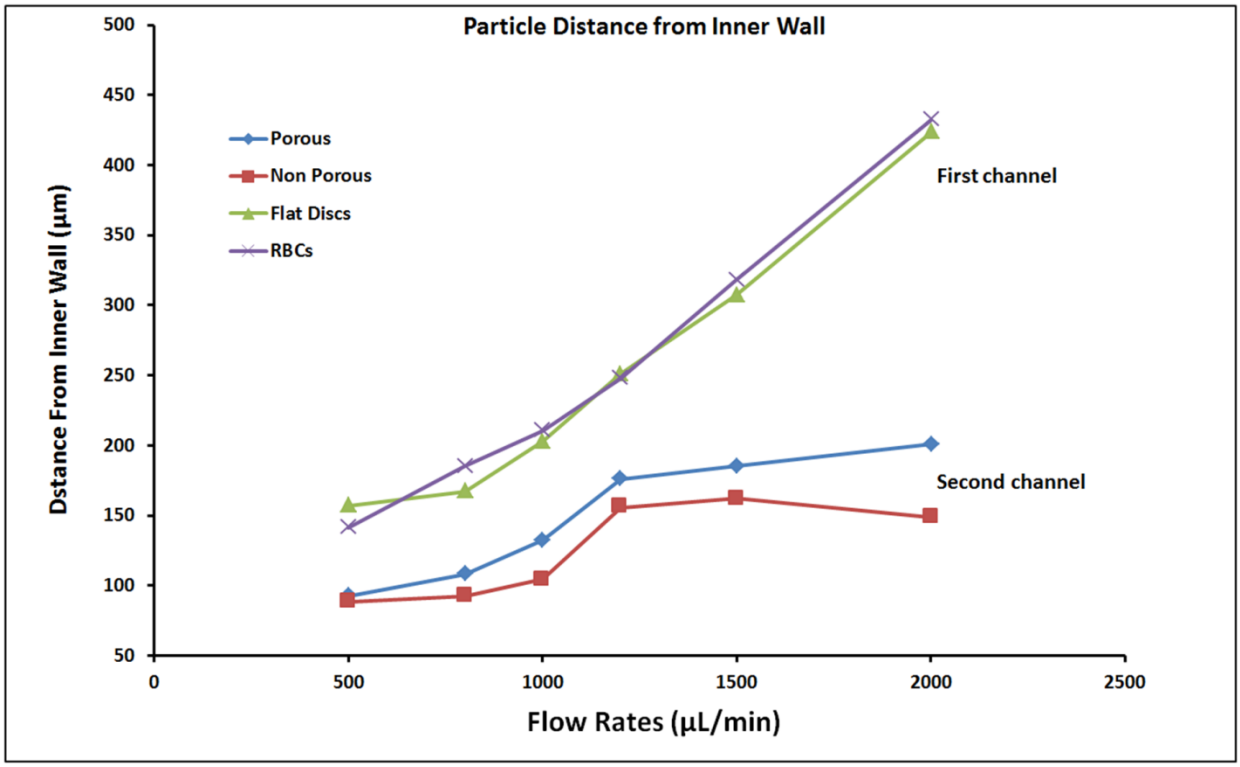

Figure 5.6: Comparing focusing of porous, non-porous, flat disc and RBC disc. Discs focus and at and emerge from the first outlet channel while spheres focus at and emerge from the second outlet channel.

5.4.4 Efficiency of PANC-1 Cell labelling with porous particles

After nonporous spheres were surface functionalized with anti-EpCAM antibody and allowed to incubate with PANC-1 cancer cells, an aliquot of the sample was quantified for the cells that showed particle attachment with at least 1 polymer particle, using fluorescence imaging. Figure 5.7 shows the results of PANC-1 cell labeling with EpCAM functionalized spheres after 5min and 15min of incubation. Results of the control experiment of cell incubation with polymer particles that were not EpCAM surface functionalized are also shown for the same incubation time periods.

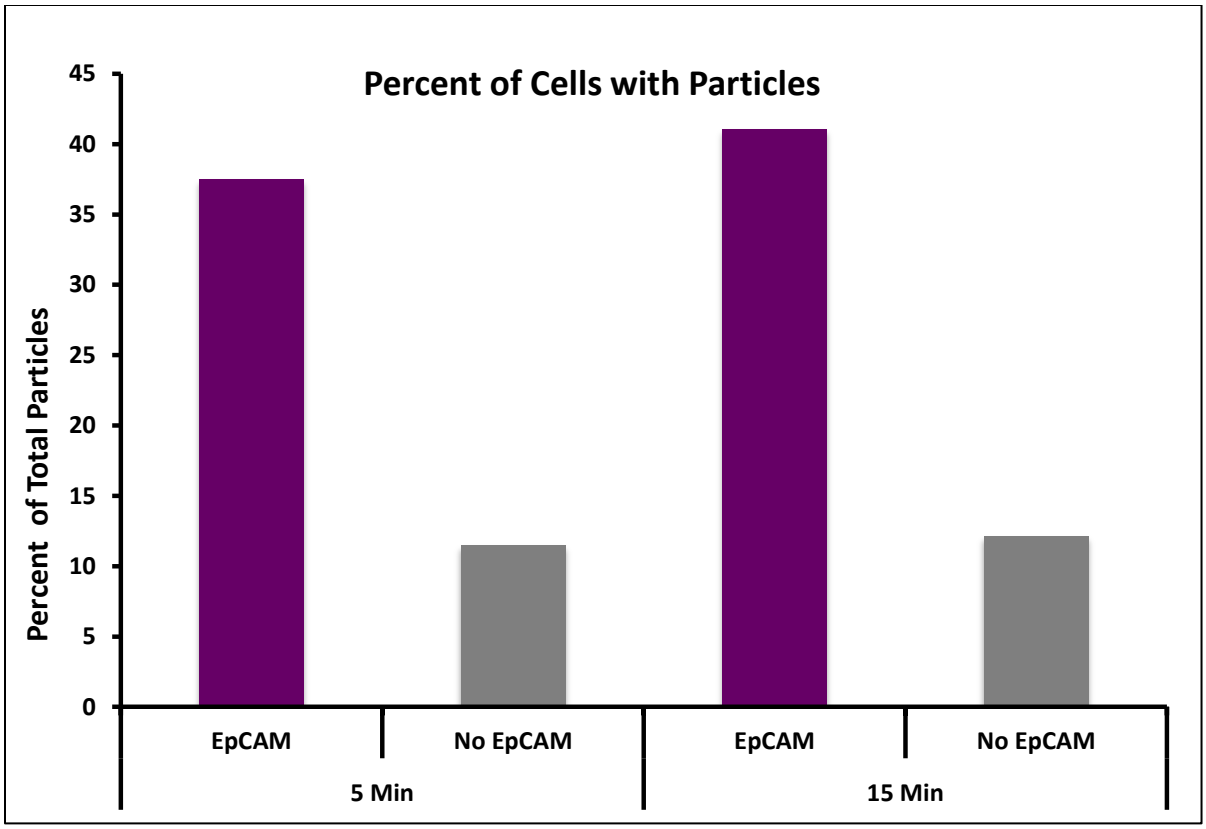

Figure 5.7: PANC-1 labeling with EpCAM functionalized and unfunctionalized spheres. EpCAM spheres show higher labeling extents compared to control spheres at both time points.

At both time points, EpCAM functionalized spheres attain higher percentages of PANC-1 cell labeling which may be reflective of higher specific labeling of the cells with the polymer spheres. Polymer spheres without EpCAM also show some degree of surface attachment to cells which may be as a result of nonspecific binding of the spheres to the cancer cells. Overall, labeling efficiency can be improved and efforts to do so will include testing particle functionalization with increased concentrations of both Neutravidin and biotinylated EpCAM, among other steps.

5.5 Discussion

Efforts are ongoing to develop the multiplexed assay of differently synthesized micron-sized polymer particles coated with unique CTC antibodies for separation of CTC subpopulations using inertial sorting in microchannels. Preliminary data showed that neither particle porosity nor minor shifts in particle shape (flat disc versus biconcave RBC disc) led to particle separation using the selected inertial sorter design at the flow rates tested. However,

polymer particles of significantly different shapes, namely discs and spheres, could potentially be separated in the inertial sorter under study. Also, initial experiments to label cancer cells with the surface functionalized polymer spheres shows promise where PANC-1 cells showed almost 40% particle attachment compared to the unfunctionalized control spheres. Further optimization will require continued testing of particle physics and inertial sorter designs. Additionally, surface functionalization of polymer particles with antibodies of interest such as CD44, CD133 and CD24 among others, still needs to be explored.

In fulfilling the objectives of this study, we imagine that we can both identify and separate CTCs according to their unique surface marker expressions. With such high throughput segregation of CTC subtypes, to yield cells that are viable, we imagine that this approach will be advantageous in studies involving, for example, development of diagnostics and patient response to therapy. Thereupon the platform can serve as a facile method of patient monitoring. Additionally, sensitive molecular analyses such as mRNA profiling and sequencing can be compared among the different CTCs to correlate their phenotype and genotype with CSCs, which have been particularly implicated in the metastasis of pancreatic cancer.

Chapter 6

Conclusions

6.1 Summary of Research Findings

6.1.1 Development of an integrated microfluidic immunomagnetic platform to isolate CTCs

An integrated microfluidic immunomagnetic platform to isolate CTCs in suspension from whole blood of patient samples was developed (chapter 2). The approach enables significant CTC enrichment in a continuous, high-throughput manner (24 mL hr^{-1}), through strategic combination of size based-inertial, on-chip CTC labeling with magnetic microbeads, and magnetic cell sorting. The clinical relevance of the platform was demonstrated by enabling unequaled CTC isolation purity rates (82.5%±23.5) among pancreatic ductal adenocarcinoma (PDAC) patient samples. Detection of >13 CTCs/mL was observed in 100% of patient samples (median = 69 CTCs/mL, mean = 146± 231 CTCs/mL). Since CTCs are isolated in suspension, the sample is amenable to CTC molecular profiling and so both MicroRNA and mRNA profiling of CTCs were carried out from CTCs isolated within the system. MicroRNA and mRNA profiling of CTCs revealed that RNAs previously reported as PDAC-associated, were among those most abundantly expressed. In summary, a microfluidic platform that enhances CTC purity and permits detailed molecular characterization of isolated CTCs was described.

6.1.2 Continuum Isolation of Sub-Populations of Pancreatic Cancer CTCs via Immunomagnetism

A method to enrich specific tumor cell groups immunomagnetically according to a continuum of EpCAM surface marker expression levels was described (chapter 3). Specifically, we categorized cells as having low, moderate and high EpCAM expression among levels which can potentially reflect different physiological contributions of each cell subset to pancreatic disease. We demonstrated that even among a relatively homogenous group of cells such as the PANC-1 cell line, cells could be separated according to their EpCAM levels into low, moderate and high expression. Additionally, a wound healing assay was performed to functionally assess each subpopulation, which revealed distinct invasive potentials among each subset. Furthermore, we described the isolation of pancreatic cancer CTCs from the same patient sample based on their varying EpCAM levels. Overall we demonstrated a robust method of capturing varying EpCAM leveled-CTCs, which could subsequently shed light on tumor heterogeneity. Among a cohort of 6 patients, 5 of 6 samples had CTCs that could be recovered at all three levels of EpCAM expression, though the majority of CTCs were recovered as low expression events. Preliminary studies that compare tumor cell subpopulations in this continuum manner can potentially increase our understanding of the dynamic nature of cell heterogeneity and how it relates to patient outcomes. Also further investigation may also reveal therapeutic targets for the different subpopulations.

6.1.3 Dual-Marker Isolation and Characterization of Pancreatic Ductal Adenocarcinoma Circulating Tumor Cells via EpCAM- and CD44- based Immunomagnetism

Efforts to study whether CD44-based CTC isolation would contribute to any observable differences among CTCs enriched from pancreatic cancer samples, compared to standalone EpCAM, has been described. Apart from the established epithelial marker EpCAM, expression of the stem cell marker CD44, among pancreatic cancer CTCs has taken on particular importance since these cells demonstrate an enhanced metastatic potential. CTCs were isolated using either anti-EpCAM as a standalone antibody or a combination of anti- EpCAM and anti-CD44 from each of ten patient samples. We show that within this patient cohort there was no significant difference ($p=0.328$) in detection rates between EpCAM+CD44 dual isolation (average CTCs/mL=64±63) compared to EpCAM only isolation (average CTCs/mL=42±33). Additionally, we describe that among the 8 samples in which CTCs appeared in clusters, their

detection was independent of whether EpCAM only or EpCAM-CD44 combination was used (p=0.593). Also we describe how mRNA profiles of CTCs isolated with EpCAM-CD44 among patients with less advanced disease clustered distinctly from those isolated solely with EpCAM (n=5). This distinction was not observed among patients with more advanced disease (n=3). Though preliminary, studies as such can be used in further characterization of metastatic advance of pancreatic cancer.

6.1.4 Inertial Sorting of polymer particles based on particle shape and porosity

In this study we proposed and described how particle physics such as shape and porosity could be leveraged in multiple-marker immunolabeling of these CTCs. In most instances CTCs that are responsible for driving the metastatic process are expected to express multiple surface proteins, the extents of which may vary. Evidence suggests that particle shape at the micron-scale enhances antibody specificity and avidity to antigens. We proposed that shapes that allow enhanced avidity can be coated with antibodies against less abundant surface proteins while other particle shapes can be used for more abundantly expressed CTC surface markers. With such an approach, not only cells can be identified as expressing multiple markers, yet the approach reduces the amount of immunofluorescence post processing if shapes are specific to unique markers of interest. Additionally, through the use of inertial microfluidic CTC sorting CTCs labeled with micron-sized particles can be enriched from patient samples in a high throughput manner. In addition to particle shape as a factor to hydrodynamically separate and sort particles, we set out to investigate whether particle porosity would facilitate enhanced particle sorting. We reported our initial findings associated with particle synthesis and subsequent sorting of particles using microfluidic inertial sorting. Using the inertial sorting device disc shaped polymer particles could be separated from polymer spheres at the flowrates tested. Additionally, we demonstrated successful labeling of PANC-1 cancer cells with EpCAM functionalized polymer spheres.

6.2 Limitations and Future Directions

6.2.1 Operation of the integrated microfluidic immunomagnetic cell sorter

To date, implementation of microfluidic based technologies to isolate and study rare CTCs has led to significant advances in our understanding of mechanisms involved in cancer and the invasive metastasis cascade. Ultimately, studies and findings predicated on these platforms represent tools that can guide identification of potential therapeutic targets. The reported integrated microfluidic immunomagnetic platform is capable of significant CTC enrichment in a high-throughput manner that is amenable to sensitive molecular characterization. Furthermore the universality of the platform allows it to be implemented in any cell isolation context wherein cell surface makers of interest have been identified. Apart from the advantages of the device there remain opportunities for improvement of the technology, as well as the associated protocol for patient sample processing.

CTC isolation with the integrated system is dependent on size-based inertial sorting as a first stage of CTC enrichment such that cells with a diameter >15μm get sorted to the innermost outlet of the inertial sorter. Previous studies have shown where CTCs with <4 μm have been recovered.[7] CTCs of this size range are likely to be unfocused in the inertial sorter at the flow rates typically used for sample processing, and may emerge from any outlet of the inertial sorter. Those that emerge from the innermost outlet of the spiral and flow into the passive mixer may successfully be immunomagnetically labeled and isolated but the CTCs that emerge from the three other waste outlets remain undetected. While a fraction of these smaller CTCs may randomly disperse to the innermost outlet, a potentially important subset of CTCs can be lost due to this device limitation.

One potential method that can be employed to recover a greater percentage of these smaller CTCs from future patient samples is to process the sample that emerges from both the first and second spiral sorter outlets. Additionally, another approach that can be tested to improve the recoveries of smaller CTC is to process the sample form the waste outlets a second time through the inertial sorter. Of the two potential methods, the second one allows for more efficient sample volume reduction overall, and so more rapid sample processing. Subsequent CTC immunomagnetic labeling and processing can be carried out as previously described. Moreover, for samples in which smaller CTCs have been successfully detected, molecular profiling and comparison of CTCs based on their size may help to identify unique molecular characteristics between the groups that affect this phenotypic difference.

The dependence of the integrated microfluidic immunomagnetic platform on immunomagnetic bead labeling for CTC isolation has a couple of drawbacks. If using a single antibody to label CTCs, cells that express the labeling antibody to a negligible degree can potentially go unlabeled and therefore undetected in the system. Such concerns can be addressed by using a cocktail of antibodies that target a range of putative CTC markers, however caution needs to be taken that such markers are specific to CTCs to avoid contamination with other hematopoietic cells. CTCs emerge from the integrated system in suspension, which is advantageous for subsequent assays such as single CTC analysis, compared to methods that immobilize CTCs in the device. However, there are concerns that unattached magnetic beads in the sample may present clogging issues with some of the more recently established platforms for single cell and molecular analysis. Methods to address such concerns include cell-picking and transferring isolated CTCs from the beads or using a rapid size based filtration method to remove the smaller beads from the magnetically labeled CTCs. Through either method, excess magnetic beads can be removed to prevent clogging issues during these subsequent CTC assays.

With the integrated microfluidic immunomagnetic device, magnetic sorting is the rate limiting step of the entire process occuring at 50μL/min. The simplicity of the design allows it to be readily multiplexed so that several magnetic sorters can be operated concurrently. Future work involves designing and optimizing a reusable multi-magnetic sorter where several magnetic sorter devices can run in parallel. To ensure reusability of the multiplexed device, the material of construct will be based on its ability to retain its engineered parameters and features over time in addition to the ease with which it can be sterilized to minimize the likelihood of cross-contamination among patient samples.

Once patient samples are processed in the device, CTC identification and enumeration are dependent on immunofluorescence staining. To reduce the cost and time associated with such procedures, on-chip automated counting of CTCs has been proposed. Future work will involve development of an on-chip CTC quantification capabilities similar to work previously described that use the electromagnetic resistance of magnetically labeled cells for detection. [205]Once the device has been calibrated, the established characteristic resistance associated with a cell magnetized with magnetic beads will be used as a basis for enumeration. As magnetized CTCs emerge through the collection outlet of the magnetic sorter, the system will enumerate and record such events. Especially in a setting where numerous patient samples are being tested, an

automated counting system enables rapid and convenient enumeration, which in turn leads to rapid identification of CTC samples that may be considered for subsequent CTC assays. Furthermore, this approach removes concerns about the loss of CTCs during centrifugation-dependent processes such as the currently used cytospin process required for sample immunofluorescence staining. Also inaccuracies surrounding the scale up of CTCs counts from small sample to the overall volume are eliminated if actual CTC counts can be determined on chip.

6.2.2 Assessing larger patient cohorts stage wise

So far, molecular profiles of <20 patient samples have been studied in any of the reported projects. While preliminary CTC data generated across small patient cohorts using the integrated system show that molecular patterns characteristic of specific disease stages may be identified among patients, tighter controls regarding patient treatment methods are required. To generate data that can have significant impact upon clinical implications of CTC studies, larger numbers of patients need to be studied. For instance in a previous study among 63 PDAC patients persistent differences in clinical outcomes were observed if patients were stratified according to early and advanced disease stages. Moreover detection of circulating tumor cell clusters before treatment was an independent predictor of survival.[177]

Pancreatic cancer progresses and disseminates rapidly compared to other cancers, and so, especially in the context of pancreatic cancer, developing a molecular fingerprint for early disease detection has the potential to significantly impact patient outcomes and reduce mortality.[206] Since CTCs can be robustly isolated with high sensitivity in the reported integrated microfluidic immunomagnetic platform, its implementation in studies with larger cohorts of patients holds promise in identifying molecular and physiologically distinct fingerprints of pancreatic cancer. Furthemre, characterizing pancreatic disease at relatively early stages may increase our understanding of what leads to disease onset and so diagnostic tools can be developed. To this end, CTC molecular profiles enriched from patients with less advanced diseases can be compared to those with more advanced disease staging. patients that are either treatment naïve or on the same treatment regimens should be compared to maintain experimental controls and to facilitate objective comparisons.

Moreover, the system can be implemented to monitor intra-patient differences that occur at the molecular level as pancreatic cancer progresses within the patient. has the potential to uncover effective therapeutic targets. To this end CTCs can be isolated from patients at distinct stages of disease and Once a sufficiently large number of patients are profiled, analysis of CTC molecular profiles associated with disease stages may potentially reveal pathways and genes characteristic of disease advance. Interrogating these pathways more deeply has the potential to identifying therapeutic targets.

6.2.3 Standardization of molecular profiling of small cell population

Molecular based assays such as microRNA and mRNA profiling have traditionally been used to assay large numbers of cells and large tissue fragments. In general, CTC molecular profiling is a less developed field and so the approaches and protocols adopted by different groups may vary.[184, 207] Furthermore, the low number of cells can present more technical challenges for specificity of profiles especially if there is contamination with other blood cells. A potential concern is that such variations in protocol can ultimately result in generation of data that cannot be objectively compared. Apart from differences in RNA extraction and profiling protocols, post profiling analysis is another potential cause of variation among studies. Overall, there is a need for standardization of molecular profiling and analysis protocols so that studies generated by different groups can be more objectively compared.[184, 207]

Given these concerns, future endeavors to standardize CTC molecular profiling methods will involve developing a detailed standard operating procedure for sample processing so that results across different platforms can be compared with confidence. For samples with relatively low RNA content such as CTC enriched samples, establishing a reliable range of values for quality control parameters such as RNA concentration (ng/µL) as well as purity (260/280 absorbance ratio) is important. Moreover, understanding how and why different RNA purification kits and methods affect the quality and reliability of results will be essential in narrowing options as a standard procedure is adopted. For the few pancreatic cancer patient samples that failed quality control tests, ascertaining the cause of failure will also be beneficial in establishing preventive measures in the future.

6.2.4 Single Cell analysis of patient CTCs

Given the heterogeneity among tumor cells of the primary tumor and the small fraction of cells that successfully disseminate and circulate form the tumor, the ability to interrogate such cells at the single level has the potential to improve our understanding of disease evolution as well as tumor biology. [184] Single CTC analysis also addresses concerns about other blood cell contamination and the effect it can have on CTC profiling.[184] With the integrated microfluidic immunomagnetic platform, since enriched CTCs emerge from the device in as single CTCs or CTC aggregates, cells can readily be made available for single cell interrogation. Future work will involve developing a method to identify and then micro-manipulate single cells from the device in order to carry out single cell molecular profiling, similar to what has been previously demonstrated.[208, 209]

Once CTCs are enriched from patient samples with the integrated device, one method of selecting single cells can be to manually manipulate and pipette cells using a hand-held pipette, combined with microscope imaging. While this process may prove to be laborious, the low WBC contamination enabled by the integrated device combined with CTC magnetic bead labeling allows for a relatively facile CTC identification and selection process. Additionally, single cell analysis can be carried out using a platform such as Fluidigm C1 (San Francisco, California) where CTCs in suspension can be encapsulated as single entities in microfluidic wells and examined for molecular sequencing and expression data. Therefore, from a single patient sample, information about the frequency as well as heterogeneity of expression of mutations and aberrations among CTCs can be generated.

Overall, the basis for future studies involving CTCs and cells enriched from the integrated device lies in molecular studies that span across large patient cohorts. Automating the CTC enumeration process is imminent as it enables rapid on-chip detection of CTCs. We imagine that detailed and well defined studies that implement CTC enrichment using the integrated device can ultimately bring insight into important mechanisms and pathways that facilitate invasive metastasis cascade in pancreatic cancer. Moreover, the idea is that with conclusive data as such, will inform future endeavors to establish effective therapies against pancreatic disease.

6.3 Conclusion

Finally, the integrated microfluidic immunomagnetic device is a versatile platform that can be recruited in CTC studies beyond just pancreatic cancer. The tunability of the system and its ability to yield highly enriched CTCs enables quality CTC fingerprinting and molecular characterization. Ultimately, such studies hold the potential to identify effective therapeutic targets and agents in the fight again cancer.

References

[1] Ashworth, T. (1869) A case of cancer in which cells similar to those in the tumours were seen in the blood after death, *Aust Med J 14*, 146-149.

[2] Pantel, K., and Brakenhoff, R. H. (2004) Dissecting the metastatic cascade, *Nature reviews. Cancer 4*, 448-456.

[3] Husemann, Y., Geigl, J. B., Schubert, F., Musiani, P., Meyer, M., Burghart, E., Forni, G., Eils, R., Fehm, T., Riethmuller, G., and Klein, C. A. (2008) Systemic spread is an early step in breast cancer, *Cancer cell 13*, 58-68.

[4] Jones, S., Zhang, X., Parsons, D. W., Lin, J. C., Leary, R. J., Angenendt, P., Mankoo, P., Carter, H., Kamiyama, H., Jimeno, A., Hong, S. M., Fu, B., Lin, M. T., Calhoun, E. S., Kamiyama, M., Walter, K., Nikolskaya, T., Nikolsky, Y., Hartigan, J., Smith, D. R., Hidalgo, M., Leach, S. D., Klein, A. P., Jaffee, E. M., Goggins, M., Maitra, A., Iacobuzio-Donahue, C., Eshleman, J. R., Kern, S. E., Hruban, R. H., Karchin, R., Papadopoulos, N., Parmigiani, G., Vogelstein, B., Velculescu, V. E., and Kinzler, K. W. (2008) Core signaling pathways in human pancreatic cancers revealed by global genomic analyses, *Science (New York, N.Y.) 321*, 1801-1806.

[5] Paterlini-Brechot, P., and Benali, N. L. (2007) Circulating tumor cells (CTC) detection: clinical impact and future directions, *Cancer letters 253*, 180-204.

[6] Pantel, K., Brakenhoff, R. H., and Brandt, B. (2008) Detection, clinical relevance and specific biological properties of disseminating tumour cells, *Nature reviews. Cancer 8*, 329-340.

[7] Allard, W. J., Matera, J., Miller, M. C., Repollet, M., Connelly, M. C., Rao, C., Tibbe, A. G., Uhr, J. W., and Terstappen, L. W. (2004) Tumor cells circulate in the peripheral blood of all major carcinomas but not in healthy subjects or patients with nonmalignant diseases, *Clinical cancer research : an official journal of the American Association for Cancer Research 10*, 6897-6904.

[8] Cristofanilli, M., Budd, G. T., Ellis, M. J., Stopeck, A., Matera, J., Miller, M. C., Reuben, J. M., Doyle, G. V., Allard, W. J., Terstappen, L. W. M. M., and Hayes, D. F. (2004) Circulating Tumor Cells, Disease Progression, and Survival in Metastatic Breast Cancer, *New England Journal of Medicine 351*, 781-791.

[9] Hayes, D. F., Cristofanilli, M., Budd, G. T., Ellis, M. J., Stopeck, A., Miller, M. C., Matera, J., Allard, W. J., Doyle, G. V., and Terstappen, L. W. (2006) Circulating tumor cells at each follow-up time point during therapy of metastatic breast cancer patients predict progression-free and overall survival, *Clinical cancer research : an official journal of the American Association for Cancer Research 12*, 4218-4224.

[10] Moreno, J. G., Miller, M. C., Gross, S., Allard, W. J., Gomella, L. G., and Terstappen, L. W. (2005) Circulating tumor cells predict survival in patients with metastatic prostate cancer, *Urology 65*, 713-718.

[11] Cohen, S. J., Punt, C. J., Iannotti, N., Saidman, B. H., Sabbath, K. D., Gabrail, N. Y., Picus, J., Morse, M. A., Mitchell, E., Miller, M. C., Doyle, G. V., Tissing, H., Terstappen, L. W., and Meropol, N. J. (2009) Prognostic significance of circulating tumor cells in patients with

metastatic colorectal cancer, *Annals of oncology : official journal of the European Society for Medical Oncology / ESMO 20*, 1223-1229.

[12] Krebs, M. G., Sloane, R., Priest, L., Lancashire, L., Hou, J. M., Greystoke, A., Ward, T. H., Ferraldeschi, R., Hughes, A., Clack, G., Ranson, M., Dive, C., and Blackhall, F. H. (2011) Evaluation and prognostic significance of circulating tumor cells in patients with non-small-cell lung cancer, *Journal of clinical oncology : official journal of the American Society of Clinical Oncology 29*, 1556-1563.

[13] Nesteruk, D., Rutkowski, A., Fabisiewicz, S., Pawlak, J., Siedlecki, J. A., and Fabisiewicz, A. (2014) Evaluation of prognostic significance of circulating tumor cells detection in rectal cancer patients treated with preoperative radiotherapy: prospectively collected material data, *BioMed research international 2014*, 712827.

[14] Stoecklein, N. H., and Klein, C. A. (2010) Genetic disparity between primary tumours, disseminated tumour cells, and manifest metastasis, *International journal of cancer. Journal international du cancer 126*, 589-598.

[15] Klein, C. A., Blankenstein, T. J., Schmidt-Kittler, O., Petronio, M., Polzer, B., Stoecklein, N. H., and Riethmuller, G. (2002) Genetic heterogeneity of single disseminated tumour cells in minimal residual cancer, *Lancet 360*, 683-689.

[16] Marrinucci, D., Bethel, K., Bruce, R. H., Curry, D. N., Hsieh, B., Humphrey, M., Krivacic, R. T., Kroener, J., Kroener, L., Ladanyi, A., Lazarus, N. H., Nieva, J., and Kuhn, P. (2007) Case study of the morphologic variation of circulating tumor cells, *Human pathology 38*, 514-519.

[17] Lin, H. K., Zheng, S., Williams, A. J., Balic, M., Groshen, S., Scher, H. I., Fleisher, M., Stadler, W., Datar, R. H., Tai, Y.-C., and Cote, R. J. (2010) Portable Filter-Based Microdevice for Detection and Characterization of Circulating Tumor Cells, *Clinical cancer research : an official journal of the American Association for Cancer Research 16*, 5011-5018.

[18] Park, S., Ang, R. R., Duffy, S. P., Bazov, J., Chi, K. N., Black, P. C., and Ma, H. (2014) Morphological differences between circulating tumor cells from prostate cancer patients and cultured prostate cancer cells, *PloS one 9*, e85264.

[19] Powell, A. A., Talasaz, A. H., Zhang, H., Coram, M. A., Reddy, A., Deng, G., Telli, M. L., Advani, R. H., Carlson, R. W., Mollick, J. A., Sheth, S., Kurian, A. W., Ford, J. M., Stockdale, F. E., Quake, S. R., Pease, R. F., Mindrinos, M. N., Bhanot, G., Dairkee, S. H., Davis, R. W., and Jeffrey, S. S. (2012) Single cell profiling of circulating tumor cells: transcriptional heterogeneity and diversity from breast cancer cell lines, *PloS one 7*, e33788.

[20] Kim, M. Y., Oskarsson, T., Acharyya, S., Nguyen, D. X., Zhang, X. H., Norton, L., and Massague, J. (2009) Tumor self-seeding by circulating cancer cells, *Cell 139*, 1315-1326.

[21] Alix-Panabières, C., Schwarzenbach, H., and Pantel, K. (2012) Circulating Tumor Cells and Circulating Tumor DNA, *Annual Review of Medicine 63*, 199-215.

[22] Polyak, K., and Weinberg, R. A. (2009) Transitions between epithelial and mesenchymal states: acquisition of malignant and stem cell traits, *Nature reviews. Cancer 9*, 265-273.

[23] Rhim, A. D., Mirek, E. T., Aiello, N. M., Maitra, A., Bailey, J. M., McAllister, F., Reichert, M., Beatty, G. L., Rustgi, A. K., Vonderheide, R. H., Leach, S. D., and Stanger, B. Z. (2012) EMT and dissemination precede pancreatic tumor formation, *Cell 148*, 349-361.

[24] Sarkar, F. H., Li, Y., Wang, Z., and Kong, D. (2009) Pancreatic cancer stem cells and EMT in drug resistance and metastasis, *Minerva chirurgica 64*, 489-500.

[25] Rhim, A. D., Thege, F. I., Santana, S. M., Lannin, T. B., Saha, T. N., Tsai, S., Maggs, L. R., Kochman, M. L., Ginsberg, G. G., Lieb, J. G., Chandrasekhara, V., Drebin, J. A., Ahmad, N., Yang, Y. X., Kirby, B. J., and Stanger, B. Z. (2014) Detection of circulating pancreas epithelial cells in patients with pancreatic cystic lesions, *Gastroenterology 146*, 647-651.

[26] Li, C., Heidt, D. G., Dalerba, P., Burant, C. F., Zhang, L., Adsay, V., Wicha, M., Clarke, M. F., and Simeone, D. M. (2007) Identification of pancreatic cancer stem cells, *Cancer research 67*, 1030-1037.

[27] Li, C., Lee, C. J., and Simeone, D. M. (2009) Identification of human pancreatic cancer stem cells, *Methods in molecular biology (Clifton, N.J.) 568*, 161-173.

[28] Autebert, J., Coudert, B., Bidard, F.-C., Pierga, J.-Y., Descroix, S., Malaquin, L., and Viovy, J.-L. (2012) Microfluidic: An innovative tool for efficient cell sorting, *Methods 57*, 297-307.

[29] Dong, Y., Skelley, A. M., Merdek, K. D., Sprott, K. M., Jiang, C., Pierceall, W. E., Lin, J., Stocum, M., Carney, W. P., and Smirnov, D. A. (2013) Microfluidics and Circulating Tumor Cells, *The Journal of Molecular Diagnostics 15*, 149-157.

[30] Nagrath, S., Sequist, L. V., Maheswaran, S., Bell, D. W., Irimia, D., Ulkus, L., Smith, M. R., Kwak, E. L., Digumarthy, S., Muzikansky, A., Ryan, P., Balis, U. J., Tompkins, R. G., Haber, D. A., and Toner, M. (2007) Isolation of rare circulating tumour cells in cancer patients by microchip technology, *Nature 450*, 1235-1239.

[31] Stott, S. L., Hsu, C. H., Tsukrov, D. I., Yu, M., Miyamoto, D. T., Waltman, B. A., Rothenberg, S. M., Shah, A. M., Smas, M. E., Korir, G. K., Floyd, F. P., Jr., Gilman, A. J., Lord, J. B., Winokur, D., Springer, S., Irimia, D., Nagrath, S., Sequist, L. V., Lee, R. J., Isselbacher, K. J., Maheswaran, S., Haber, D. A., and Toner, M. (2010) Isolation of circulating tumor cells using a microvortex-generating herringbone-chip, *Proc Natl Acad Sci U S A 107*, 18392-18397.

[32] Wang, S., Liu, K., Liu, J., Yu, Z. T., Xu, X., Zhao, L., Lee, T., Lee, E. K., Reiss, J., Lee, Y. K., Chung, L. W., Huang, J., Rettig, M., Seligson, D., Duraiswamy, K. N., Shen, C. K., and Tseng, H. R. (2011) Highly efficient capture of circulating tumor cells by using nanostructured silicon substrates with integrated chaotic micromixers, *Angewandte Chemie (International ed. in English) 50*, 3084-3088.

[33] Lin, M., Chen, J. F., Lu, Y. T., Zhang, Y., Song, J., Hou, S., Ke, Z., and Tseng, H. R. (2014) Nanostructure embedded microchips for detection, isolation, and characterization of circulating tumor cells, *Acc Chem Res 47*, 2941-2950.

[34] Ke, Z., Lin, M., Chen, J. F., Choi, J. S., Zhang, Y., Fong, A., Liang, A. J., Chen, S. F., Li, Q., Fang, W., Zhang, P., Garcia, M. A., Lee, T., Song, M., Lin, H. A., Zhao, H., Luo, S. C., Hou, S., Yu, H. H., and Tseng, H. R. (2015) Programming thermoresponsiveness of NanoVelcro substrates enables effective purification of circulating tumor cells in lung cancer patients, *ACS Nano 9*, 62-70.

[35] Hughes, A. D., Mattison, J., Western, L. T., Powderly, J. D., Greene, B. T., and King, M. R. (2012) Microtube device for selectin-mediated capture of viable circulating tumor cells from blood, *Clinical chemistry 58*, 846-853.

[36] Gleghorn, J. P., Pratt, E. D., Denning, D., Liu, H., Bander, N. H., Tagawa, S. T., Nanus, D. M., Giannakakou, P. A., and Kirby, B. J. (2010) Capture of circulating tumor cells from whole blood of prostate cancer patients using geometrically enhanced differential immunocapture (GEDI) and a prostate-specific antibody, *Lab Chip 10*, 27-29.

[37] Adams, A. A., Okagbare, P. I., Feng, J., Hupert, M. L., Patterson, D., Göttert, J., McCarley, R. L., Nikitopoulos, D., Murphy, M. C., and Soper, S. A. (2008) Highly Efficient Circulating Tumor Cell Isolation from Whole Blood and Label-Free Enumeration Using Polymer-Based Microfluidics with an Integrated Conductivity Sensor, *Journal of the American Chemical Society 130*, 8633-8641.

[38] Earhart, C. M., Hughes, C. E., Gaster, R. S., Ooi, C. C., Wilson, R. J., Zhou, L. Y., Humke, E. W., Xu, L., Wong, D. J., Willingham, S. B., Schwartz, E. J., Weissman, I. L., Jeffrey, S. S., Neal, J. W., Rohatgi, R., Wakelee, H. A., and Wang, S. X. (2014) Isolation and mutational analysis of circulating tumor cells from lung cancer patients with magnetic sifters and biochips, *Lab Chip 14*, 78-88.

[39] Murlidhar, V., Zeinali, M., Grabauskiene, S., Ghannad-Rezaie, M., Wicha, M. S., Simeone, D. M., Ramnath, N., Reddy, R. M., and Nagrath, S. (2014) A radial flow microfluidic device for ultra-high-throughput affinity-based isolation of circulating tumor cells, *Small (Weinheim an der Bergstrasse, Germany) 10*, 4895-4904.

[40] Yoon, H. J., Kim, T. H., Zhang, Z., Azizi, E., Pham, T. M., Paoletti, C., Lin, J., Ramnath, N., Wicha, M. S., Hayes, D. F., Simeone, D. M., and Nagrath, S. (2013) Sensitive capture of circulating tumour cells by functionalised graphene oxide nanosheets, *Nature nanotechnology 8*, 735-741.

[41] Went, P. T., Lugli, A., Meier, S., Bundi, M., Mirlacher, M., Sauter, G., and Dirnhofer, S. (2004) Frequent EpCam protein expression in human carcinomas, *Human pathology 35*, 122-128.

[42] Gastl, G., Spizzo, G., Obrist, P., Dunser, M., and Mikuz, G. (2000) Ep-CAM overexpression in breast cancer as a predictor of survival, *Lancet 356*, 1981-1982.

[43] Spizzo, G., Gastl, G., Obrist, P., Went, P., Dirnhofer, S., Bischoff, S., Mirlacher, M., Sauter, G., Simon, R., Stopatschinskaya, S., Haas, P., Bart, R., Köchli, O., Spichtin, H., Maurer, R., Metzger, U., von Castelberg, B., Zuber, M., Mross, F., and Dietrich, H. (2004) High Ep-CAM Expression is Associated with Poor Prognosis in Node-positive Breast Cancer, *Breast cancer research and treatment 86*, 207-213.

[44] Spizzo, G., Gastl, G., Wolf, D., Gunsilius, E., Steurer, M., Fong, D., Amberger, A., Margreiter, R., and Obrist, P. (0000) Correlation of COX-2 and Ep-CAM overexpression in human invasive breast cancer and its impact on survival, *Br J Cancer 88*, 574-578.

[45] Lim, L. S., Hu, M., Huang, M. C., Cheong, W. C., Gan, A. T., Looi, X. L., Leong, S. M., Koay, E. S., and Li, M. H. (2012) Microsieve lab-chip device for rapid enumeration and fluorescence in situ hybridization of circulating tumor cells, *Lab Chip 12*, 4388-4396.

[46] Kim, M. S., Sim, T. S., Kim, Y. J., Kim, S. S., Jeong, H., Park, J.-M., Moon, H.-S., Kim, S. I., Gurel, O., Lee, S. S., Lee, J.-G., and Park, J. C. (2012) SSA-MOA: a novel CTC isolation platform using

selective size amplification (SSA) and a multi-obstacle architecture (MOA) filter, *Lab on a Chip 12*, 2874-2880.

[47] Tan, S. J., Yobas, L., Lee, G. Y. H., Ong, C. N., and Lim, C. T. (2009) Microdevice for Trapping Circulating Tumor Cells for Cancer Diagnostics

13th International Conference on Biomedical Engineering, (Lim, C. T., and Goh, J. C. H., Eds.), pp 774-777, Springer Berlin Heidelberg.

[48] Tan, S. J., Lakshmi, R. L., Chen, P., Lim, W. T., Yobas, L., and Lim, C. T. (2010) Versatile label free biochip for the detection of circulating tumor cells from peripheral blood in cancer patients, *Biosensors & bioelectronics 26*, 1701-1705.

[49] Zheng, S., Lin, H., Lu, B., Williams, A., Datar, R., Cote, R., and Tai, Y.-C. (2011) 3D microfilter device for viable circulating tumor cell (CTC) enrichment from blood, *Biomedical Microdevices 13*, 203-213.

[50] Di Carlo, D. (2009) Inertial microfluidics, *Lab on a Chip 9*, 3038-3046.

[51] Di Carlo, D., Edd, J. F., Irimia, D., Tompkins, R. G., and Toner, M. (2008) Equilibrium Separation and Filtration of Particles Using Differential Inertial Focusing, *Analytical Chemistry 80*, 2204-2211.

[52] Kuntaegowdanahalli, S. S., Bhagat, A. A. S., Kumar, G., and Papautsky, I. (2009) Inertial microfluidics for continuous particle separation in spiral microchannels, *Lab on a Chip 9*.

[53] Bhagat, A. A. S., Kuntaegowdanahalli, S. S., and Papautsky, I. (2008) Continuous particle separation in spiral microchannels using dean flows and differential migration, *Lab on a Chip 8*.

[54] Sollier, E., Go, D. E., Che, J., Gossett, D. R., O'Byrne, S., Weaver, W. M., Kummer, N., Rettig, M., Goldman, J., Nickols, N., McCloskey, S., Kulkarni, R. P., and Di Carlo, D. (2014) Size-selective collection of circulating tumor cells using Vortex technology, *Lab Chip 14*, 63-77.

[55] Bhagat, A. A., Hou, H. W., Li, L. D., Lim, C. T., and Han, J. (2011) Pinched flow coupled shear-modulated inertial microfluidics for high-throughput rare blood cell separation, *Lab Chip 11*, 1870-1878.

[56] Hou, H. W., Warkiani, M. E., Khoo, B. L., Li, Z. R., Soo, R. A., Tan, D. S.-W., Lim, W.-T., Han, J., Bhagat, A. A. S., and Lim, C. T. (2013) Isolation and retrieval of circulating tumor cells using centrifugal forces, *Scientific Reports 3*, 1259.

[57] Sun, J., Li, M., Liu, C., Zhang, Y., Liu, D., Liu, W., Hu, G., and Jiang, X. (2012) Double spiral microchannel for label-free tumor cell separation and enrichment, *Lab Chip 12*, 3952-3960.

[58] Warkiani, M. E., Guan, G., Luan, K. B., Lee, W. C., Bhagat, A. A. S., Kant Chaudhuri, P., Tan, D. S.-W., Lim, W. T., Lee, S. C., Chen, P. C. Y., Lim, C. T., and Han, J. (2014) Slanted spiral microfluidics for the ultra-fast, label-free isolation of circulating tumor cells, *Lab on a Chip 14*, 128-137.

[59] Mohamed, H., Murray, M., Turner, J. N., and Caggana, M. (2009) Isolation of tumor cells using size and deformation, *Journal of Chromatography A 1216*, 8289-8295.

[60] Rinker-Schaeffer, C. W., Partin, A. W., Isaacs, W. B., Coffey, D. S., and Isaacs, J. T. (1994) Molecular and cellular changes associated with the acquisition of metastatic ability by prostatic cancer cells, *The Prostate 25*, 249-265.

[61] Ozkumur, E., Shah, A. M., Ciciliano, J. C., Emmink, B. L., Miyamoto, D. T., Brachtel, E., Yu, M., Chen, P.-i., Morgan, B., Trautwein, J., Kimura, A., Sengupta, S., Stott, S. L., Karabacak, N. M., Barber, T. A., Walsh, J. R., Smith, K., Spuhler, P. S., Sullivan, J. P., Lee, R. J., Ting, D. T., Luo, X., Shaw, A. T., Bardia, A., Sequist, L. V., Louis, D. N., Maheswaran, S., Kapur, R., Haber, D. A., and Toner, M. (2013) Inertial Focusing for Tumor Antigen–Dependent and –Independent Sorting of Rare Circulating Tumor Cells, *Science Translational Medicine 5*, 179ra147.

[62] Harb, W., Fan, A., Tran, T., Danila, D. C., Keys, D., Schwartz, M., and Ionescu-Zanetti, C. (2013) Mutational Analysis of Circulating Tumor Cells Using a Novel Microfluidic Collection Device and qPCR Assay, *Translational oncology 6*, 528-538.

[63] Chang, C.-L., Huang, W., Jalal, S. I., Chan, B.-D., Mahmood, A., Shahda, S., O'Neil, B. H., Matei, D. E., and Savran, C. A. (2015) Circulating tumor cell detection using a parallel flow micro-aperture chip system, *Lab on a Chip 15*, 1677-1688.

[64] Hezel, A. F., Kimmelman, A. C., Stanger, B. Z., Bardeesy, N., and Depinho, R. A. (2006) Genetics and biology of pancreatic ductal adenocarcinoma, *Genes & development 20*, 1218-1249.

[65] Sergeant, G., Roskams, T., van Pelt, J., Houtmeyers, F., Aerts, R., and Topal, B. (2011) Perioperative cancer cell dissemination detected with a real-time RT-PCR assay for EpCAM is not associated with worse prognosis in pancreatic ductal adenocarcinoma, *BMC cancer 11*, 47.

[66] Logsdon, C. D., Simeone, D. M., Binkley, C., Arumugam, T., Greenson, J. K., Giordano, T. J., Misek, D. E., Kuick, R., and Hanash, S. (2003) Molecular profiling of pancreatic adenocarcinoma and chronic pancreatitis identifies multiple genes differentially regulated in pancreatic cancer, *Cancer research 63*, 2649-2657.

[67] Adwan, H., Zhivkova-Galunska, M., Georges, R., Eyol, E., Kleeff, J., Giese, N. A., Friess, H., Bergmann, F., and Berger, M. R. (2011) Expression of HOXC8 is inversely related to the progression and metastasis of pancreatic ductal adenocarcinoma, *Br J Cancer 105*, 288-295.

[68] Collisson, E. A., Sadanandam, A., Olson, P., Gibb, W. J., Truitt, M., Gu, S., Cooc, J., Weinkle, J., Kim, G. E., Jakkula, L., Feiler, H. S., Ko, A. H., Olshen, A. B., Danenberg, K. L., Tempero, M. A., Spellman, P. T., Hanahan, D., and Gray, J. W. (2011) Subtypes of pancreatic ductal adenocarcinoma and their differing responses to therapy, *Nature medicine 17*, 500-503.

[69] Biankin, A. V., and Waddell, N., and Kassahn, K. S., and Gingras, M. C., and Muthuswamy, L. B., and Johns, A. L., and Miller, D. K., and Wilson, P. J., and Patch, A. M., and Wu, J., and Chang, D. K., and Cowley, M. J., and Gardiner, B. B., and Song, S., and Harliwong, I., and Idrisoglu, S., and Nourse, C., and Nourbakhsh, E., and Manning, S., and Wani, S., and Gongora, M., and Pajic, M., and Scarlett, C. J., and Gill, A. J., and Pinho, A. V., and Rooman, I., and Anderson, M., and Holmes, O., and Leonard, C., and Taylor, D., and Wood, S., and Xu, Q., and Nones, K., and Fink, J. L., and Christ, A., and Bruxner, T., and Cloonan, N., and Kolle, G., and Newell, F., and Pinese, M., and Mead, R. S., and Humphris, J. L., and Kaplan, W., and Jones, M. D., and Colvin, E. K., and Nagrial, A. M., and Humphrey, E. S., and Chou, A., and Chin, V. T., and Chantrill, L. A., and Mawson, A., and Samra, J. S., and Kench, J. G., and Lovell, J. A., and Daly, R. J., and Merrett, N. D., and Toon, C., and Epari, K., and Nguyen, N. Q., and Barbour, A., and Zeps, N., and Australian Pancreatic Cancer Genome, I., and Kakkar, N., and Zhao, F., and Wu, Y. Q., and

Wang, M., and Muzny, D. M., and Fisher, W. E., and Brunicardi, F. C., and Hodges, S. E., and Reid, J. G., and Drummond, J., and Chang, K., and Han, Y., and Lewis, L. R., and Dinh, H., and Buhay, C. J., and Beck, T., and Timms, L., and Sam, M., and Begley, K., and Brown, A., and Pai, D., and Panchal, A., and Buchner, N., and De Borja, R., and Denroche, R. E., and Yung, C. K., and Serra, S., and Onetto, N., and Mukhopadhyay, D., and Tsao, M. S., and Shaw, P. A., and Petersen, G. M., and Gallinger, S., and Hruban, R. H., and Maitra, A., and Iacobuzio-Donahue, C. A., and Schulick, R. D., and Wolfgang, C. L., and Morgan, R. A., and Lawlor, R. T., and Capelli, P., and Corbo, V., and Scardoni, M., and Tortora, G., and Tempero, M. A., and Mann, K. M., and Jenkins, N. A., and Perez-Mancera, P. A., and Adams, D. J., and Largaespada, D. A., and Wessels, L. F., and Rust, A. G., and Stein, L. D., and Tuveson, D. A., and Copeland, N. G., and Musgrove, E. A., and Scarpa, A., and Eshleman, J. R., and Hudson, T. J., and Sutherland, R. L., and Wheeler, D. A., and Pearson, J. V., and McPherson, J. D., and Gibbs, R. A., and Grimmond, S. M. (2012) Pancreatic cancer genomes reveal aberrations in axon guidance pathway genes, *Nature 491*, 399-405.

[70] Kim, M. S., Zhong, Y., Yachida, S., Rajeshkumar, N. V., Abel, M. L., Marimuthu, A., Mudgal, K., Hruban, R. H., Poling, J. S., Tyner, J. W., Maitra, A., Iacobuzio-Donahue, C. A., and Pandey, A. (2014) Heterogeneity of pancreatic cancer metastases in a single patient revealed by quantitative proteomics, *Molecular & cellular proteomics : MCP 13*, 2803-2811.

[71] Clarke, D. L., Clarke, B. A., Thomson, S. R., Garden, O. J., and Lazarus, N. G. (2004) The role of preoperative biopsy in pancreatic cancer, *HPB : the official journal of the International Hepato Pancreato Biliary Association 6*, 144-153.

[72] Riethdorf, S., Fritsche, H., Muller, V., Rau, T., Schindlbeck, C., Rack, B., Janni, W., Coith, C., Beck, K., Janicke, F., Jackson, S., Gornet, T., Cristofanilli, M., and Pantel, K. (2007) Detection of circulating tumor cells in peripheral blood of patients with metastatic breast cancer: a validation study of the CellSearch system, *Clinical cancer research : an official journal of the American Association for Cancer Research 13*, 920-928.

[73] Hayes, D. F., and Smerage, J. (2008) Is there a role for circulating tumor cells in the management of breast cancer?, *Clinical cancer research : an official journal of the American Association for Cancer Research 14*, 3646-3650.

[74] Ren, C., Han, C., Zhang, J., He, P., Wang, D., Wang, B., Zhao, P., and Zhao, X. (2011) Detection of apoptotic circulating tumor cells in advanced pancreatic cancer following 5-fluorouracil chemotherapy, *Cancer biology & therapy 12*, 700-706.

[75] Marrinucci, D., Bethel, K., Kolatkar, A., Luttgen, M. S., Malchiodi, M., Baehring, F., Voigt, K., Lazar, D., Nieva, J., Bazhenova, L., Ko, A. H., Korn, W. M., Schram, E., Coward, M., Yang, X., Metzner, T., Lamy, R., Honnatti, M., Yoshioka, C., Kunken, J., Petrova, Y., Sok, D., Nelson, D., and Kuhn, P. (2012) Fluid biopsy in patients with metastatic prostate, pancreatic and breast cancers, *Physical biology 9*, 016003.

[76] Marrinucci, D., Bethel, K., Luttgen, M., Bruce, R. H., Nieva, J., and Kuhn, P. (2009) Circulating tumor cells from well-differentiated lung adenocarcinoma retain cytomorphologic features of primary tumor type, *Arch Pathol Lab Med 133*, 1468-1471.

[77] Bobek, V., Gurlich, R., Eliasova, P., and Kolostova, K. (2014) Circulating tumor cells in pancreatic cancer patients: Enrichment and cultivation, *World journal of gastroenterology : WJG 20*, 17163-17170.

[78] Iwanicki-Caron, I., Basile, P., Toure, E., Antonietti, M., Lecleire, S., Di Fiore, A., Oden-Gangloff, A., Blanchard, F., Lemoine, F., Di Fiore, F., Sabourin, J. C., and Michel, P. (2013) Usefulness of circulating tumor cell detection in pancreatic adenocarcinoma diagnosis, *The American journal of gastroenterology 108*, 152-155.

[79] Krebs, M. G., Sloane, R., Priest, L., Lancashire, L., Hou, J.-M., Greystoke, A., Ward, T. H., Ferraldeschi, R., Hughes, A., Clack, G., Ranson, M., Dive, C., and Blackhall, F. H. (2011) Evaluation and Prognostic Significance of Circulating Tumor Cells in Patients With Non–Small-Cell Lung Cancer, *Journal of Clinical Oncology 29*, 1556-1563.

[80] Wang, Z. P., Eisenberger, M. A., Carducci, M. A., Partin, A. W., Scher, H. I., and Ts'o, P. O. (2000) Identification and characterization of circulating prostate carcinoma cells, *Cancer 88*, 2787-2795.

[81] Stott, S. L., Lee, R. J., Nagrath, S., Yu, M., Miyamoto, D. T., Ulkus, L., Inserra, E. J., Ulman, M., Springer, S., Nakamura, Z., Moore, A. L., Tsukrov, D. I., Kempner, M. E., Dahl, D. M., Wu, C.-L., Iafrate, A. J., Smith, M. R., Tompkins, R. G., Sequist, L. V., Toner, M., Haber, D. A., and Maheswaran, S. (2010) Isolation and Characterization of Circulating Tumor Cells from Patients with Localized and Metastatic Prostate Cancer, *Science translational medicine 2*, 25ra23-25ra23.

[82] Kirby, B. J., Jodari, M., Loftus, M. S., Gakhar, G., Pratt, E. D., Chanel-Vos, C., Gleghorn, J. P., Santana, S. M., Liu, H., Smith, J. P., Navarro, V. N., Tagawa, S. T., Bander, N. H., Nanus, D. M., and Giannakakou, P. (2012) Functional characterization of circulating tumor cells with a prostate-cancer-specific microfluidic device, *PloS one 7*, e35976.

[83] Pestrin, M., Bessi, S., Galardi, F., Truglia, M., Biggeri, A., Biagioni, C., Cappadona, S., Biganzoli, L., Giannini, A., and Di Leo, A. (2009) Correlation of HER2 status between primary tumors and corresponding circulating tumor cells in advanced breast cancer patients, *Breast cancer research and treatment 118*, 523-530.

[84] Riethdorf, S., Muller, V., Zhang, L., Rau, T., Loibl, S., Komor, M., Roller, M., Huober, J., Fehm, T., Schrader, I., Hilfrich, J., Holms, F., Tesch, H., Eidtmann, H., Untch, M., von Minckwitz, G., and Pantel, K. (2010) Detection and HER2 expression of circulating tumor cells: prospective monitoring in breast cancer patients treated in the neoadjuvant GeparQuattro trial, *Clinical cancer research : an official journal of the American Association for Cancer Research 16*, 2634-2645.

[85] Ignatiadis, M., Rothe, F., Chaboteaux, C., Durbecq, V., Rouas, G., Criscitiello, C., Metallo, J., Kheddoumi, N., Singhal, S. K., Michiels, S., Veys, I., Rossari, J., Larsimont, D., Carly, B., Pestrin, M., Bessi, S., Buxant, F., Liebens, F., Piccart, M., and Sotiriou, C. (2011) HER2-positive circulating tumor cells in breast cancer, *PloS one 6*, e15624.

[86] Theodoropoulos, P. A., Polioudaki, H., Agelaki, S., Kallergi, G., Saridaki, Z., Mavroudis, D., and Georgoulias, V. (2010) Circulating tumor cells with a putative stem cell phenotype in peripheral blood of patients with breast cancer, *Cancer letters 288*, 99-106.

[87] Armstrong, A. J., Marengo, M. S., Oltean, S., Kemeny, G., Bitting, R. L., Turnbull, J. D., Herold, C. I., Marcom, P. K., George, D. J., and Garcia-Blanco, M. A. (2011) Circulating tumor cells from patients with advanced prostate and breast cancer display both epithelial and mesenchymal markers, *Mol Cancer Res 9*, 997-1007.

[88] Kallergi, G., Papadaki, M. A., Politaki, E., Mavroudis, D., Georgoulias, V., and Agelaki, S. (2011) Epithelial to mesenchymal transition markers expressed in circulating tumour cells of early and metastatic breast cancer patients, *Breast Cancer Res 13*, R59.

[89] Lecharpentier, A., Vielh, P., Perez-Moreno, P., Planchard, D., Soria, J. C., and Farace, F. (2011) Detection of circulating tumour cells with a hybrid (epithelial/mesenchymal) phenotype in patients with metastatic non-small cell lung cancer, *Br J Cancer 105*, 1338-1341.

[90] Alix-Panabieres, C., Brouillet, J. P., Fabbro, M., Yssel, H., Rousset, T., Maudelonde, T., Choquet-Kastylevsky, G., and Vendrell, J. P. (2005) Characterization and enumeration of cells secreting tumor markers in the peripheral blood of breast cancer patients, *J Immunol Methods 299*, 177-188.

[91] Alix-Panabières, C., Vendrell, J.-P., Slijper, M., Pellé, O., Barbotte, E., Mercier, G., Jacot, W., Fabbro, M., and Pantel, K. (2009) Full-length cytokeratin-19 is released by human tumor cells: a potential role in metastatic progression of breast cancer, *Breast Cancer Research : BCR 11*, R39-R39.

[92] Maheswaran, S., Sequist, L. V., Nagrath, S., Ulkus, L., Brannigan, B., Collura, C. V., Inserra, E., Diederichs, S., Iafrate, A. J., Bell, D. W., Digumarthy, S., Muzikansky, A., Irimia, D., Settleman, J., Tompkins, R. G., Lynch, T. J., Toner, M., and Haber, D. A. (2008) Detection of Mutations in EGFR in Circulating Lung-Cancer Cells, *New England Journal of Medicine 359*, 366-377.

[93] Ghossein, R. A., Rosai, J., Scher, H. I., Seiden, M., Zhang, Z. F., Sun, M., Chang, G., Berlane, K., Krithivas, K., and Kantoff, P. W. (1997) Prognostic significance of detection of prostate-specific antigen transcripts in the peripheral blood of patients with metastatic androgen-independent prostatic carcinoma, *Urology 50*, 100-105.

[94] Helo, P., Cronin, A. M., Danila, D. C., Wenske, S., Gonzalez-Espinoza, R., Anand, A., Koscuiszka, M., Vaananen, R. M., Pettersson, K., Chun, F. K., Steuber, T., Huland, H., Guillonneau, B. D., Eastham, J. A., Scardino, P. T., Fleisher, M., Scher, H. I., and Lilja, H. (2009) Circulating prostate tumor cells detected by reverse transcription-PCR in men with localized or castration-refractory prostate cancer: concordance with CellSearch assay and association with bone metastases and with survival, *Clinical chemistry 55*, 765-773.

[95] Aktas, B., Tewes, M., Fehm, T., Hauch, S., Kimmig, R., and Kasimir-Bauer, S. (2009) Stem cell and epithelial-mesenchymal transition markers are frequently overexpressed in circulating tumor cells of metastatic breast cancer patients, *Breast Cancer Res 11*, R46.

[96] Aktas, B., Kasimir-Bauer, S., Heubner, M., Kimmig, R., and Wimberger, P. (2011) Molecular profiling and prognostic relevance of circulating tumor cells in the blood of ovarian cancer patients at primary diagnosis and after platinum-based chemotherapy, *International journal of gynecological cancer : official journal of the International Gynecological Cancer Society 21*, 822-830.

[97] Aktas, B., Muller, V., Tewes, M., Zeitz, J., Kasimir-Bauer, S., Loehberg, C. R., Rack, B., Schneeweiss, A., and Fehm, T. (2011) Comparison of estrogen and progesterone receptor status of circulating tumor cells and the primary tumor in metastatic breast cancer patients, *Gynecol Oncol 122*, 356-360.

[98] Sieuwerts, A. M., Mostert, B., Bolt-de Vries, J., Peeters, D., de Jongh, F. E., Stouthard, J. M., Dirix, L. Y., van Dam, P. A., Van Galen, A., de Weerd, V., Kraan, J., van der Spoel, P., Ramirez-Moreno, R., van Deurzen, C. H., Smid, M., Yu, J. X., Jiang, J., Wang, Y., Gratama, J. W., Sleijfer, S., Foekens, J. A., and Martens, J. W. (2011) mRNA and microRNA expression profiles in circulating tumor cells and primary tumors of metastatic breast cancer patients, *Clinical cancer research : an official journal of the American Association for Cancer Research 17*, 3600-3618.

[99] Yu, M., Ting, D. T., Stott, S. L., Wittner, B. S., Ozsolak, F., Paul, S., Ciciliano, J. C., Smas, M. E., Winokur, D., Gilman, A. J., Ulman, M. J., Xega, K., Contino, G., Alagesan, B., Brannigan, B. W., Milos, P. M., Ryan, D. P., Sequist, L. V., Bardeesy, N., Ramaswamy, S., Toner, M., Maheswaran, S., and Haber, D. A. (2012) RNA sequencing of pancreatic circulating tumour cells implicates WNT signalling in metastasis, *Nature 487*, 510-513.

[100] Ting, D. T., Wittner, B. S., Ligorio, M., Vincent Jordan, N., Shah, A. M., Miyamoto, D. T., Aceto, N., Bersani, F., Brannigan, B. W., Xega, K., Ciciliano, J. C., Zhu, H., MacKenzie, O. C., Trautwein, J., Arora, K. S., Shahid, M., Ellis, H. L., Qu, N., Bardeesy, N., Rivera, M. N., Deshpande, V., Ferrone, C. R., Kapur, R., Ramaswamy, S., Shioda, T., Toner, M., Maheswaran, S., and Haber, D. A. (2014) Single-cell RNA sequencing identifies extracellular matrix gene expression by pancreatic circulating tumor cells, *Cell reports 8*, 1905-1918.

[101] Meng, S., Tripathy, D., Shete, S., Ashfaq, R., Haley, B., Perkins, S., Beitsch, P., Khan, A., Euhus, D., Osborne, C., Frenkel, E., Hoover, S., Leitch, M., Clifford, E., Vitetta, E., Morrison, L., Herlyn, D., Terstappen, L. W., Fleming, T., Fehm, T., Tucker, T., Lane, N., Wang, J., and Uhr, J. (2004) HER-2 gene amplification can be acquired as breast cancer progresses, *Proc Natl Acad Sci U S A 101*, 9393-9398.

[102] Leversha, M. A., Han, J., Asgari, Z., Danila, D. C., Lin, O., Gonzalez-Espinoza, R., Anand, A., Lilja, H., Heller, G., Fleisher, M., and Scher, H. I. (2009) Fluorescence in situ hybridization analysis of circulating tumor cells in metastatic prostate cancer, *Clinical cancer research : an official journal of the American Association for Cancer Research 15*, 2091-2097.

[103] El Sherif, M., Schneider, C. P., Rabenstein, C., Hassab, A. H., El Bordiny, M. M., Ayad, M. W., and Pachmann, K. (2013) Behavior of circulating epithelial tumor cells (CETC) and FISH (fluorescence in situ hybridisation) of epidermal growth factor receptor (EGFR)-gene amplification in lung cancer patients during the course of therapy.

[104] Yu, M., Bardia, A., Wittner, B. S., Stott, S. L., Smas, M. E., Ting, D. T., Isakoff, S. J., Ciciliano, J. C., Wells, M. N., Shah, A. M., Concannon, K. F., Donaldson, M. C., Sequist, L. V., Brachtel, E., Sgroi, D., Baselga, J., Ramaswamy, S., Toner, M., Haber, D. A., and Maheswaran, S. (2013) Circulating breast tumor cells exhibit dynamic changes in epithelial and mesenchymal composition, *Science (New York, N.Y.) 339*, 580-584.

[105] Ulmer, A., Schmidt-Kittler, O., Fischer, J., Ellwanger, U., Rassner, G., Riethmuller, G., Fierlbeck, G., and Klein, C. A. (2004) Immunomagnetic enrichment, genomic characterization, and prognostic impact of circulating melanoma cells, *Clinical cancer research : an official journal of the American Association for Cancer Research 10*, 531-537.

[106] Ramskold, D., Luo, S., Wang, Y. C., Li, R., Deng, Q., Faridani, O. R., Daniels, G. A., Khrebtukova, I., Loring, J. F., Laurent, L. C., Schroth, G. P., and Sandberg, R. (2012) Full-length mRNA-Seq from single-cell levels of RNA and individual circulating tumor cells, *Nat Biotechnol 30*, 777-782.

[107] Cann, G. M., Gulzar, Z. G., Cooper, S., Li, R., Luo, S., Tat, M., Stuart, S., Schroth, G., Srinivas, S., Ronaghi, M., Brooks, J. D., and Talasaz, A. H. (2012) mRNA-Seq of single prostate cancer circulating tumor cells reveals recapitulation of gene expression and pathways found in prostate cancer, *PloS one 7*, e49144.

[108] Chen, C. L., Mahalingam, D., Osmulski, P., Jadhav, R. R., Wang, C. M., Leach, R. J., Chang, T. C., Weitman, S. D., Kumar, A. P., Sun, L., Gaczynska, M. E., Thompson, I. M., and Huang, T. H.

(2013) Single-cell analysis of circulating tumor cells identifies cumulative expression patterns of EMT-related genes in metastatic prostate cancer, *The Prostate 73*, 813-826.

[109] Klein, C. A., Schmidt-Kittler, O., Schardt, J. A., Pantel, K., Speicher, M. R., and Riethmuller, G. (1999) Comparative genomic hybridization, loss of heterozygosity, and DNA sequence analysis of single cells, *Proc Natl Acad Sci U S A 96*, 4494-4499.

[110] Gasch, C., Bauernhofer, T., Pichler, M., Langer-Freitag, S., Reeh, M., Seifert, A. M., Mauermann, O., Izbicki, J. R., Pantel, K., and Riethdorf, S. (2013) Heterogeneity of epidermal growth factor receptor status and mutations of KRAS/PIK3CA in circulating tumor cells of patients with colorectal cancer, *Clinical chemistry 59*, 252-260.

[111] Klapman, J., and Malafa, M. P. (2008) Early detection of pancreatic cancer: why, who, and how to screen, *Cancer control : journal of the Moffitt Cancer Center 15*, 280-287.

[112] Zhou, J., Hu, L., Yu, Z., Zheng, J., Yang, D., Bouvet, M., and Hoffman, R. M. (2011) Marker expression in circulating cancer cells of pancreatic cancer patients, *The Journal of surgical research 171*, 631-636.

[113] Z'Graggen, K., Centeno, B. A., Fernandez-del Castillo, C., Jimenez, R. E., Werner, J., and Warshaw, A. L. (2001) Biological implications of tumor cells in blood and bone marrow of pancreatic cancer patients, *Surgery 129*, 537-546.

[114] Kurihara, T., Itoi, T., Sofuni, A., Itokawa, F., Tsuchiya, T., Tsuji, S., Ishii, K., Ikeuchi, N., Tsuchida, A., Kasuya, K., Kawai, T., Sakai, Y., and Moriyasu, F. (2008) Detection of circulating tumor cells in patients with pancreatic cancer: a preliminary result, *Journal of hepato-biliary-pancreatic surgery 15*, 189-195.

[115] Khoja, L., Backen, A., Sloane, R., Menasce, L., Ryder, D., Krebs, M., Board, R., Clack, G., Hughes, A., Blackhall, F., Valle, J. W., and Dive, C. (2012) A pilot study to explore circulating tumour cells in pancreatic cancer as a novel biomarker, *Br J Cancer 106*, 508-516.

[116] Han, L., Chen, W., and Zhao, Q. (2014) Prognostic value of circulating tumor cells in patients with pancreatic cancer: a meta-analysis, *Tumour biology : the journal of the International Society for Oncodevelopmental Biology and Medicine 35*, 2473-2480.

[117] Soeth, E., Grigoleit, U., Moellmann, B., Roder, C., Schniewind, B., Kremer, B., Kalthoff, H., and Vogel, I. (2005) Detection of tumor cell dissemination in pancreatic ductal carcinoma patients by CK 20 RT-PCR indicates poor survival, *Journal of cancer research and clinical oncology 131*, 669-676.

[118] Hoffmann, K., Kerner, C., Wilfert, W., Mueller, M., Thiery, J., Hauss, J., and Witzigmann, H. (2007) Detection of disseminated pancreatic cells by amplification of cytokeratin-19 with quantitative RT-PCR in blood, bone marrow and peritoneal lavage of pancreatic carcinoma patients, *World journal of gastroenterology : WJG 13*, 257-263.

[119] de Albuquerque, A., Kubisch, I., Breier, G., Stamminger, G., Fersis, N., Eichler, A., Kaul, S., and Stolzel, U. (2012) Multimarker gene analysis of circulating tumor cells in pancreatic cancer patients: a feasibility study, *Oncology 82*, 3-10.

[120] Zhang, Y., Wang, F., Ning, N., Chen, Q., Yang, Z., Guo, Y., Xu, D., Zhang, D., Zhan, T., and Cui, W. (2015) Patterns of circulating tumor cells identified by CEP8, CK and CD45 in pancreatic cancer, *International journal of cancer. Journal international du cancer 136*, 1228-1233.

[121] Bidard, F. C., Huguet, F., Louvet, C., Mineur, L., Bouche, O., Chibaudel, B., Artru, P., Desseigne, F., Bachet, J. B., Mathiot, C., Pierga, J. Y., and Hammel, P. (2013) Circulating tumor cells in locally advanced pancreatic adenocarcinoma: the ancillary CirCe 07 study to the LAP 07 trial, *Annals of oncology : official journal of the European Society for Medical Oncology / ESMO 24*, 2057-2061.

[122] Yu, K. H., Ricigliano, M., Hidalgo, M., Abou-Alfa, G. K., Lowery, M. A., Saltz, L. B., Crotty, J. F., Gary, K., Cooper, B., Lapidus, R., Sadowska, M., and O'Reilly, E. M. (2014) Pharmacogenomic modeling of circulating tumor and invasive cells for prediction of chemotherapy response and resistance in pancreatic cancer, *Clinical cancer research : an official journal of the American Association for Cancer Research 20*, 5281-5289.

[123] Yu, M., Bardia, A., Aceto, N., Bersani, F., Madden, M. W., Donaldson, M. C., Desai, R., Zhu, H., Comaills, V., Zheng, Z., Wittner, B. S., Stojanov, P., Brachtel, E., Sgroi, D., Kapur, R., Shioda, T., Ting, D. T., Ramaswamy, S., Getz, G., Iafrate, A. J., Benes, C., Toner, M., Maheswaran, S., and Haber, D. A. (2014) Cancer therapy. Ex vivo culture of circulating breast tumor cells for individualized testing of drug susceptibility, *Science (New York, N.Y.) 345*, 216-220.

[124] Zhang, Z., Shiratsuchi, H., Lin, J., Chen, G., Reddy, R. M., Azizi, E., Fouladdel, S., Chang, A. C., Lin, L., Jiang, H., Waghray, M., Luker, G., Simeone, D. M., Wicha, M. S., Beer, D. G., Ramnath, N., and Nagrath, S. (2014) *Expansion of CTCs from early stage lung cancer patients using a microfluidic co-culture model*.

[125] Torphy, R. J., Tignanelli, C. J., Kamande, J. W., Moffitt, R. A., Herrera Loeza, S. G., Soper, S. A., and Yeh, J. J. (2014) Circulating tumor cells as a biomarker of response to treatment in patient-derived xenograft mouse models of pancreatic adenocarcinoma, *PloS one 9*, e89474.

[126] Skvortsova, T. E., Rykova, E. Y., Tamkovich, S. N., Bryzgunova, O. E., Starikov, A. V., Kuznetsova, N. P., Vlassov, V. V., and Laktionov, P. P. (2006) Cell-free and cell-bound circulating DNA in breast tumours: DNA quantification and analysis of tumour-related gene methylation, *Br J Cancer 94*, 1492-1495.

[127] Kidess, E., and Jeffrey, S. S. (2013) Circulating tumor cells versus tumor-derived cell-free DNA: rivals or partners in cancer care in the era of single-cell analysis?, *Genome Med 5*, 70.

[128] Bettegowda, C., Sausen, M., Leary, R. J., Kinde, I., Wang, Y., Agrawal, N., Bartlett, B. R., Wang, H., Luber, B., Alani, R. M., Antonarakis, E. S., Azad, N. S., Bardelli, A., Brem, H., Cameron, J. L., Lee, C. C., Fecher, L. A., Gallia, G. L., Gibbs, P., Le, D., Giuntoli, R. L., Goggins, M., Hogarty, M. D., Holdhoff, M., Hong, S.-M., Jiao, Y., Juhl, H. H., Kim, J. J., Siravegna, G., Laheru, D. A., Lauricella, C., Lim, M., Lipson, E. J., Marie, S. K. N., Netto, G. J., Oliner, K. S., Olivi, A., Olsson, L., Riggins, G. J., Sartore-Bianchi, A., Schmidt, K., Shih, l.-M., Oba-Shinjo, S. M., Siena, S., Theodorescu, D., Tie, J., Harkins, T. T., Veronese, S., Wang, T.-L., Weingart, J. D., Wolfgang, C. L., Wood, L. D., Xing, D., Hruban, R. H., Wu, J., Allen, P. J., Schmidt, C. M., Choti, M. A., Velculescu, V. E., Kinzler, K. W., Vogelstein, B., Papadopoulos, N., and Diaz, L. A. (2014) Detection of Circulating Tumor DNA in Early- and Late-Stage Human Malignancies, *Science Translational Medicine 6*, 224ra224.

[129] Crowley, E., Di Nicolantonio, F., Loupakis, F., and Bardelli, A. (2013) Liquid biopsy: monitoring cancer-genetics in the blood, *Nat Rev Clin Oncol 10*, 472-484.

[130] De Mattos-Arruda, L., Cortes, J., Santarpia, L., Vivancos, A., Tabernero, J., Reis-Filho, J. S., and Seoane, J. (2013) Circulating tumour cells and cell-free DNA as tools for managing breast cancer, *Nat Rev Clin Oncol 10*, 377-389.

[131] Wu, T. L., Zhang, D., Chia, J. H., Tsao, K., Sun, C. F., and Wu, J. T. (2002) Cell-free DNA: measurement in various carcinomas and establishment of normal reference range, *Clin Chim Acta 321*, 77-87.

[132] Dawson, S. J., Tsui, D. W., Murtaza, M., Biggs, H., Rueda, O. M., Chin, S. F., Dunning, M. J., Gale, D., Forshew, T., Mahler-Araujo, B., Rajan, S., Humphray, S., Becq, J., Halsall, D., Wallis, M., Bentley, D., Caldas, C., and Rosenfeld, N. (2013) Analysis of circulating tumor DNA to monitor metastatic breast cancer, *The New England journal of medicine 368*, 1199-1209.

[133] Anker, P., and Stroun, M. (2001) Tumor-related alterations in circulating DNA, potential for diagnosis, prognosis and detection of minimal residual disease, *Leukemia 15*, 289-291.

[134] Diehl, F., Schmidt, K., Choti, M. A., Romans, K., Goodman, S., Li, M., Thornton, K., Agrawal, N., Sokoll, L., Szabo, S. A., Kinzler, K. W., Vogelstein, B., and Diaz, L. A., Jr. (2008) Circulating mutant DNA to assess tumor dynamics, *Nature medicine 14*, 985-990.

[135] Cristofanilli, M. (2013) Circulating Tumor DNA to Monitor Metastatic Breast Cancer, *New England Journal of Medicine 369*, 93-94.

[136] Misale, S., Yaeger, R., Hobor, S., Scala, E., Janakiraman, M., Liska, D., Valtorta, E., Schiavo, R., Buscarino, M., Siravegna, G., Bencardino, K., Cercek, A., Chen, C. T., Veronese, S., Zanon, C., Sartore-Bianchi, A., Gambacorta, M., Gallicchio, M., Vakiani, E., Boscaro, V., Medico, E., Weiser, M., Siena, S., Di Nicolantonio, F., Solit, D., and Bardelli, A. (2012) Emergence of KRAS mutations and acquired resistance to anti-EGFR therapy in colorectal cancer, *Nature 486*, 532-536.

[137] Diaz, L. A., Jr., Williams, R. T., Wu, J., Kinde, I., Hecht, J. R., Berlin, J., Allen, B., Bozic, I., Reiter, J. G., Nowak, M. A., Kinzler, K. W., Oliner, K. S., and Vogelstein, B. (2012) The molecular evolution of acquired resistance to targeted EGFR blockade in colorectal cancers, *Nature 486*, 537-540.

[138] Murtaza, M., Dawson, S. J., Tsui, D. W., Gale, D., Forshew, T., Piskorz, A. M., Parkinson, C., Chin, S. F., Kingsbury, Z., Wong, A. S., Marass, F., Humphray, S., Hadfield, J., Bentley, D., Chin, T. M., Brenton, J. D., Caldas, C., and Rosenfeld, N. (2013) Non-invasive analysis of acquired resistance to cancer therapy by sequencing of plasma DNA, *Nature 497*, 108-112.

[139] Taniguchi, K., Uchida, J., Nishino, K., Kumagai, T., Okuyama, T., Okami, J., Higashiyama, M., Kodama, K., Imamura, F., and Kato, K. (2011) Quantitative detection of EGFR mutations in circulating tumor DNA derived from lung adenocarcinomas, *Clinical cancer research : an official journal of the American Association for Cancer Research 17*, 7808-7815.

[140] Mulcahy, H. E., Lyautey, J., Lederrey, C., qi Chen, X., Anker, P., Alstead, E. M., Ballinger, A., Farthing, M. J., and Stroun, M. (1998) A prospective study of K-ras mutations in the plasma of pancreatic cancer patients, *Clinical cancer research : an official journal of the American Association for Cancer Research 4*, 271-275.

[141] Yamada, T., Nakamori, S., Ohzato, H., Oshima, S., Aoki, T., Higaki, N., Sugimoto, K., Akagi, K., Fujiwara, Y., Nishisho, I., Sakon, M., Gotoh, M., and Monden, M. (1998) Detection of K-ras gene mutations in plasma DNA of patients with pancreatic adenocarcinoma: correlation with clinicopathological features, *Clinical cancer research : an official journal of the American Association for Cancer Research 4*, 1527-1532.

[142] Liggett, T., Melnikov, A., Yi, Q. L., Replogle, C., Brand, R., Kaul, K., Talamonti, M., Abrams, R. A., and Levenson, V. (2010) Differential methylation of cell-free circulating DNA among patients with pancreatic cancer versus chronic pancreatitis, *Cancer 116*, 1674-1680.

[143] Scheel, C., and Weinberg, R. A. (2012) Cancer stem cells and epithelial–mesenchymal transition: Concepts and molecular links, *Seminars in Cancer Biology*.

[144] Negin, B., and Cohen, S. (2010) Circulating Tumor Cells in Colorectal Cancer: Past, Present, and Future Challenges, *Current Treatment Options in Oncology 11*, 1-13.

[145] Yu, M., Stott, S., Toner, M., Maheswaran, S., and Haber, D. A. (2011) Circulating tumor cells: approaches to isolation and characterization, *The Journal of Cell Biology 192*, 373-382.

[146] Wang, S., Wang, H., Jiao, J., Chen, K. J., Owens, G. E., Kamei, K. i., Sun, J., Sherman, D. J., Behrenbruch, C. P., and Wu, H. (2009) Three-Dimensional Nanostructured Substrates toward Efficient Capture of Circulating Tumor Cells, *Angewandte Chemie 121*, 9132-9135.

[147] Liu, H., Liu, X., Meng, J., Zhang, P., Yang, G., Su, B., Sun, K., Chen, L., Han, D., and Wang, S. (2013) Hydrophobic Interaction-Mediated Capture and Release of Cancer Cells on Thermoresponsive Nanostructured Surfaces, *Advanced Materials 25*, 922-927.

[148] Jack, R. M., Grafton, M. M. G., Rodrigues, D., Giraldez, M. D., Griffith, C., Cieslak, R., Zeinali, M., Kumar Sinha, C., Azizi, E., Wicha, M., Tewari, M., Simeone, D. M., and Nagrath, S. (2016) Ultra-Specific Isolation of Circulating Tumor Cells Enables Rare-Cell RNA Profiling, *Advanced Science*, n/a-n/a.

[149] Melin, J., Gimenez, G., Roxhed, N., van der Wijngaart, W., and Stemme, G. (2004) A fast passive and planar liquid sample micromixer, *Lab Chip 4*, 214-219.

[150] Hong, C. C., Choi, J. W., and Ahn, C. H. (2004) A novel in-plane passive microfluidic mixer with modified Tesla structures, *Lab Chip 4*, 109-113.

[151] Jung, J. H., Kim, G.-Y., and Seo, T. S. (2011) An integrated passive micromixer-magnetic separation-capillary electrophoresis microdevice for rapid and multiplex pathogen detection at the single-cell level, *Lab on a chip 11*, 3465-3470.

[152] Liu, R. H., Stremler, M. A., Sharp, K. V., Olsen, M. G., Santiago, J. G., Adrian, R. J., Aref, H., and Beebe, D. J. (2000) Passive mixing in a three-dimensional serpentine microchannel, *Microelectromechanical Systems, Journal of 9*, 190-197.

[153] Gleghorn, J. P., Pratt, E. D., Denning, D., Liu, H., Bander, N. H., Tagawa, S. T., Nanus, D. M., Giannakakou, P. A., and Kirby, B. J. (2010) Capture of circulating tumor cells from whole blood of prostate cancer patients using geometrically enhanced differential immunocapture (GEDI) and a prostate-specific antibody, *Lab on a Chip 10*, 27-29.

[154] Stott, S. L., Hsu, C.-H., Tsukrov, D. I., Yu, M., Miyamoto, D. T., Waltman, B. A., Rothenberg, S. M., Shah, A. M., Smas, M. E., Korir, G. K., Floyd, F. P., Gilman, A. J., Lord, J. B., Winokur, D., Springer, S., Irimia, D., Nagrath, S., Sequist, L. V., Lee, R. J., Isselbacher, K. J., Maheswaran, S., Haber, D. A., and Toner, M. (2010) Isolation of circulating tumor cells using a microvortex-generating herringbone-chip, *Proceedings of the National Academy of Sciences*.

[155] Buchholz, M., Schatz, A., Wagner, M., Michl, P., Linhart, T., Adler, G., Gress, T. M., and Ellenrieder, V. (2006) Overexpression of c-myc in pancreatic cancer caused by ectopic activation of NFATc1 and the Ca2+/calcineurin signaling pathway, *The EMBO journal 25*, 3714-3724.

[156] Bronsert, P., Kohler, I., Timme, S., Kiefer, S., Werner, M., Schilling, O., Vashist, Y., Makowiec, F., Brabletz, T., Hopt, U. T., Bausch, D., Kulemann, B., Keck, T., and Wellner, U. F. (2014) Prognostic significance of Zinc finger E-box binding homeobox 1 (ZEB1) expression in cancer cells and cancer-associated fibroblasts in pancreatic head cancer, *Surgery 156*, 97-108.

[157] Rowland, B. D., and Peeper, D. S. (2006) KLF4, p21 and context-dependent opposing forces in cancer, *Nature reviews. Cancer 6*, 11-23.

[158] Beger, C., Ramadani, M., Meyer, S., Leder, G., Kruger, M., Welte, K., Gansauge, F., and Beger, H. G. (2004) Down-regulation of BRCA1 in chronic pancreatitis and sporadic pancreatic adenocarcinoma, *Clinical cancer research : an official journal of the American Association for Cancer Research 10*, 3780-3787.

[159] Chou, A., Waddell, N., Cowley, M. J., Gill, A. J., Chang, D. K., Patch, A. M., Nones, K., Wu, J., Pinese, M., Johns, A. L., Miller, D. K., Kassahn, K. S., Nagrial, A. M., Wasan, H., Goldstein, D., Toon, C. W., Chin, V., Chantrill, L., Humphris, J., Mead, R. S., Rooman, I., Samra, J. S., Pajic, M., Musgrove, E. A., Pearson, J. V., Morey, A. L., Grimmond, S. M., and Biankin, A. V. (2013) Clinical and molecular characterization of HER2 amplified-pancreatic cancer, *Genome Med 5*, 78.

[160] Bloomston, M., Frankel, W. L., Petrocca, F., Volinia, S., Alder, H., Hagan, J. P., Liu, C. G., Bhatt, D., Taccioli, C., and Croce, C. M. (2007) MicroRNA expression patterns to differentiate pancreatic adenocarcinoma from normal pancreas and chronic pancreatitis, *JAMA 297*, 1901-1908.

[161] Lopez-Casas, P. P., and Lopez-Fernandez, L. A. (2010) Gene-expression profiling in pancreatic cancer, *Expert review of molecular diagnostics 10*, 591-601.

[162] Dillhoff, M., Liu, J., Frankel, W., Croce, C., and Bloomston, M. (2008) MicroRNA-21 is overexpressed in pancreatic cancer and a potential predictor of survival, *J Gastrointest Surg 12*, 2171-2176.

[163] Sadakari, Y., Ohtsuka, T., Ohuchida, K., Tsutsumi, K., Takahata, S., Nakamura, M., Mizumoto, K., and Tanaka, M. (2010) MicroRNA expression analyses in preoperative pancreatic juice samples of pancreatic ductal adenocarcinoma, *JOP 11*, 587-592.

[164] Szafranska, A. E., Davison, T. S., John, J., Cannon, T., Sipos, B., Maghnouj, A., Labourier, E., and Hahn, S. A. (2007) MicroRNA expression alterations are linked to tumorigenesis and non-neoplastic processes in pancreatic ductal adenocarcinoma, *Oncogene 26*, 4442-4452.

[165] Palumbo, T., Faucz, F. R., Azevedo, M., Xekouki, P., Iliopoulos, D., and Stratakis, C. A. (2013) Functional screen analysis reveals miR-26b and miR-128 as central regulators of pituitary

somatomammotrophic tumor growth through activation the PTEN-AKT pathway, *Oncogene 32*, 1651-1659.

[166] Landau, Dan A., Carter, Scott L., Stojanov, P., McKenna, A., Stevenson, K., Lawrence, Michael S., Sougnez, C., Stewart, C., Sivachenko, A., Wang, L., Wan, Y., Zhang, W., Shukla, Sachet A., Vartanov, A., Fernandes, Stacey M., Saksena, G., Cibulskis, K., Tesar, B., Gabriel, S., Hacohen, N., Meyerson, M., Lander, Eric S., Neuberg, D., Brown, Jennifer R., Getz, G., and Wu, Catherine J. Evolution and Impact of Subclonal Mutations in Chronic Lymphocytic Leukemia, *Cell 152*, 714-726.

[167] Mroz, E. A., and Rocco, J. W. (2013) MATH, a novel measure of intratumor genetic heterogeneity, is high in poor-outcome classes of head and neck squamous cell carcinoma, *Oral Oncology 49*, 211-215.

[168] Zhang, J., Fujimoto, J., Zhang, J., Wedge, D. C., Song, X., Zhang, J., Seth, S., Chow, C.-W., Cao, Y., Gumbs, C., Gold, K. A., Kalhor, N., Little, L., Mahadeshwar, H., Moran, C., Protopopov, A., Sun, H., Tang, J., Wu, X., Ye, Y., William, W. N., Lee, J. J., Heymach, J. V., Hong, W. K., Swisher, S., Wistuba, I. I., and Futreal, P. A. (2014) Intratumor heterogeneity in localized lung adenocarcinomas delineated by multiregion sequencing, *Science (New York, N.Y.) 346*, 256-259.

[169] McGranahan, N., and Swanton, C. Biological and Therapeutic Impact of Intratumor Heterogeneity in Cancer Evolution, *Cancer cell 27*, 15-26.

[170] Calbo, J., van Montfort, E., Proost, N., van Drunen, E., Beverloo, H. B., Meuwissen, R., and Berns, A. A Functional Role for Tumor Cell Heterogeneity in a Mouse Model of Small Cell Lung Cancer, *Cancer cell 19*, 244-256.

[171] Bedard, P. L., Hansen, A. R., Ratain, M. J., and Siu, L. L. (2013) Tumour heterogeneity in the clinic, *Nature 501*, 355-364.

[172] Castle, J., Shaker, H., Morris, K., Tugwood, J. D., and Kirwan, C. C. (2014) The significance of circulating tumour cells in breast cancer: A review, *The Breast 23*, 552-560.

[173] Aceto, N., Bardia, A., Miyamoto, D. T., Donaldson, M. C., Wittner, B. S., Spencer, J. A., Yu, M., Pely, A., Engstrom, A., Zhu, H., Brannigan, B. W., Kapur, R., Stott, S. L., Shioda, T., Ramaswamy, S., Ting, D. T., Lin, C. P., Toner, M., Haber, D. A., and Maheswaran, S. (2014) Circulating tumor cell clusters are oligoclonal precursors of breast cancer metastasis, *Cell 158*, 1110-1122.

[174] Cleary, A. S., Leonard, T. L., Gestl, S. A., and Gunther, E. J. (2014) Tumour cell heterogeneity maintained by cooperating subclones in Wnt-driven mammary cancers, *Nature 508*, 113-117.

[175] Boiko, A. (2013) Isolation of Melanoma Tumor-Initiating Cells from Surgical Tissues, In *Molecular Dermatology* (Has, C., and Sitaru, C., Eds.), pp 253-259, Humana Press.

[176] Cheung, K. J., Padmanaban, V., Silvestri, V., Schipper, K., Cohen, J. D., Fairchild, A. N., Gorin, M. A., Verdone, J. E., Pienta, K. J., and Bader, J. S. (2016) Polyclonal breast cancer metastases arise from collective dissemination of keratin 14-expressing tumor cell clusters, *Proceedings of the National Academy of Sciences 113*, E854-E863.

[177] Chang, M.-C., Chang, Y.-T., Chen, J.-Y., Jeng, Y.-M., Yang, C.-Y., Tien, Y.-W., Yang, S.-H., Chen, H.-L., Liang, T.-Y., and Wang, C.-F. (2016) Clinical Significance of Circulating Tumor

Microemboli as a Prognostic Marker in Patients with Pancreatic Ductal Adenocarcinoma, *Clinical chemistry*, clinchem. 2015.248260.

[178] Mohamadi, R. M., Besant, J. D., Mepham, A., Green, B., Mahmoudian, L., Gibbs, T., Ivanov, I., Malvea, A., Stojcic, J., Allan, A. L., Lowes, L. E., Sargent, E. H., Nam, R. K., and Kelley, S. O. (2015) Nanoparticle-Mediated Binning and Profiling of Heterogeneous Circulating Tumor Cell Subpopulations, *Angewandte Chemie International Edition 54*, 139-143.

[179] Wit, S. d., Dalum, G. v., Lenferink, A. T. M., Tibbe, A. G. J., Hiltermann, T. J. N., Groen, H. J. M., van Rijn, C. J. M., and Terstappen, L. W. M. M. (2015) The detection of EpCAM+ and EpCAM– circulating tumor cells, *Scientific Reports 5*, 12270.

[180] Kokkinis, G., Keplinger, F., and Giouroudi, I. (2013) On-chip microfluidic biosensor using superparamagnetic microparticles, *Biomicrofluidics 7*, 054117.

[181] Derec, C., Wilhelm, C., Servais, J., and Bacri, J.-C. (2009) Local control of magnetic objects in microfluidic channels, *Microfluidics and Nanofluidics 8*, 123-130.

[182] Lampugnani, M. G. (1999) Cell migration into a wounded area in vitro, *Methods in molecular biology (Clifton, N.J.) 96*, 177-182.

[183] Chen, Y., Lu, B., Yang, Q., Fearns, C., Yates, J. R., 3rd, and Lee, J. D. (2009) Combined integrin phosphoproteomic analyses and small interfering RNA--based functional screening identify key regulators for cancer cell adhesion and migration, *Cancer research 69*, 3713-3720.

[184] Krebs, M. G., Metcalf, R. L., Carter, L., Brady, G., Blackhall, F. H., and Dive, C. (2014) Molecular analysis of circulating tumour cells[mdash]biology and biomarkers, *Nat Rev Clin Oncol 11*, 129-144.

[185] Diepenbruck, M., and Christofori, G. (2016) Epithelial-mesenchymal transition (EMT) and metastasis: yes, no, maybe?, *Current opinion in cell biology 43*, 7-13.

[186] Jolly, M. K., Boareto, M., Huang, B., Jia, D., Lu, M., Ben-Jacob, E., Onuchic, J. N., and Levine, H. (2015) Implications of the Hybrid Epithelial/Mesenchymal Phenotype in Metastasis, *Frontiers in Oncology 5*.

[187] Leong, S. M., Tan, K. M., Chua, H. W., Tan, D., Fareda, D., Osmany, S., Li, M.-H., Tucker, S., and Koay, E. S. (2015) Sampling circulating tumor cells for clinical benefits: how frequent?, *Journal of Hematology & Oncology 8*, 1-8.

[188] Ye, X., and Weinberg, R. A. (2015) Epithelial–mesenchymal plasticity: a central regulator of cancer progression, *Trends in cell biology 25*, 675-686.

[189] Hermann, P. C., Huber, S. L., Herrler, T., Aicher, A., Ellwart, J. W., Guba, M., Bruns, C. J., and Heeschen, C. (2007) Distinct populations of cancer stem cells determine tumor growth and metastatic activity in human pancreatic cancer, *Cell stem cell 1*, 313-323.

[190] Visvader, J. E., and Lindeman, G. J. (2008) Cancer stem cells in solid tumours: accumulating evidence and unresolved questions, *Nature reviews. Cancer 8*, 755-768.

[191] Oskarsson, T., Batlle, E., and Massagué, J. (2014) Metastatic Stem Cells: Sources, Niches, and Vital Pathways, *Cell stem cell 14*, 306-321.

[192] Zhang, Y., Toy, K. A., and Kleer, C. G. (2012) Metaplastic breast carcinomas are enriched in markers of tumor-initiating cells and epithelial to mesenchymal transition, *Mod Pathol 25*, 178-184.

[193] Ratajczak, M. Z. (2005) Cancer stem cells--normal stem cells "Jedi" that went over to the "dark side", *Folia histochemica et cytobiologica / Polish Academy of Sciences, Polish Histochemical and Cytochemical Society 43*, 175-181.

[194] Zöller, M. (2011) CD44: can a cancer-initiating cell profit from an abundantly expressed molecule?, *Nature reviews. Cancer 11*, 254-267.

[195] Hong, S. P., Wen, J., Bang, S., Park, S., and Song, S. Y. (2009) CD44-positive cells are responsible for gemcitabine resistance in pancreatic cancer cells, *International journal of cancer. Journal international du cancer 125*, 2323-2331.

[196] Mascalchi, M., Falchini, M., Maddau, C., Salvianti, F., Nistri, M., Bertelli, E., Sali, L., Zuccherelli, S., Vella, A., Matucci, M., Voltolini, L., Pegna, A. L., Luconi, M., Pinzani, P., and Pazzagli, M. (2015) Prevalence and number of circulating tumour cells and microemboli at diagnosis of advanced NSCLC, *Journal of cancer research and clinical oncology*.

[197] Krebs, M. G., Hou, J. M., Sloane, R., Lancashire, L., Priest, L., Nonaka, D., Ward, T. H., Backen, A., Clack, G., Hughes, A., Ranson, M., Blackhall, F. H., and Dive, C. (2012) Analysis of circulating tumor cells in patients with non-small cell lung cancer using epithelial marker-dependent and -independent approaches, *Journal of thoracic oncology : official publication of the International Association for the Study of Lung Cancer 7*, 306-315.

[198] Wendel, M., Bazhenova, L., Boshuizen, R., Kolatkar, A., Honnatti, M., Cho, E. H., Marrinucci, D., Sandhu, A., Perricone, A., Thistlethwaite, P., Bethel, K., Nieva, J., Heuvel, M., and Kuhn, P. (2012) Fluid biopsy for circulating tumor cell identification in patients with early-and late-stage non-small cell lung cancer: a glimpse into lung cancer biology, *Physical biology 9*, 016005.

[199] Cho, E. H., Wendel, M., Luttgen, M., Yoshioka, C., Marrinucci, D., Lazar, D., Schram, E., Nieva, J., Bazhenova, L., Morgan, A., Ko, A. H., Korn, W. M., Kolatkar, A., Bethel, K., and Kuhn, P. (2012) Characterization of circulating tumor cell aggregates identified in patients with epithelial tumors, *Physical biology 9*, 016001.

[200] Mitra, A., Satelli, A., Xia, X., Cutrera, J., Mishra, L., and Li, S. (2015) Cell-surface Vimentin: A mislocalized protein for isolating csVimentin(+) CD133(-) novel stem-like hepatocellular carcinoma cells expressing EMT markers, *International journal of cancer. Journal international du cancer 137*, 491-496.

[201] Barua, S., Yoo, J.-W., Kolhar, P., Wakankar, A., Gokarn, Y. R., and Mitragotri, S. (2013) Particle shape enhances specificity of antibody-displaying nanoparticles, *Proceedings of the National Academy of Sciences*.

[202] Hur, S. C., Choi, S.-E., Kwon, S., and Carlo, D. D. (2011) Inertial focusing of non-spherical microparticles, *Applied Physics Letters 99*, 044101.

[203] Lee, C. J., Dosch, J., and Simeone, D. M. (2008) Pancreatic cancer stem cells, *Journal of clinical oncology : official journal of the American Society of Clinical Oncology 26*, 2806-2812.

[204] Bhaskar, S., Pollock, K. M., Yoshida, M., and Lahann, J. (2010) Towards designer microparticles: simultaneous control of anisotropy, shape, and size, *Small (Weinheim an der Bergstrasse, Germany) 6*, 404-411.

[205] Lee, W., Joo, S., Kim, S. U., Rhie, K., Hong, J., Shin, K.-H., and Kim, K. H. (2009) Magnetic bead counter using a micro-Hall sensor for biological applications, *Applied Physics Letters 94*, 153903.

[206] Hingorani, S. R., Petricoin Iii, E. F., Maitra, A., Rajapakse, V., King, C., Jacobetz, M. A., Ross, S., Conrads, T. P., Veenstra, T. D., Hitt, B. A., Kawaguchi, Y., Johann, D., Liotta, L. A., Crawford, H. C., Putt, M. E., Jacks, T., Wright, C. V. E., Hruban, R. H., Lowy, A. M., and Tuveson, D. A. (2003) Preinvasive and invasive ductal pancreatic cancer and its early detection in the mouse, *Cancer cell 4*, 437-450.

[207] Rothwell, D. G., Li, Y., Ayub, M., Tate, C., Newton, G., Hey, Y., Carter, L., Faulkner, S., Moro, M., Pepper, S., Miller, C., Blackhall, F., Bertolini, G., Roz, L., Dive, C., and Brady, G. (2014) Evaluation and validation of a robust single cell RNA-amplification protocol through transcriptional profiling of enriched lung cancer initiating cells, *BMC Genomics 15*, 1129.

[208] Gasch, C., Bauernhofer, T., Pichler, M., Langer-Freitag, S., Reeh, M., Seifert, A. M., Mauermann, O., Izbicki, J. R., Pantel, K., and Riethdorf, S. (2013) Heterogeneity of Epidermal Growth Factor Receptor Status and Mutations of KRAS/PIK3CA in Circulating Tumor Cells of Patients with Colorectal Cancer , *Clinical chemistry 59*, 252-260.

[209] Heitzer, E., Auer, M., Gasch, C., Pichler, M., Ulz, P., Hoffmann, E. M., Lax, S., Waldispuehl-Geigl, J., Mauermann, O., Lackner, C., Hofler, G., Eisner, F., Sill, H., Samonigg, H., Pantel, K., Riethdorf, S., Bauernhofer, T., Geigl, J. B., and Speicher, M. R. (2013) Complex tumor genomes inferred from single circulating tumor cells by array-CGH and next-generation sequencing, *Cancer research 73*, 2965-2975.